(12) INTERNATIONAL APPLICATION PUBLISHED UNDER THE PATENT COOPERATION TREATY (PCT)

(19) World Intellectual Property Organization
International Bureau

(43) International Publication Date
13 July 2017 (13.07.2017)

WIPO | PCT

(10) International Publication Number
WO 2017/120322 A1

(51) International Patent Classification:
A61K 39/35 (2006.01) *A61K 38/19* (2006.01)
A61K 39/39 (2006.01) *A61K 9/00* (2006.01)

(21) International Application Number:
PCT/US2017/012315

(22) International Filing Date:
5 January 2017 (05.01.2017)

(25) Filing Language: English

(26) Publication Language: English

(30) Priority Data:
62/275,167 5 January 2016 (05.01.2016) US

(71) Applicant: **UNIVERSITY OF PITTSBURGH-OF THE COMMONWEALTH SYSTEM OF HIGHER EDUCATION** [US/US]; 1st Floor Gardner Steel Conference Center, 130 Thackeray Avenue, Pittsburgh, PA 15260 (US).

(72) Inventors: **FALO JR., Louis, D.;** 2698 Timberglen Drive, Wexford, PA 15090 (US). **LARREGINA DE MORELLI, Adriana, Teresita;** 631 Bigelow St., Pittsburgh, PA 15207 (US).

(74) Agent: **LAUER, Deakin,** T.; Klarquist Sparkman, LLP, One World Trade Center, Suite 1600, 121 Sw Salmon Street, Portland, OR 97204 (US).

(81) Designated States *(unless otherwise indicated, for every kind of national protection available):* AE, AG, AL, AM, AO, AT, AU, AZ, BA, BB, BG, BH, BN, BR, BW, BY, BZ, CA, CH, CL, CN, CO, CR, CU, CZ, DE, DJ, DK, DM, DO, DZ, EC, EE, EG, ES, FI, GB, GD, GE, GH, GM, GT, HN, HR, HU, ID, IL, IN, IR, IS, JP, KE, KG, KH, KN, KP, KR, KW, KZ, LA, LC, LK, LR, LS, LU, LY, MA, MD, ME, MG, MK, MN, MW, MX, MY, MZ, NA, NG, NI, NO, NZ, OM, PA, PE, PG, PH, PL, PT, QA, RO, RS, RU, RW, SA, SC, SD, SE, SG, SK, SL, SM, ST, SV, SY, TH, TJ, TM, TN, TR, TT, TZ, UA, UG, US, UZ, VC, VN, ZA, ZM, ZW.

(84) Designated States *(unless otherwise indicated, for every kind of regional protection available):* ARIPO (BW, GH, GM, KE, LR, LS, MW, MZ, NA, RW, SD, SL, ST, SZ, TZ, UG, ZM, ZW), Eurasian (AM, AZ, BY, KG, KZ, RU, TJ, TM), European (AL, AT, BE, BG, CH, CY, CZ, DE, DK, EE, ES, FI, FR, GB, GR, HR, HU, IE, IS, IT, LT, LU, LV, MC, MK, MT, NL, NO, PL, PT, RO, RS, SE, SI, SK, SM, TR), OAPI (BF, BJ, CF, CG, CI, CM, GA, GN, GQ, GW, KM, ML, MR, NE, SN, TD, TG).

[Continued on nextpage]

(54) Title: SKIN MICROENVIRONMENT TARGETED DELIVERY FOR PROMOTING IMMUNE AND OTHER RESPONSES

(57) Abstract: Methods are provided for promoting, reducing, or desensitizing various immune responses by delivery of sub-immunogenic doses of an allergen, alone or with other agents, or by delivery of antigens and adjuvants to a cutaneous microenvironment of a subject. Microneedle arrays can be used in connection with this delivery.

FIG. 1

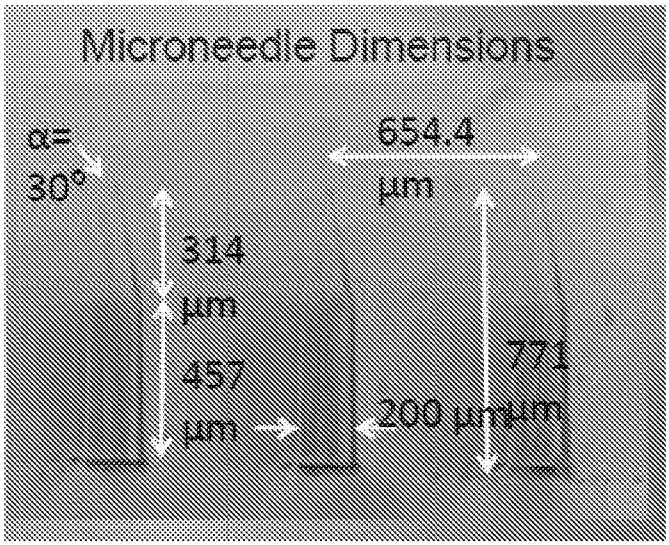

WO 2017/120322 A1

Declarations under Rule 4.17:

— *of inventorship (Rule 4.17(iv))*

Published:

— *with international search report (Art. 21(3))*

SKIN MICROENVIRONMENT TARGETED DELIVERY FOR PROMOTING IMMUNE AND OTHER RESPONSES

CROSS REFERENCE TO RELATED APPLICATION

This application claims the benefit of U.S. Provisional Application No. 62/275,167 filed January 5, 2016, which is herein incorporated by reference in its entirety.

FIELD

The disclosure pertains to systems and methods for transdermal drug delivery, including microneedle arrays and, in particular, to systems and methods for promoting, enhancing, dampening, suppressing, desensitizing, or otherwise modifying an immune response of a subject.

ACKNOWLEDGMENT OF GOVERNMENT SUPPORT

This invention was made with government support under grant number EBO 12776 awarded by the National Institutes of Health. The government has certain rights in the invention.

BACKGROUND

The immune system protects the body of a subject from possibly harmful substances by recognizing and responding to antigens. The body's response to antigens can be used to treat or affect various health conditions or diseases by provoking a desired immune response in the subject. However, in some cases, overactive or non-specific immune responses can result in pathology or disease. Precise control of the nature of the provoked immune response is difficult and, as a result, conventional methods suffer various shortcomings. As such, there remains a need for improved methods for promoting, enhancing, dampening, suppressing, desensitizing, or otherwise modifying an immune response in a subject.

SUMMARY

In some embodiments, methods for reducing or desensitizing an immune response of a subject in need thereof are provided. The methods can include administering one or more sub-immunogenic doses of an allergen to a specific cutaneous microenvironment of the subject, and thereby reducing or desensitizing the immune response of the subject. In some embodiments, the one or more sub-immunogenic doses of the allergen can be contained in microneedle arrays.

In other embodiments methods can include administering one or more sub-immunogenic or non-immunogenic doses of an allergen and one or more immunoregulatory molecule to a specific

cutaneous microenvironment of the subject, and thereby reducing or desensitizing the immune response of the subject. In some embodiments, the one or more sub-immunogenic or non-immunogenic doses of the allergan and adjuvant(s) can be contained in microneedle arrays.

In other embodiments, methods for promoting a pro-inflammatory and an adaptive immune response to provide a positive immunization against tumors and infectious diseases to a subject in need thereof are provide. The methods can include administering an antigen and at least one adjuvant in a cutaneous microenvironment of the subject, thereby promoting the pro-inflammatory and adaptive immune response in the subject. In some embodiments, the antigen and at least adjuvant administration can be achieved using microneedle arrays that contain the antigen and the at least one adjuvant therein.

In other embodiments, methods for promoting an immune response to a subject in need thereof are provide that include administering an antigen and at least one adjuvant in a cutaneous microenvironment of the subject, thereby promoting the immune response in the subject.

In other embodiments, a method for promoting an immune response to a subject in need thereof can include administering an antigen and at least two adjuvants in a cutaneous microenvironment of the subject, thereby promoting the immune response in the subject.

The systems and methods disclosed herein include cutaneous delivery platforms based on dissolvable microneedle arrays that can provide efficient, precise, and reproducible delivery of biologically active molecules to human skin. The microneedle array delivery platforms can be used to deliver a broad range of bioactive components to a patient. In still other embodiments, specific implementations of the methods and systems disclosed herein are achieved using microneedle arrays to deliver cargo to the desired cutaneous microenvironment of the subject.

The foregoing and other objects, features, and advantages of the disclosed embodiments will become more apparent from the following detailed description, which proceeds with reference to the accompanying figures.

BRIEF DESCRIPTION OF THE DRAWINGS

FTG. 1 illustrates exemplary microneedles and their dimensions.

FTG. 2 illustrates an exemplary microneedle array and its dimensions.

FIGS. 3A and 3B illustrate exemplary microneedles with tip-loaded active components.

FIGS. 4A and 4B illustrate exemplary microneedles with tip-loaded active components.

FIGS. 5A and 5B illustrate exemplary microneedles with tip-loaded active components.

FIGS. 6A and 6B illustrate exemplary microneedles with tip-loaded active components.

FIG. 7 illustrates a miniature precision-micromilling system used for fabricating microneedle mastermolds.

FIG. 8 is an SEM image of a micromilled mastermold with pyramidal needles.

FIG. 9 is an SEM image of a pyramidal production mold.

FIG. 10 is an SEM image of an enlarged segment of the production mold, illustrating a pyramidal needle molding well in the center of the image.

FIGS. 11A-11D illustrate exemplary CMC-solids and embedded active components.

FIGS. 12A-12B illustrate exemplary CMC-solids and embedded active components.

FIG. 13 is a schematic illustration of exemplary vertical multi-layered deposition structures and methods of fabricating the same.

FIG. 14 is a schematic illustration of exemplary microneedle arrays fabricated using layering and spatial distribution techniques of embedded active components.

FIG. 15 is a schematic illustration of exemplary microneedle arrays fabricated in a spatially controlled manner.

FIG. 16A is an SEM image of a plurality of pyramidal-type molded microneedles.

FIG. 16B is an SEM image of a single pyramidal-type molded microneedle.

FIG. 17 is an SEM image of a pillar type molded microneedle.

FIG. 18 is a micrograph of pyramidal type molded microneedles.

FIG. 19 is a micrograph of pillar type molded microneedles.

FIG. 20 illustrates various microneedle geometries that can be formed using micromilled mastermolds or by direct micromilling of a block of material.

FIG. 21 illustrates a test apparatus for performing failure and piercing tests.

FIG. 22 illustrates force-displacement curves for pillar type microneedles (left) and pyramidal type microneedles (right).

FIG. 23 illustrates a finite elements model of microneedle deflections for pillar type microneedles (left) and pyramidal type microneedles (right).

FIG. 24 show various stereo micrographs of the penetration of pyramidal (A, C, E) and pillar (B, D, F) type microneedles in skin explants.

FIGS. 25A, 25B, and 25C illustrate the effectiveness of microneedle arrays in penetrating skin explants.

FIGS. 26A and 26B illustrate *in vivo* delivery of particulates to the skin draining lymph nodes of microneedle array immunized mice.

FIG. 27 is a bar graph showing immunogenicity of microneedle delivered model antigens.

FIG. 28 is a bar graph showing the stability of the active cargo of CMC-microneedle arrays in storage.

FIGS. 29A and 29B show induction of apoptosis in epidermal cells that have been delivered Cytoxan® (cyclophosphamide) through a microneedle array.

FIG. 30 illustrates a microneedle geometry that can be formed by direct micromilling of a block of material.

FIG. 31 is a stereo microscopic image of a direct-fabricated solid CMC-microneedle array.

FIG. 32 is a stereo microscopic image of a portion of the microneedle array of FIG. 31.

FIG. 33 is a schematic cross-sectional view of a casting-mold assembly for creating a block or sheet of material for direct micromilling.

FIG. 34 is a schematic cross-sectional view of a drying apparatus that can be used to dry a block or sheet of material for direct micromilling.

FIG. 35 is a flow cytometry analysis of GFP expressing target 293T cells.

FIG. 36 illustrates the stability of microneedle embedded viruses after a number of days in storage.

FIG. 37 illustrates the expression and immunogenicity of microneedle array delivered adenovectors.

FIGS. 38A-C show sustained-release-polymer embedded cargos in microneedle arrays.

FIGS. 39A-C illustrate the time dependent cargo release of single and double loaded microneedle arrays.

FIG. 40 illustrates various controlled release activities that can be incorporated into microneedle arrays for coordinated kinetic and/or spatial co-delivery.

FIGS. 41A-41D show various indications of functional NK1R expression in mouse skin.

FIGS. 42A-D show various indications of NK1R expression by human skin dendritic cells and SarSP increasing T-cell stimulatory function.

FIG. 43 is a table showing a quantitative comparison of conventional pyramid-shaped microneedles and obelisk microneedles.

FIGS. 44A-44D illustrate penetration and delivery of MNA cargo to mouse and human skin.

FIGS. 45A-45D illustrate inflammatory responses observed in cross sections of abdominal skin and skin draining lymph nodes of sensitized mice and controls.

FIG. 46 illustrates a DTH effector response expressed as percent of ear thickness increase.

FIGS. 47A and 47B show the lack of an immune- stimulatory response in microneedle arrays generally.

FIG. 48 show immunizations with DNCB-MNA or with DNCB-L733,060-MNA.

FIGS. 49A-49C illustrate an approach for desensitization of contact dermatitis by MNA negative immunization.

FIGS. 50A and 50B show the effects of NK1R blockade on migration and T-cell stimulatory function in human skin.

FIGS. 51A and 51B demonstrate the immunogenicity of skin microenvironment targeted delivery of a representative hapten antigen, and characterizes the contact hypersensitivity response generated.

FIGS. 52A, 52B, and 52C demonstrate that skin microenvironment targeted delivery of a hapten antigen with a potent NK1R antagonist, prevents an acute inflammatory response against that same hapten.

FIGS. 53A and 53B illustrate additional exemplary results from negative immunization MNA systems.

FIGS. 54A, 54B, and 54C illustrate additional exemplary results from negative immunization MNA systems.

FIGS. 55A, 55B, 55C, and 55D illustrate the activation and migration of human skin dendritic cell subsets.

FIGS. 56A and 56B illustrate additional exemplary results from negative immunization MNA systems.

DETAILED DESCRIPTION

The following description is exemplary in nature and is not intended to limit the scope, applicability, or configuration of the disclosed embodiments in any way. Various changes to the described embodiment may be made in the function and arrangement of the elements described herein without departing from the scope of the disclosure.

As used in this application and in the claims, the singular forms "a," "an," and "the" include the plural forms unless the context clearly dictates otherwise. Additionally, the term "includes" means "comprises." As used herein, the terms "biologic," "active component," "bioactive component," "bioactive material," or "cargo" refer to pharmaceutically active agents, such as analgesic agents, anesthetic agents, anti-asthmatic agents, antibiotics, anti-depressant agents, anti-diabetic agents, anti-fungal agents, anti-hypertensive agents, anti-inflammatory agents, anti-neoplastic agents, anxiolytic agents, enzymatically active agents, nucleic acid constructs,

immunostimulating agents, immunosuppressive agents, vaccines, and the like. The bioactive material can comprise dissoluble materials, insoluble but dispersible materials, natural or formulated macro, micro and nano particulates, and/or mixtures of two or more of dissoluble, dispersible insoluble materials and natural and/or formulated macro, micro and nano particulates.

As used herein, the terms "controlled release" or "controlled release profile" refer to the characteristics of the release of the bioactive agent from another material (such as a composition containing the bioactive agent and a biocompatible polymer). Controlled release encompasses delayed, sustained or prolonged release, and other pre-determined release mechanisms. Use of the materials described herein allows a controlled release of the bioactive agent after delivery of the microneedle or microneedle array to the subject. The selection of the desired release profile depends on considerations known to those skilled in the art, such as the disease or indication to be treated, the treatment regimen, the patient to be treated, the route of administration and/or the site of administration, etc. In some embodiments, controlled release is achieved by combining the bioactive agent with a polymer in some manner, such as complexing the bioactive component with the polymer, encapsulating the bioactive component, or otherwise integrating the two components to provide for a change in release activity from that of the bioactive component itself.

As used herein, the terms "complexed" or "integrated" with means the bioactive component is interconnected with, intermingled with, deposited with, dispersed within, and/or bonded to another material. As used herein, the term "encapsulated" means that the bioactive component is dissolved or dispersed in another material such as a polymer.

As used herein, the term "conjugate" means two or more moieties directly or indirectly coupled together. For example, a first moiety may be covalently or noncovalently *(e.g.* , electrostatically) coupled to a second moiety. Indirect attachment is possible, such as by using a "linker" (a molecule or group of atoms positioned between two moieties).

As used herein, the term "pre-formed" means that a structure or element is made, constructed, and/or formed into a particular shape or configuration prior to use. Accordingly, the shape or configuration of a pre-formed microneedle array is the shape or configuration of that microneedle array prior to insertion of one or more of the microneedles of the microneedle array into the patient.

As used herein, the term "sub-immunogenic" means conditions which avoid activation of antigen presenting cells. As used herein, the term "antigen" means any immunogenic moiety or agent, generally a macromolecule, that elicits an immunological response in an individual. As used herein, the term "allergen" means any substance that causes an enhanced cell response (e.g., an allergic or asthmatic response) in a susceptible subject. Allergens are commonly proteins, or

chemicals bound to proteins, that have the property of being allergenic; however, allergens can also include organic or inorganic materials derived from a variety of man-made or natural sources such as plant materials, metals, ingredients in cosmetics or detergents, latexes, or the like. The term "allergy" refers to acquired hypersensitivity to a substance (allergen). An "allergic reaction" is the response of an immune system to an allegen in a subject allergic to the allergen. Allergic conditions include eczema, allergic rhinitis or coryza, hay fever, bronchial asthma, urticaria (hives) and food allergies, and other atopic conditions. As used herein, "subject" means a mammal, including but not limited to humans, dogs, cats, and rodents.

Although the operations of exemplary embodiments of the disclosed method may be described in a particular, sequential order for convenient presentation, it should be understood that disclosed embodiments can encompass an order of operations other than the particular, sequential order disclosed. For example, operations described sequentially may in some cases be rearranged or performed concurrently. Further, descriptions and disclosures provided in association with one particular embodiment are not limited to that embodiment, and may be applied to any embodiment disclosed.

Moreover, for the sake of simplicity, the attached figures may not show the various ways (readily discernable, based on this disclosure, by one of ordinary skill in the art) in which the disclosed system, method, and apparatus can be used in combination with other systems, methods, and apparatuses. Additionally, the description sometimes uses terms such as "produce" and "provide" to describe the disclosed method. These terms are high-level abstractions of the actual operations that can be performed. The actual operations that correspond to these terms can vary depending on the particular implementation and are, based on this disclosure, readily discernible by one of ordinary skill in the art.

Tip-Loaded Microneedle Arrays

Dissolvable microneedle arrays enable efficient and safe drug and vaccine delivery to the skin and mucosal surfaces. However, inefficient drug delivery can result from the homogenous nature of conventional microneedle array fabrication. Although the drugs or other cargo that is to be delivered to the patient are generally incorporated into the entire microneedle array matrix, in practice only the microneedles enter the skin and therefore, only cargo contained in the volume of the individual needles is deliverable. Accordingly, the vast majority of the drugs or other cargo that is localized in the non-needle components (e.g., the supporting structure of the array) is never delivered to the patient and is generally discarded as waste.

FIGS. 1 and 2 illustrate exemplary dimensions of microneedles and microneedle arrays. Based on the illustrative sizes shown in FIGS. 1 and 2, a microneedle array that comprises an active

component homogenously distributed throughout the array exhibits active component waste of greater than 40 percent. For example, if the entire area of the array is 61 mm^2 and the microneedle array area is 36 mm^2, then the percent utilization of the active component is less than 60 percent. Although the dimensions reflected in FIGS. 1 and 2 illustrate a particular size array and shape of microneedles, it should be understood that similar waste is present in any other size microneedle array in which the active component is homogenously distributed throughout the array, regardless of the size of the array or the shape of the microneedles involved.

The systems and methods described herein provide novel microneedle array fabrication technology that utilizes a fully-dissolvable microneedle array substrate and unique microneedle geometries that enable effective delivery of a broad range of active components, including a broad range of protein and/or small molecule medicines and vaccines.

As described in more detail herein, in some embodiments, this technology can also uniquely enable the simultaneous co-delivery of multiple chemically distinct agents for polyfunctional drug delivery. Examples of the utility of these devices include, for example, (1) simultaneous delivery of multiple antigens and adjuvants to generate a polyvalent immune response relevant to infectious disease prevention and cancer therapy, (2) co-delivery of chemotherapeutic agents, immune stimulators, adjuvants, and antigens to enable simultaneous adjunct tumor therapies, and (3) localized skin delivery of multiple therapeutic agents without systemic exposure for the treatment of a wide variety of skin diseases.

In some embodiments, the systems and method disclosed herein relate to a novel fabrication technology that enables various active components to be incorporated into the needle tips. Thus, by localizing the active components in this manner, the remainder of the microneedle array volume can be prepared using less expensive matrix material that is non-active and generally regarded as safe. The net result is greatly improved efficiency of drug delivery based on (1) reduced waste of non-deliverable active components incorporated into the non-needle portions of the microneedle array, and (2) higher drug concentration in the skin penetrating needle tips. This technological advance results in dramatically improved economic feasibility proportional to the cost of drug cargo, and increased effective cargo delivery capacity per needle of these novel microneedle arrays.

FIGS. 3A, 3B, 4A, and 4B illustrate various embodiments of microneedle arrays wherein the active component is concentrated in the microneedle tips of the respective arrays. Thus, in contrast to conventional microneedle arrays, the active component is not present at even concentration throughout the microneedle array since there is little or no active component present in the supporting base structure. In addition, in some embodiments (as shown, for example, in FIGS. 3A, 3B, 4A, and 4B), not only is there little or no active component in the supporting

structures, the location of the active component is concentrated in the upper half of the individual microneedles in the array.

FIGS. 5A and 5B illustrate exemplary images of microneedles of a microneedle array that contains active component concentrated in the upper half of the individual microneedles. The active component is illustrated as fluorescent particles that are concentrated in the tip of the microneedle, with the tip being defined by an area of the microneedle that extends from a base portion in a narrowing and/or tapered manner. The base portion, in turn, extends from the supporting structure of the array.

FIGS. 6A and 6B illustrate additional exemplary images of microneedles of microneedle arrays that contain active components concentrated in the upper half of the individual microneedles. In FIG. 6A, the active component, which is concentrated in the tip of the microneedles, is BSA-FITC. In FIG. 6B, the active component, which is also concentrated in the tip of the microneedles, is OVA-FITC.

As noted above, in some embodiments, individual microneedles can comprise active components only in the upper half of the microneedle. In other embodiments, individual microneedles can comprise active components only in the tips or in a narrowing portion near the tip of the microneedle. In still other embodiments, individual needles can comprise active components throughout the entire microneedle portion that extends from the supporting structure.

The following embodiments describe various exemplary methods for fabricating microneedle arrays with one or more active component concentrated in the upper halves and/or tips of microneedles in respective microneedle arrays.

Microneedle Arrays Fabricated by Sequential Micro-Molding and Spin-Drying Methods

The following steps describe an exemplary method of fabricating microneedle arrays using sequential micro-molding and spin-drying. Active components/cargo can be prepared at a desired useful concentration in a compatible solvent. As described herein, the solvents of the active component(s) can be cargo specific and can comprise a broad range of liquids, including for example, water, organic polar, and/or apolar liquids. Examples of active components are discussed in more detail below and various information about those active components, including tested and maximum loading capacity of various microneedle arrays are also discussed in more detail below.

If desired, multiple loading cycles can be performed to achieve higher active cargo loads as necessary for specific applications. In addition, multiple active cargos can be loaded in a single loading cycle as a complex solution, or as single solutions in multiple cycles (e.g., repeating the loading cycle described below) as per specific cargo-compatibility requirements of individual

cargos. Also, particulate cargos (including those with nano- and micro- sized geometries) can be prepared as suspensions at the desired particle number/volume density.

Example 1

a) As described in more detail below in the micromilling embodiments, an active cargo's working stock solution/suspension can be applied to the surface of microneedle array production molds at, for example, about 40 μï per cm^2 surface area.

b) The microneedle array production molds with active cargo(s) can be centrifuged at 4500 rpm for 10 minutes to fill the microneedle array production molds needles with the working cargo stock.

c) The excess cargo solution/suspension can be removed and the surface of the microneedle array production molds, washed with 100 μï phosphate buffer saline (PBS) per cm^2 mold-surface area, or with the solvent used for the preparation of the active cargo's working stock.

d) The microneedle array production molds containing the active cargo stock solution/suspension in the needle's cavity can be spin-dried at 3500 rpm for 30 minutes at the required temperature with continues purging gas flow through the centrifuge at 0-50 L/min to facilitate concentration of the drying active cargo(s) in the needle-tips. The purging gas can be introduced into the centrifuge chamber through tubular inlets. Moisture content can be reduced using a dehumidifier tempered to the required temperature with recirculation into the centrifuge chamber. The purging gas can be air, nitrogen, carbon dioxide or another inert or active gas as required for specific cargo(s). The flow rate is measured by flow-meters and controlled by a circulating pump device.

e) 100 μï 20% CMC90 hydrogel in H20 can be added to the surface microneedle array production molds' per cm^2 microneedle array production molds-area to load the structural component of the microneedle array device.

f) The microneedle array production molds can be centrifuged at 4500 rpm for 10 min at the required temperature without purging gas exchange in the centrifuge chamber to fill up the microneedle array production molds needle cavities with the CMC90 hydrogel. This can be followed by a 30 min incubation period to enable rehydration of the active cargo(s) previously deposited in the microneedle array tips.

g) The microneedle array production molds can centrifuged at 3500 rpm for 3 hours or longer at the required temperature with 0-50 L/min constant purging gas flow through the centrifuge chamber to spin-dry the MNA devices to less than 5% moisture content.

h) The dried microneedle array devices can then be separated from the microneedle array production molds for storage under the desired conditions. In some embodiments, CMC90 based devices can be storable between about 50 °C to -86 °C.

Examples of fabricated tip-loaded active cargo carrying microneedle arrays can be seen in FIGS. 3A-6B.

Micromilled Master Molds and Spin-molded Microneedle Arrays

In the following embodiments, micromilling steps are preformed to create microneedle arrays of various specifications. It should be understood, however, that the following embodiments describe certain details of microneedle array fabrication that can be applicable to processes of microneedle array fabrication that do not involve micromilling steps, including the process described above in the previous example.

In the following embodiments, apparatuses and methods are described for fabricating dissolvable microneedle arrays using master molds formed by micromilling techniques. For example, microneedle arrays can be fabricated based on a mastermold (positive) to production mold (negative) to array (positive) methodology. Micromilling technology can be used to generate various micro-scale geometries on virtually any type of material, including metal, polymer, and ceramic parts. Micromilled mastermolds of various shapes and configurations can be effectively used to generate multiple identical female production molds. The female production molds can then be used to microcast various microneedle arrays.

FIG. 7 illustrates an example of a precision-micromilling system that can be used for fabricating a microneedle mastermold. Mechanical micromilling uses micro-scale (for example, as small as 10 μιη) milling tools within precision computer controlled miniature machine-tool platforms. The system can include a microscope to view the surface of the workpiece that is being cut by the micro-tool. The micro-tool can be rotated at ultra-high speeds (200,000 rpm) to cut the workpiece to create the desired shapes. As noted above, the micromilling process can be used to create complex geometric features with many kinds of material. Various types of tooling can be used in the micromilling process, including, for example, carbide micro-tools. In a preferred embodiment, however, diamond tools can be used to fabricate the microneedle arrays on the master mold. Diamond tooling can be preferable over other types of tooling because it is harder than conventional materials, such as carbide, and can provide cleaner cuts on the surface of the workpiece.

Mastermolds can be micromilled from various materials, including, for example, Cirlex® (DuPont, Kapton® polyimide), which is the mastermold material described in the exemplary embodiment. Mastermolds can be used to fabricate flexible production molds from a suitable

material, such as SYLGARD® 184 (Dow Corning), which is the production material described in the exemplary embodiment below. The mastermold is desirably formed of a material that is capable of being reused so that a single mastermold can be repeatedly used to fabricate a large number of production molds. Similarly each production mold is desirably able to fabricate multiple microneedle arrays.

Mastermolds can be created relatively quickly using micromiUing technology. For example, a mastermold that comprises a 10 mm x 10 mm array with 100 microneedles can take less than a couple of hours and, in some embodiments, less than about 30 minutes to micromill. Thus, a short ramp-up time enables rapid fabrication of different geometries, which permits the rapid development of microneedle arrays and also facilitates the experimentation and study of various microneedle parameters.

The mastermold material preferably is able to be cleanly separated from the production mold material and preferably is able to withstand any heighted curing temperatures that may be necessary to cure the production mold material. For example, in an illustrated embodiment, the silicone-based compound SYLGARD® 184 (Dow Corning) is the production mold material and that material generally requires a curing temperature of about 80-90 degrees Celsius.

Mastermolds can be created in various sizes. For example, in an exemplary embodiment, a mastermold was created on 1.8 mm thick Cirlex® (DuPont, Kapton® polyimide) and 5.0 mm thick acrylic sheets. Each sheet can be flattened first by micromiUing tools, and the location where the microneedles are to be created can be raised from the rest of the surface. Micro-tools can be used in conjunction with a numerically controlled micromiUing machine (FIG. 1) to create the microneedle features *(e.g.* , as defined by the mastermold). In that manner, the micromiUing process can provide full control of the dimensions, sharpness, and spatial distribution of the microneedles.

FIG. 8 is an image from a scanning electron microscope (SEM) showing the structure of a micromilled mastermold with a plurality of pyramidal needles. As shown in FIG. 8, a circular groove can be formed around the microneedle array of the mastermold to produce an annular (for example, circular) wall section in the production mold. The circular wall section of the production mold can facilitate the spincasting processes discussed below. Although the wall sections illustrated in FIG. 9 and the respective mastermold structure shown in FIG. 8 is circular, it should be understood that wall sections or containment means of other geometries can be provided. For example, depending on what shape is desired for the microneedle array device, the containment means can be formed in a variety of shapes including, for example, square, rectangular, trapezoidal, polygonal, or various irregular shapes.

As discussed above, the production molds can be made from SYLGARD® 184 (Dow Corning), which is a two component clear curable silicone elastomer that can be mixed at a 10: 1 SYLGARD® to curing agent ratio. The mixture can be degassed for about 10 minutes and poured over the mastermold to form an approximately 8 mm layer, subsequently degassed again for about 30 minutes and cured at 85 °C for 45 minutes. After cooling down to room temperature, the mastermold can be separated from the cured silicone, and the silicone production mold trimmed to the edge of the circular wall section that surrounds the array (FIG. 9.). From a single mastermold, a large number of production molds *(e.g.* , 100 or more) can be produced with very little, if any, apparent deterioration of the Cirlex® or acrylic mastermolds.

FIG. 9 is an SEM image of a pyramidal production mold created as described above. FIG. 10 illustrates an enlarged segment of the production mold with a pyramidal needle molding well in the center of the image. The molding well is configured to receive a base material (and any components added to the base material) to form microneedles with an external shape defined by the molding well.

To construct the microneedle arrays, a base material can be used to form portions of each microneedle that have bioactive components and portions that do not. As discussed above, each microneedle can comprise bioactive components only in the microneedles, or in some embodiments, only in the upper half of the microneedles, or in other embodiments, only in a portion of the microneedle that tapers near the tip. Thus, to control the delivery of the bioactive component(s) and to control the cost of the microneedle arrays, each microneedle preferably has a portion with a bioactive component and a portion without a bioactive component. In the embodiments described herein, the portion without the bioactive component includes the supporting structure of the microneedle array and, in some embodiments, a base portion (e.g., a lower half) of each microneedle in the array.

Various materials can be used as the base material for the microneedle arrays. The structural substrates of biodegradable solid microneedles most commonly include poly(lactic-co-glycolic acid) (PLGA) or carboxymethylcellulose (CMC) based formulations; however, other bases can be used.

CMC is generally preferable to PLGA as the base material of the microneedle arrays described herein. The PLGA based devices can limit drug delivery and vaccine applications due to the relatively high temperature *(e.g.* , 135 degrees Celsius or higher) and vacuum required for fabrication. In contrast, a CMC-based matrix can be formed at room temperature in a simple spin-casting and drying process, making CMC-microneedle arrays more desirable for incorporation of sensitive biologies, peptides, proteins, nucleic acids, and other various bioactive components.

CMC-hydrogel can be prepared from low viscosity sodium salt of CMC with or without active components (as described below) in sterile dH_2O. In the exemplary embodiment, CMC can be mixed with sterile distilled water (dH_2O) and with the active components to achieve about 25 wt% CMC concentration. The resulting mixture can be stirred to homogeneity and equilibrated at about 4 degrees Celsius for 24 hours. During this period, the CMC and any other components can be hydrated and a hydrogel can be formed. The hydrogel can be degassed in a vacuum for about an hour and centrifuged at about 20,000 g for an hour to remove residual micro-sized air bubbles that might interfere with a spincasting/drying process of the CMC-microneedle arrays. The dry matter content of the hydrogel can be tested by drying a fraction (lOg) of it at 85 degrees Celsius for about 72 hours. The ready-to-use CMC-hydrogel is desirably stored at about 4 degrees Celsius until use.

Active components can be incorporated in a hydrogel of CMC at a relatively high (20-30%) CMC-dry biologies weight ratio before the spin-casting process. Arrays can be spin-cast at room temperature, making the process compatible with the functional stability of a structurally broad range of bioactive components. Since the master and production molds can be reusable for a large number of fabrication cycles, the fabrication costs can be greatly reduced. The resulting dehydrated CMC-microneedle arrays are generally stable at room temperature or slightly lower temperatures (such as about 4 degrees Celsius), and preserve the activity of the incorporated biologies, facilitating easy, low cost storage and distribution.

In an exemplary embodiment, the surface of the production molds can be covered with about 50 μï (for molds with 11 mm diameter) of CMC-hydrogel and spin-casted by centrifugation at 2,500 g for about 5 minutes. After the initial CMC-hydrogel layer, another 50 μï CMC-hydrogel can be layered over the mold and centrifuged for about 4 hours at 2,500 g. At the end of a drying process, the CMC-microneedle arrays can be separated from the molds, trimmed off from excess material at the edges, collected and stored at about 4 degrees Celsuis. The production molds can be cleaned and reused for further casting of microneedle arrays.

In some embodiments, CMC-solids can be formed with layers that do not contain active components and layers that contain active components. FIGS. 11A-D illustrate CMC-solids with different shapes (FIG. 11A and 1IB) and embedded active cargos on an upper layer which becomes, after micromilling, the portions of the microneedle with the active components. FIG. llC illustrates micron sized fluorescent particles layered on a surface of a non-active component containing layer and FIG. 1ID illustrates toluidine blue examples layered on a surface of a non-active component containing layer.

FIGS. 12A and 12B also illustrate CMC-solids with different shapes, with FIG. 12B showing a square shape and FIG. 12B showing a rectangular shape. Both CMC solids can be

milled to dimensions for further processing as described herein. It should be understood that the geometries and the active cargo shown herein are not intended to be limited to the exemplary embodiments.

Example 2

CMC-solids can be prepared with defined geometry and active cargo contents in one or more layers of the prepared structure. Examples of active cargos integrated into CMC-solids are described more detail herein. Upon construction of the CMC-solids with embedded active cargo contained in at least one layer of the CMC-solid, the CMC solids can be milled to project-specific dimensions and micro-milled to fabricate microneedle devices as described herein.

Example 3

In another embodiment, one or more layers of active cargo can be embedded on CMC-solids for direct micromilling of the microneedle array. FIG. 13 illustrates a sample representation of vertical multi-layered deposition and CMC embedding of active cargos on CMC-solids for direct micro-milling of MNA devices.

In one exemplary method, microneedle arrays can be fabricated by preparing CMC-solids with a defined geometries and without any active cargo contained therein. Then, blank CMC-solids can be milled to a desired dimension.

As shown in FIG. 13, active cargo(s) can be deposited onto the CMC-solid in project specific geometric patterns for inclusion of the active cargo(s) specifically in the tips of micro-milled MNA devices.

The methods active cargo deposition onto the CMC-solid blank can include, for example:

1) Direct printing with micro-nozzle aided droplet deposition.
2) Transfer from preprinted matrices.
3) Droplet-deposition with computer controlled robotic systems.

FIG. 14 illustrates layering and spatial distribution of embedded active cargos in a CMC-solid block. After the first layer is deposited (A) it can be covered with a CMC layer (B) that provides the surface for the subsequent deposition of the active cargo (C). The process can be repeated until all desired layers are deposited and encased in a solid CMC-block suitable for the micro-milling process (D-F).

FIG. 15 illustrates a schematic view of a cross-section of a CMC-block encasing the deposits of the active cargo in a spatially controlled manner (A). The method allows 3-dimensional control and placement of the active components after micro-milling in the MNA-device (B). In panel (B) of FIG. 15, the placement of the active cargos are shown in the stems of the active cargo; however through the control of the milling process the placement can be controlled vertically from

the tip to the base of the microneedles. Colors represent different active components or different amount/concentration of the same material.

Thus, a method of vertically layered deposition of active cargos in microneedles is provided by depositing one or more active cargos sequentially on the surface of the CMC-solids in contact with each other or separated by layers of CMC. In some embodiments, horizontal pattern deposition of the active cargos can result in spatial separation of the cargos. By combining vertical and horizontal patterning of active cargo deposition, 3 dimensional delivery and distribution of each of the defined active components can be achieved, further reducing waste of active components during fabrication of microneedle arrays.

Microneedle Integrated Adenovectors

The following embodiments are directed to dissolvable microneedle arrays, such as those described herein, that incorporate infectious viral vectors into the dissolvable matrix of microneedle arrays. Using this technology, for the first time, living viral vectors can be incorporated into microneedle arrays. As described herein, the incorporation of viral vectors within the disclosed microneedle arrays stabilizes the viral vectors so that they maintain their infectivity after incorporation and after prolonged periods of storage. The application of microneedle array incorporated adenovectors (MIAs) to the skin results in transfection of skin cells. In a vaccine setting, we have demonstrated that skin application of MIAs encoding an HIV antigen results in potent HIV specific immune responses. These results are described in detail in the examples below.

Example 4

The microneedle integrated adenovectors preparation method described herein preserves the viability of the adenoviral particles during the preparation and in dry storage. These steps were specifically designed based on the physical and chemical properties of CMC microneedle arrays. Viral viability in CMC microneedle arrays was achieved by

- Inclusion of low viscosity carboxymethyl cellulose (CMC90) at 2.5% final concentration (step 2.) and by
- Timed and temperature controlled spin-drying concentration of the adenoviral particles in the tips of the microneedle array devices (step 6.).
- Controlled partial rehydration of the needle-tip loaded adenoviral particles (step 8.)

Preparation of Tip-loaded Microneedle Integrated Adenovectors (MIAs):

1) Resuspend adenoviral particles at 2x109 particles/ml density in Trehalose-storage buffer (5% trehalose Sigma-Aldrich USA, 20 mM Tris pH7.8, 75 mM NaCl, 2 mM MgC12, 0.025 % Tween 80)

2) Mix resuspended viral stock with equal volume of 5% CMC90 prepared in Trehasole-storage buffer, resulting in a 1x109 particles/ml density adenoviral working stock.

3) Add adenoviral working stock suspension to the surface of microneedle array production molds (as described in detail in other embodiments herein) at 40 µï per cm2 surface area.

4) The molds are centrifuged at 4500 rpm for 10 minutes at 22 °C to fill the needle tips with adenoviral working stock.

5) The excess viral stock is removed and the surface of the molds washed with 100 µï (phosphate buffer saline (PBS) solution per cm2 mold-surface area.

6) The microneedle array-molds containing the adenoviral stock solution only in the needle's cavity are partially spin-dried at 3500 rpm for 10 minutes at 22 °C.

7) 100 µï 20% structural, non-cargo containing CMC90 hydrogel in H20 added to the surface microneedle array-molds' per cm2 mold-area to form the structure of the MIA device.

8) Centrifuge at 4500 rpm for 10 min at 22 °C to fill up the needle cavities with 20 % CMC90 and allow 30 min incubation for the rehydration of the adenoviral particles dried in the tips (step 3-6, above).

9) By centrifugation spin-dry the MIA devices to less than 5% moisture content at 3500 rpm for 3 hours at 22 °C with 10 L/min constant air flow through the centrifuge chamber.

10) De-mold the dried MIA devices for storage at 4 °C or -80 °C.

Example 5

We have evaluated the potency and stability MNA incorporated recombinant adenoviral particles. Ad5.EGFP was incorporated into CMC hydrogel MNAs to fabricate a final product that contained 1010 virus particles/MNA. Control blank MNAs were prepared identically but without the virus. Batches of Ad5.EGFP and control MNAs were stored at RT, 4 °C and at -86 °C and viral stability was evaluated in infectious assays. Specific transduction activity of the MNA incorporated Ad5.EGFP virus was assessed in vitro using 293T cells. Cells were plated at 2 xl06/ well in six well plates and transduced in duplicate with diluted virus suspension, suspension + empty MNA (control), or Ad5.EGFP MNAs stored at RT, 4 °C and -86 °C for the indicated time periods. As a negative control untransduced wells were included. Initially cell populations were analyzed after 24h by flow cytometry for GFP expression (representative histogram is shown in FIG. 35.).

As shown in FIG. 35, the incorporation of Ad5.EGFP into MNAs does not reduce transduction efficiency. Flow cytometry analysis of GFP expressing target 293T cells 24h after transduction with identical titers of Ad5.EGFP either in suspension or incorporated into CMC-patches vs. untransfected control cells. FIG. 36 shows the stability of MNA embedded Ad5.EGFP

virus. GFP gene expression was assayed by flow cytometry as in FIG. 37 and normalized to the infection efficiency of -86 °C preserved Ad5.EGFP suspension.

It has been found that the infection efficiency using MNA Ad5.EGFP virus was 87.92 ±4.5%, which is similar to that observed for traditional -86 °C preserved Ad5.EGFP suspension (FIGS. 35 and 36), suggesting that the manufacturing process does not adversely affect the transduction efficiency of Ad-EGFP viral particles. To asses infectivity over time, the transfection efficiency of freshly prepared -86 °C preserved Ad5.EGFP suspensions was compared to that of MNA incorporated Ad5.EGFP stored for prolonged periods of time at either RT, 4C, or -86C. Infectivity (normalized to Ad5.EGFP suspension + empty CMC-patch) is reported for storage periods of up to 365 days (FIG. 36). These results suggest that the infectiousness of MNA Ad5.EGFP is remarkably stable with storage at either 4C or -86C, and somewhat stable at RT for up to 30 days.

These results demonstrate that microneedle array delivered Ad transgenes are expressed in the skin and induce potent cellular immune responses. To specifically evaluate gene expression in vivo, we determined GFP expression in skin following either traditional intradermal injection (I.D.) or microneedle array-mediated intracutaneous delivery. We delivered 108 Ad5.GFP viral particles by ID injection or topically via a single microneedle array application (FIG. 37). Skin was harvested 48h later, cryosectioned, counter-stained using blue fluorescent DAPI to identify cell nuclei, and then imaged by fluorescent microscopy. Significant cellular GFP expression was observed following both I.D. and microneedle array delivery. To evaluate immunogenicity, we evaluated antigen-specific lytic activity in vivo following a single I.D. or microneedle array immunization without boosting. For this purpose we immunized groups of mice with El/E3-deleted Ad5-based vectors that encode codon-optimized SIVmac239 gag full-length or SIVmac239 gag pl7 antigens (Ad5.SIV gag, Ad5.SIV gag pl7). Empty vector was used as a control (Ad5). We observed potent and similar levels of in vivo lytic activity specific for the dominant SIVgag pl7-derived peptide KSLYNTVCV (SIVmac239 gag 76-84) following either I.D. or microneedle array immunization with either Ad5.SIV gag or Ad5.SIV gag pl7 (FIG. 37, CTL).

The microneedle array technology disclosed herein can also facilitate clinical gene therapy. It addresses, for example, at least two major limitations of conventional approaches. First, it enables stabilization and storage of recombinant viral vectors for prolonged periods of time. By rendering live virus vectors resistant to high and low temperatures with proven seroequivalence to frozen liquid formulations, microneedle array stabilization will relieve pressures related to the 'cold chain.' Further, integration in microneedle arrays enables precise, consistent and reproducible dosing of viral vectors not achievable by conventional methods. Finally, the viral vector is

repackaged in the only necessary delivery device, the biocompatible and completely disposable microneedle array that directs delivery precisely to the superficial layers of the skin.

Such a gene delivery platform is useful in providing patient-friendly, clinical gene therapy. Since these microneedle arrays have been engineered to not penetrate to the depth of vascular or neural structures, gene delivery to human skin will be both painless and bloodless. In addition, the fabrication process is flexible, enabling simple and rapid low cost production with efficient scale-up potential. Also, as a final product, the MIA device it is stable at room temperature and is inexpensive to transport and store. In combination, these structural and manufacturing advantages can enable broad and rapid clinical deployment, making this gene delivery technology readily applicable to the prevention and/or treatment of a broad range of human diseases. Moreover, this approach can be extended to other vector-based vaccine platforms that are currently restricted by the same limitations (e.g., vaccinia virus, AAV etc.). For at least these reasons, the disclosed microneedle arrays and methods of using the same significantly advance the recombinant gene therapy field.

Microneedle Arrays - Exemplary Active Components

Various active components are described in detail below. For convenience, the following examples are based on an microneedle array which is 6.3 x 6.3 mm. This size, and hence cargo delivery can be varied by increasing or decreasing 2-100 fold.

General considerations for the maximum active cargo quantities include, for example, total needle volume in the array and solubility of the active component(s) in the solvent (generally expected to be <50%).

Tip Loaded Components:	Amount Tip Loaded into MNA device µg/device (unless indicated differently)	Max. predicted loading capacity
	Live viruses(1)	
Ad5.GFP (adeno viral GFP expression vector)	$5x10^8$ particles/MNA	$2\text{-}5x10^9$ particles/MNA

Ad-SIVgag (adeno viral gag expression vector)	$5xl0^{8}$ particles/MNA	$2\text{-}5xl0^{9}$ particles/MNA
Ad-SIVpl7 (adeno viral gag-pl7 expression vector)	$5xl0^{8}$ particles/MNA	$2\text{-}5xl0^{9}$ particles/MNA
Ψ5 (non-recombinant Ad vector)	$5xl0^{8}$ particles/MNA	$2\text{-}5xl0^{9}$ particles/MNA
Lenti-GFP® (Lenti viral GFP expression vector)	$5xl0^{6}$ particles/MNA	$2\text{-}5xl0^{7}$ particles/MNA

Vaccinia virus (immunization)

Recombinant vaccinia virus (gene therapy, genetic engineering)

Seasonal influenza

MMR (Measles, Mumps, Rubella)

Proteins/Peptides

BSA (FITC labeled)	240	400
OVA (FITC labeled)	100	400
OVA (no label)	240	400
Flu (split vaccine)	0.22	(2-5)

Epitope Peptides®

TRP-2	50	200
EphA2 (a)	50	400
EphA2 (b)	50	400
DLK-1	50	200
Multiple epitopes in one MNA	200	400-600
Substance-P	15	

(NK-1R ligand)

Nucleic acids		
CpG 1668	120	250
CpG 2006	120	250
Poly(I:C)	250	250
Plasmid vectors (High mol. weight DNA)	100	200
Peptides/Nucleic acid combos		
OVA/CpG		250/120
OVA/CpG/poly(I:C)		250/120/250
Epitope peptides/poly(I:C)		200/250
Organics		
Doxorubicin	1-1000 μg	
R848 (**TLR7/8** ligand)	6	
L733 (NK-1 antagonist)	2	
DNCB (irritant)	100	
Particulates		
Micro-particles (1 μ diameter microsphares)	lxlO^6 particles/MNA	2-5xl0^7 particles/MNA
Nano scale particles		
PLG/PLA based		

Other Biologic	
tumor lysate/CpG	250/120
tumor lysate/CpG/poly(I:C)	250/120/250
tumor lysates/poly(I:C)	200/250

Tip-loading of live adenoviruses generally includes the following modifications:

a) The presence of 5% trehalose and 2.5% CMC90 in the tip-loading hydrogel suspension.

b) The temperature of the process is maintained at 22 °C.

In addition, Lenti viral vectors generally require 4 °C processing and vapor trap based humidity controls. Also, short epitope peptides generally are solubilized in DMSO, with the evaporation time of the solvent during tip-loading is 4 hours.

Microneedle Structures and Shapes

For each of the embodiments below, it should be understood that one or more layers of active components can be provided in the microneedles of the microneedle arrays as described above. Thus, for example, in some embodiments, active components are only provided in the area of the microneedle—not in the structural support of the array, such as shown in FIG. 15. Moreover, in other embodiments, the active components are concentrated in the upper half of the microneedles, such as in the tips of the microneedles as shown in FIGS. 3A-4B.

FIGS. 16A and 16B are SEM images of a CMC-microneedle array formed with a plurality of pyramidal projections *(i.e.,* microneedles). The average tip diameter of the pyramidal needles shown in FIG. 16A is about 5-10 μιη. As shown in FIG. 16B, the sides of the pyramidal needles can be formed with curved and/or arcuate faces that can facilitate insertion in skin.

FIG 17 is another SEM image of a single needle of a microneedle array. The microneedle shown in FIG. 17 is a base-extended pillar type molded CMC-microneedle. The base-extended pillar type microneedle comprises a base portion, which is generally polyagonal (for example, rectangular) in cross section, and a projecting portion that extends from the base portion. The projecting portion has a lower portion that is substantially rectangular and tip portion that generally tapers to a point. The tip portion is generally pyramidal in shape, and the exposed faces of the pyramid can be either flat or arcuate. The projecting portion can be half or more the entire length of the needle.

FIGS. 18 and 19 illustrate micrographs of pyramidal (FIG. 18) and pillar type (FIG. 19) molded CMC-microneedles. Because the pyramidal needles have a continually increasing cross-sectional profile (dimension) from the needle point to the needle base, as the needle enters the skin,

the force required to continue pushing the pyramidal needle into the skin increases. In contrast, pillar type needles have a generally continuous cross-sectional profile (dimension) once the generally rectangular portion of the projection portion is reached. Thus, pillar type needles can be preferable over pyramidal type needles because they can allow for the introduction of the needle into the skin with less force.

FIG. 20 illustrates schematic representation of microneedle shapes and structures that are generally suitable for fabrication by spin-casting material into a mastermold formed by micromilling. Since the shapes and structures shown in FIG. 20 do not contain any undercuts, they generally will not interfere with the molding/de-molding process. The structures in FIG. 20 include (a) a generally pyramidal microneedle, (b) a "sharp" pillar type microneedle (without the base member of FIG. 8), (c) a "wide" pillar type microneedle, (d) a "short" pillar type microneedle (having a short pillar section and a longer pointed section), and (e) a "filleted" pillar type microneedle.

While the volume of the pyramidal microneedles can be greater than that of the pillar type microneedles, their increasing cross-sectional profile (dimension) requires an increasing insertion force. Accordingly, the geometry of the pyramidal microneedles can result in reduced insertion depths and a reduced effective delivery volume. On the other hand, the smaller cross-sectional area and larger aspect ratio of the pillar microneedles may cause the failure force limit to be lower. The smaller the apex angle a, the "sharper" the tip of the microneedle. However, by making the apex angle too small *(e.g.* , below about 30 degrees), the resulting microneedle volume and mechanical strength may be reduced to an undesirable level.

The penetration force of a microneedle is inversely proportional to the microneedle sharpness, which is characterized not only by the included (apex) angle of the microneedles, but also by the radius of the microneedle tip. While the apex angle is prescribed by the mastermold geometry, the tip sharpness also depends on the reliability of the mold. Micromilling of mastermolds as described herein allows for increased accuracy in mold geometry which, in turn, results in an increased accuracy and reliability in the resulting production mold and the microneedle array formed by the production mold.

The increased accuracy of micromilling permits more accurate and detailed elements to be included in the mold design. For example, as discussed in the next section below, the formation of a fillet at the base of a pillar type microneedle can significantly increase the structural integrity of the microneedle, which reduces the likelihood that the microneedle will fail or break when it impacts the skin. While these fillets can significantly increase the strength of the microneedles, they do not interfere with the functional requirements of the microneedles *(e.g.* , penetration depth

and biologies volume). Such fillets are very small features that can be difficult to create in a master mold formed by conventional techniques. However, the micromilling techniques described above permit the inclusion of such small features with little or no difficulty.

Mechanical Integrity and Penetration Capabilities

Microneedle arrays are preferably configured to penetrate the stratum corneum to deliver their cargo *(e.g.,* biologies or bioactive components) to the epidermis and/or dermis, while minimizing pain and bleeding by preventing penetration to deeper layers that may contain nerve endings and vessels. To assess the mechanical viability of the fabricated microneedle arrays, tests were performed on the pyramidal and pillar type microneedle arrays as representative variants of array geometry (shown, *e.g.,* in FIGS. 7B and 8). The first set of tests illustrate the failure limit of microneedles, and include pressing the microneedle array against a solid acrylic surface with a constant approach speed, while simultaneously measuring the force and the displacement until failure occurs. The second set of tests illustrate the piercing capability of the microneedles on human skin explants.

Figure 21 illustrates a test apparatus designed for functional testing. The sample *(i.e.,* microneedle array) was attached to a fixture, which was advanced toward a stationary acrylic artifact (PMMA surface) at a constant speed of about 10 mm/s speed using a computer-controlled motion stage (ES 14283-52 Aerotech, Inc.). A tri-axial dynamometer (9256C1, Kistler, Inc.) that hosted the acrylic artifact enabled high-sensitivity measurement of the forces.

FIG. 22 illustrates force-displacement curves of data measured during failure tests. The curve on the left is representative of data obtained from testing a pillar microneedle sample and the curve on the right is representative of data obtained from testing a pyramid microneedle. As seen in FIG. 22, the failure of these two kinds of microneedles are significantly different; while the pyramidal arrays plastically deform (bend), the pillar type arrays exhibit breakage of the pillars at their base. This different failure behavior lends itself to considerably different displacement-force data. The failure (breakage) event can be easily identified from the displacement-force data as indicated in the figure. Based on the obtained data, the failure point of pillar type microneedles was seen to be 100 mN in average. As only about 40 mN of force is required for penetration through the stratum corneum, the microneedles are strong enough to penetrate human skin without failure. Furthermore, since parallelism between microneedle tips and the acrylic artifact cannot be established perfectly, the actual failure limit will likely be significantly higher than 100 mN *(i.e.,* microneedles broke in a successive manner, rather than simultaneous breakage of most/all microneedles).

The pyramidal microneedles presented a continuously increasing force signature with no clear indication of point of failure. To identify the failure limit for the pyramidal microneedles, interrupted tests were conducted in which the microneedles were advanced into the artifact by a certain amount, and retreated and examined through optical microscope images. This process was continued until failure was observed. For this purpose, the failure was defined as the bending of the pyramidal microneedles beyond 15 degrees.

To further analyze the failure of the microneedles, the finite-elements model (FEM) of the microneedle arrays shown in FIG. 23 was developed. To obtain the mechanical properties (elastic modulus and strength limit) of the CMC material, a series of nanoindentation tests (using a Hysitron nanoindentor). The average elastic modulus and yield strength of the CMC material (as prepared) were 10.8 GPa and 173 MPa, respectively. This indicates that the prepared CMC material has a higher elastic modulus and yield strength than both PMMA (elastic modulus: 3.1 GPa, yield strength: 103 MPa) and polycarbonate (elastic modulus: 2.2 GPa, yield strength: 75 MPa), indicating the superior strength and stiffness of CMC material with respect to other polymers.

Using this data, a series of FEM simulations were conducted. It was predicted from the FEM models that failure limit of pyramidal and sharp-pillar (width=134 um) microneedles with 600 μιη height, 30 degree apex angle, and 20 μιη fillet radius were 400 mN (pyramid) and 290 mN (sharp-pillar) for asymmetric loading (5 degrees loading misorientation). Considering that the minimum piercing force requirement is about 40 mN, pyramid and sharp-pillar microneedles would have factors of safety of about 10 and 7.25, respectively.

When the fillet radius is doubled to 40 μιη, the failure load for the pillar was increased to 350 mN, and when the fillet radius is reduced to 5 μιη, the failure load was reduced to 160 mN, which is close to the experimentally determined failure load. The height and width of the pillars had a significant effect on failure load. For instance, for 100 μιη width pillars, increasing the height from 500 μιη to 1000 μιη reduced the failure load from 230 mN to 150 mN. When the width is reduced to 75 μιη, for a 750 μιη high pillar, the failure load was seen to be 87 mN.

To evaluate penetration capability, pyramidal and sharp-pillar microneedle arrays were tested for piercing on water-based model elastic substrates and on full thickness human skin. FIG. 24 illustrates stereo micrographs of pyramidal (Panels A, C, and E) and pillar type microneedle arrays (B, D, and F) after 4 minutes of exposure to model elastics. In particular, toluene blue tracer dye was deposited in model elastic substrates (Panels C and D) or freshly excised full thickness human skin explants (Panels E and F) after application of pyramidal or pillar type microneedle arrays.

The model elastic substrate comprised about 10 % CMC and about 10 % porcine gelatin in PBS gelled at about 4 degrees Celsius for about 24 hours or longer. The surface of the elastics was covered with about 100 μιη thick parafilm to prevent the immediate contact of the needle-tips and the patch materials with the water based model elastics. To enable stereo microscopic-imaging, trypan blue tracer dye (Sigma Chem., cat # T6146) was incorporated into the CMC-hydrogel at 0.1 % concentration. The patches were applied using a spring-loaded applicator and analyzed after about a 4 minute exposure. Based on physical observation of the dye in the target substrates, the dissolution of the microneedles of the two different geometries was markedly different.

The sharp-pillar needles applied to the model elastic substrate released substantially more tracer dye to the gel matrix than that observed for the pyramidal design (FIG. 24, C vs. D). Images of the recovered patches (FIG. 24, A vs. B) were consistent with this observation, as the degradation of the sharp-pillar needles was more advanced than that of the pyramidal needles. To extrapolate this analysis to a more clinically relevant model, pyramidal and pillar type microneedle arrays were applied to freshly excised full thickness human skin explants using the same force from the spring loaded applicator. Consistent with results from the elastic model, the pyramidal microneedle arrays deposited visibly less tracer dye than the sharp-pillar microneedle arrays (FIG. 24, E vs. F).

To further evaluate penetration and to assess delivery effectiveness to human skin, CMC-microneedle arrays were fabricated with BioMag (Polysciences, Inc., cat#. 84100) beads or fluorescent particulate tracers (Fluoresbrite YG Ιμιη, Polysciences Inc., cat#. 15702). The pyramidal CMC-microneedle arrays containing fluorescent or solid particulates were applied to living human skin explants as described previously. Five minutes after the application, surface residues were removed and skin samples were cryo-sectioned and then counterstained with toluene blue for imaging by light microscopy (FIGS. 25A and 25B) or by fluorescent microscopy (FIG. 25C).

Pyramidal CMC-microneedles effectively penetrated the stratum corneum, epidermis, and dermis of living human skin explants, as evidenced by the deposition of Biomag beads lining penetration cavities corresponding to individual needle insertion points (representative sections shown in FIGS 25A and 25B). In particular, ordered cavities (FIG. 25A, cavities numbered 1-4, toluene blue counterstain, lOx) and deposits of BioMag particles (brown) lining penetration cavities were evident (FIG. 25B, 40x), indicating microneedle penetrated of human skin. Further, analysis of sections from living human explants stained with DAPI to identify cell nuclei and anti-HLA-DR to identify MHC class 11+ antigen presenting cells revealed high density fluorescent particulates deposited in the superficial epidermis and dermis, including several particles co-localized with class

11+ antigen presenting cells (FIG. 25C, DAPI (blue), HLA-DR+ (red) and fluorescent particles (green), 40x).

These results further demonstrate that the CMC microneedle arrays described herein can effectively penetrate human skin and deliver integral cargo (bioactive components), including insoluble particulates. They are consistent with effective delivery of particulate antigens to antigen presenting cells in human skin, currently a major goal of rational vaccine design.

To further address microneedle array delivery *in vivo*, the cutaneous delivery of particulate antigen *in vivo* was modeled by similarly applying fluorescent particle containing arrays to the dorsal aspect of the ears of anesthetized mice. After 5 minutes, patches were removed and mice resumed their normal activity. Three hours or 3 days, ear skin and draining lymph nodes were analyzed for the presence of fluorescent particles. Consistent with observations of human skin, particulates were evident in the skin excised from the array application site (data not shown). Further, at the 3 day time point, substantial numbers of particles were evident in the draining lymph nodes . FIGS. *26A* and 26B illustrates substantial numbers of particles that were evident in the draining lymph Nodes (FIG 26A, lOx), including clusters of particulates closely associated with Class 11+ cells (FIG. 26B, 60x) suggesting the presence of lymph node resident antigen presenting cells with internalized particulates.

To quantitatively evaluate the effects of needle geometry on cargo delivery using microneedle arrays, 3H-tracer labeled CMC-microneedle arrays were constructed. The CMC-hydrogel was prepared with 5% wt ovalbumin as a model active component at 25 wt % final dry weight content (5g/95g OVA/CMC) and trace labeled with 0.1 wt % trypan blue and 0.5x106 dpm/mg dry weight 3H-tracer in the form of 3H-thymidine (ICN Inc., cat # 2406005). From a single batch of labeled CMC-hydrogel-preparation four batches of 3H-CMC-microneedle arrays were fabricated, containing several individual patches of pyramidal and sharp-pillar needle geometry. The patches were applied to human skin explants as described above and removed after 30 min exposure. The patch-treated area was tape-striped to remove surface debris and cut using a 10 mm biopsy punch. The 3H content of the excised human skin explants-discs was determined by scintillation counting. The specific activity of the 3H-CMC-microneedle patch-material was determined and calculated to be 72,372 cpm/mg dry weight. This specific activity was used to indirectly determine the amount of ovalbumin delivered to and retained in the skin. The resulting data is summarized in Table 1 below.

The tested types of patches were consistent from microneedle array to microneedle array (average standard deviation 24-35 %) and batch to batch (average standard deviation 7-19 %). The intra-batch variability for both needle geometry was lower than the in-batch value indicating that

the insertion process and the characteristics of the target likely plays a primary role in the successful transdermal material delivery and retention. The patch-material retention data clearly demonstrate the foremost importance of the microneedle geometry in transdermal cargo delivery. Pillar- type needle geometry afforded an overall 3.89 fold greater deposition of the 3H labeled needle material than that of the pyramidal needles. On the basis of the deposited radioactive material, it is estimated that the pyramidal needles were inserted about 200 μιη deep while the pillar-type were inserted about 400 μιη or more.

Table 5. Transfer of ^{3}H-labeled CMC-micro needle material *into* human skin explants by pyramidal and pillar -type needles.

Array Batches	Pyramid Needles (cpm/patch)	STDev (%)	Pyramidal Needles OVA Transferred (μg/patch)	Pillar-Type Needles (cpm/patch)	%TDev (%)	Pillar-Type Needles OVA Transferred (μg /patch)	Pillar to Pyramid Ratio
Batch A	2453.00	17.56	1.75	11733.55	31.52	5.55	4.78
Batch B	3273.50	57.39	2.26	12815.50	21.45	5.35	3.92
Batch C	2757.75	48.14	1.55	12245.50	26.71	6.46	4.44
Batch D	3782.00	33.27	2.61	9521.50	7.32	7.58	2.52
Intra-Batch AVG	3068.06	13.86	2.12	11913.53	6.77	6.21	3.55

Desirably, the microneedle arrays described herein can be used for cutaneous immunization. The development of strategies for effective delivery of antigens and adjuvants is a major goal of vaccine design, and immunization strategies targeting cutaneous dendritic cells have various advantages over traditional vaccines.

The microneedle arrays described herein can also be effective in chemotherapy and immunochemotherapy applications. Effective and specific delivery of chemotherapeutic agents to tumors, including skin tumors is a major goal of modern tumor therapy. However, systemic delivery of chemotherapeutic agents is limited by multiple well-established toxicities. In the case of cutaneous tumors, including skin derived tumors (such as basal cell, squamous cell, Merkel cell, and melanomas) and tumors metastatic to skin (such as breast cancer, melanoma), topical delivery can be effective. Current methods of topical delivery generally require the application of creams or repeated local injections. The effectiveness of these approaches is currently limited by limited penetration of active agents into the skin, non-specificity, and unwanted side effects.

The microneedle arrays of the present disclosure can be used as an alternative to or in addition to traditional topical chemotherapy approaches. The microneedle arrays of the present disclosure can penetrate the outer layers of the skin and effectively deliver the active biologic to living cells in the dermis and epidermis. Delivery of a chemotherapeutic agents results in the apoptosis and death of skin cells.

Further, multiple bioactive agents can be delivered in a single microneedle array (patch). This enables an immunochemotherapeutic approach based on the co-delivery of a cytotoxic agent

with and immune stimulant (adjuvants). In an immunogenic environment created by the adjuvant, tumor antigens releases from dying tumor cells will be presented to the immune system, inducing a local and systemic anti-tumor immune response capable of rejecting tumor cells at the site of the treatment and throughout the body.

In an exemplary embodiment, the delivery of a biologically active small molecule was studied. In particular, the activity of the chemotherapeutic agent Cytoxan® delivered to the skin with CMC microneedle arrays was studied. The use of Cytoxan® enables direct measurement of biologic activity (Cytoxan® induced apoptosis in the skin) with a representative of a class of agents with potential clinical utility for the localized treatment of a range of cutaneous malignancies.

To directly evaluate the immunogenicity of CMC microneedle array incorporated antigens, the well characterized model antigen ovalbumin was used. Pyramidal arrays were fabricated incorporating either soluble ovalbumin (sOVA), particulate ovalbumin (pOVA), or arrays containing both pOVA along with CpGs. The adjuvant effects of CpGs are well characterized in animal models, and their adjuvanticity in humans is currently being evaluated in clinical trials.

Immunization was achieved by applying antigen containing CMC-microneedle arrays to the ears of anesthetized mice using a spring-loaded applicator as described above, followed by removal of the arrays 5 minutes after application. These pyramidal microneedle arrays contained about 5 wt% OVA in CMC and about 0.075 wt % (20 μM) CpG. As a positive control, gene gun based genetic immunization strategy using plasmid DNA encoding OVA was used. Gene gun immunization is among the most potent and reproducible methods for the induction of CTL mediated immune responses in murine models, suggesting its use as a "gold standard" for comparison in these assays.

Mice were immunized, boosted one week later, and then assayed for OVA-specific CTL activity in vivo. Notably, immunization with arrays containing small quantities of OVA and CpG induced high levels of CTL activity, similar to those observed by gene gun immunization (FIG. 27). Significant OVA-specific CTL activity was elicited even in the absence of adjuvant, both with particulate and soluble array delivered OVA antigen. It is well established that similar responses require substantially higher doses of antigen when delivered by traditional needle injection.

To evaluate the stability of fabricated arrays, batches of arrays were fabricated, stored, and then used over an extended period of time. As shown in FIG. 28, no significant deterioration of immunogenicity was observed over storage periods spanning up to 80 days (longest time point evaluated). Thus, the CMC microneedle arrays and this delivery technology can enable effective cutaneous delivery of antigen and adjuvants to elicit antigen specific immunity.

To evaluate the delivery of a biologically active small molecule, pyramidal CMC-microneedle arrays were fabricated with the low molecular weight chemotherapeutic agent Cytoxan® (cyclophosphamide), or with FluoresBrite green fluorescent particles as a control. Cytoxan® was integrated at a concentration of 5 mg/g of CMC, enabling delivery of approximately about 140 µg per array. This is a therapeutically relevant concentration based on the area of skin targeted, yet well below levels associated with systemic toxicities. Living human skin organ cultures were used to assess the cytotoxicty of Cytoxan®. Cytoxan® was delivered by application of arrays to skin explants as we previously described. Arrays and residual material were removed 5 minutes after application, and after 72 hours of exposure, culture living skin explants were cryo-sectioned and fixed. Apoptosis was evaluated using green fluorescent TUNEL assay (In Situ Cell Death Detection Kit, TMR Green, Roche, cat#: 11-684-795-910). Fluorescent microscopic image analysis of the human skin sections revealed extensive apoptosis of epidermal cells in Cytoxan® treated skin as shown in FIG. 29A. As shown in FIG. 29B, no visible apoptosis was observed in fluorescent particle treated skin though these particles were evident, validating that the observed area was accurately targeted by the microneedle array.

Direct Fabricated Microneedle Arrays

The micromilling of mastermolds described above allows the production of microneedle arrays with a variety of geometries. In another embodiment, systems and methods are provided for fabricating a microneedle array by directly micromilling various materials, such as dried CMC sheets. The same general tooling that was described above with respect to the micromilling of mastermolds can be used to directly micromilling microneedle arrays.

Direct micromilling of microneedle arrays eliminates the need for molding steps and enables a simplified, scalable, and precisely reproducible production strategy that will be compatible with large scale clinical use. Moreover, direct fabrication of the microneedle arrays through micromilling enables greater control of microneedle geometries. For example, micromilling permits the inclusion of microneedle retaining features such as undercuts and/or bevels, which cannot be achieved using molding processes.

The reproducibility of direct milling of microneedle arrays is particular beneficial. That is, in direct micromilling all of the microneedles are identical as a result of the milling fabrication process. In molding operations, it is not uncommon for some needles to be missing or broken from a given patch as a result of the process of physically separating them from the molds. For use in certain medical applications, the reproducibility of the amount of bioactive components in the array is very important to provide an appropriate level of "quality control" over the process, since irregularities in the needles from patch to patch would likely result in variability in the dose of

drug/vaccine delivered. Of course, reproducibility will also be an important benefit to any application that requires FDA approval. Spincast/molded patches would require special processes to assure acceptable uniformity for consistent drug delivery. This quality control would also be likely to result in a certain percentage of the patches "failing" this release test, introducing waste into the production process. Direct micromilling eliminates or at least significantly reduces these potential problems.

Molding processes also have inherent limitations because of the need to be able to fill a well or concavity and remove the cured molded part from that well or concavity. That is because of mold geometries, undercuts must generally be avoided when molding parts or the part will not be removable from the mold. That is, a geometrical limitation of a molded part, such as a molded microneedle array, is that any feature located closer to the apex must be narrower than any feature located toward the base.

Accordingly, in view of these limitations, FIG. 20 illustrates schematic representation of microneedle shapes and structures that are generally suitable for fabrication by molding. That is, the shapes and structures shown in FIG. 20 do not contain any undercuts that would prevent the part (i.e., the microneedles) from being removed from a production mold. In contrast, FIG. 30 illustrates a beveled, undercut microneedle shape that cannot be molded in the manners described herein.

This geometry can only be created through direct fabrication using the proposed micromilling technology. The negative (bevel) angle facilitates better retention of the microneedles in the tissue. In addition, because the microneedle of FIG. 30 has a wider intermediate portion (with a larger cross-sectional dimension) above a lower portion (with a smaller cross-sectional dimension), a greater amount of the bioactive material can be delivered by configuring the microneedle to hold or store the bioactive material in the wider section, which is configured to be retained within the skin. Thus, the larger cross-sectional dimension of the intermediate portion can "carry" the bulk of the bioactive component. Since the lower portion tapers to a narrower cross-sectional dimension, the wider intermediate portion will obtain good penetration for delivery of the bioactive component into the skin layer. A portion above the intermediate portion desirably narrows to a point to facilitate entry of the microneedles into the skin layers.

Another limitation of molded parts is that it can be difficult to precisely fill a very small section of a mold. Since production molds for microneedle arrays comprise numerous very small sections, it can be difficult to accurately fill each well. This can be particularly problematic when the mold must be filled with different materials, such as a material that contains a bioactive component and a material that does not contain a bioactive component. Thus, if the production

mold is to be filled with layers, it can be difficult to accurately fill the tiny wells that are associated with each microneedle. Such reproducibility is particularly important, since the microneedles are intended to deliver one or more bioactive components. Thus, even slight variations in the amounts of bioactive component used to fill production molds can be very undesirable.

Also, by using a lamination structure to form a sheet or block that can be micromilled, various active components can be integrated into a single microneedle by vertical layering. For example, in an exemplary embodiment, CMC-hydrogel and CMC-sOVA-hydrogel (80% CMC/ 20 wt% OVA) were layered into the form of a sheet or block. This composite sheet can be micro-machined using the direct micromilling techniques described herein.

FIG. 31 is a stereo-microscopic image analysis of an entire microneedle array. The microneedle comprises a 10 x 10 array of microneedles. FIG. 32 is an enlarged segment of the microneedle array of FIG. 31. The layering of two components is shown in FIG. 32, which illustrates darker areas of the microneedles at tip portions and lighter areas of the microneedles at base portions. The darker layer at the tip represents the layer comprising a bioactive component, in this case soluble ovalbumin contained in a CMC layer.

Although the formation of a layer containing active material *(e.g. ,* antigen) and the subsequent micromilling of the layer (and any other adjacent layers) may require the use of relatively large amounts of the active material, the material can be removed *(e.g. ,* in the form of chips), recovered, and recycled. Direct machining technology is not restricted by the geometrical constraints arising from the molding/de-molding approach, and thus, is capable of creating more innovative needle designs *(e.g. ,* FIG. 30), which can significantly improve the retained needle-volume and needle retention time in the skin.

The production of sheets or blocks by forming a plurality of layers can provide a solid material that can be micro-machined and which can comprise one or more layers with a bioactive component. For example, a dissoluble solid carboxymethylcellulose polymer based block or sheet with well-defined and controlled dimensions can be fabricated by a lamination process. The resulting sheet or block can be fully machineable, similar to the machining of plastic or metal sheets or blocks. As described herein, the fabrication process can be suitable for the incorporation of bioactive components into the matrix without significantly reducing their activity levels.

As described below, a fabricated sheet of material (such as a CMC based material) can be directly micro-machined/micromilled) to produce one or more microneedle arrays suitable for delivering active ingredients through the skin. This dissoluble biocompatible CMC block-material can be used for the delivery of soluble or insoluble and particulate agents in a time release manner for body surface application.

The biocompatible material can be suitable for implants in deeper soft or hard tissue when dissolution of the scaffolding material is required and useful.

The following method can be used to prepare a carboxymethylcellulose (CMC) polymer low viscosity hydrogel to 12.5% concentration. The 12.5% carboxymethylcellulose (CMC) low viscosity hydrogel can be prepared in water or other biocompatible buffer, such as (but not limited to) PBS or HBS. During the preparation of the polymer solution, soluble agents (such as nucleic acid, peptides, proteins, lipids or other organic and inorganic biologically active components) and particulates can be added *(e.g.* ovalbumin, a soluble agent). Ferrous particulates carrying active ingredients at 20 w/w% of CMC can be used.

The preparation of 1000 g sterile 12.5% CMC hydrogel with no active component can be achieved as follows:

1) Measure 125 g CMC, add 875 g water or other water based solvent.

2) Stir to homogeneity in overhead mixer.

3) Autoclave homogenate to sterility at 121 degrees Celsius for 1 hour (the autoclaving step can reduce viscosity for improved layering)

4) Cool to 22 degrees Celsius.

5) Vacuum treat the resulting material at 10 torr and 22 degrees Celsius for 1 hour to remove trapped micro-bubbles.

6) Centrifuge product at 25,000g for 1 hour in vacuum chambered centrifuge (for floating and further removing residual micro bubbles).

7) Store the CMC-hydrogel product at 4 degrees Celsius.

The preparation of 1000 g sterile 12.5 w/w% dry content 20/80% ovalbumin/CMC hydrogel can be achieved as follows:

1) Measure 100 g CMC add 650 g water or other water based solvent.

2) Stir to homogeneity in overhead mixer.

3) Autoclave homogenate to sterility at 121 degrees Celsius for 1 hour (this autoclaving step can reduce viscosity for improved layering).

4) Cool to 22 degrees Celsius.

5a) Dissolve 25 g ovalbumin in 225 g water.

5b) Sterile filter ovalbumin solution on 0.22 μιη pore sized filter.

6) Mix to homogeneity, under sterile conditions the 750 g CMC hydrogel with 250 g sterile ovalbumin solution.

7) Vacuum treat the resulting material at 10 torr and 22 degrees Celsius for 1 hour to remove trapped micro-bubbles.

8) Centrifuge product at 25,000g for 1 hour in vacuum chambered centrifuge (for floating and further removing residual micro bubbles).

9) Store the CMC-hydrogel product at 4 degrees Celsius.

The preparation of 100 g sterile 12.5 w/w% dry content 20/80% particulate-ovalbumin/CMC hydrogel can be achieved as follows:

1) Measure 10 g CMC add 87.5 g water or other water based solvent.

2) Stir to homogeneity in overhead mixer.

3) Autoclave homogenate to sterility at 121 degrees Celsius for 1 hour (this autoclaving step can reduce viscosity for improved layering).

4) Cool to 22 degrees Celsius.

5) Disperse 2.5 g particulate-ovalbumin in the 97.5 g, 22 degrees Celsius CMC-hydrogel and mix to homogeneity, under sterile conditions.

6) Vacuum treat the resulting material at 10 torr and 22 degrees Celsius for 2 hour to remove trapped micro-bubbles.

7) Centrifuge product at 3,000g for 1 hour in vacuum chambered centrifuge (for floating and further removing residual micro bubbles).

8) Store the CMC-hydrogel product at 4 degrees Celsius.

Note in this example, particulate-ovalbumin is prepared from activated iron beads reaction to ovalbumin. However, it should be noted that the above descriptions are only exemplary embodiments and other compounds and active ingredients can be used.

A solid block/sheet carboxymethylcellulose (CMC) can be fabricated in the following manner using the low viscosity CMC-hydrogels described above.

The fabrication process can comprise a laminar spreading of the polymer at a defined thickness and a drying of the layered polymer to less than about 5% water content using sterile dried air flow over the surface of the polymer layer. The above two acts can repeated until the desired block thickness is achieved.

A method of performing a laminar CMC-hydrogel layering of a defined thickness over the casting mold assembly is described with reference to FIG. 33. FIG. 33 illustrates a cross-sectional view of the casting-mold assembly which includes: (a) casting bed; (b) adjustable casting bed wall; (c) casting-bed depth adjustment assembly; and (d) an acrylic spreader. It should be noted that FIG. 33 is not drawn to scale or otherwise shown with elements in their proper proportions.

The casting mold assembly can be constructed from acrylic (Plexiglas) and can comprise a casting bed base unit, a vertically adjustable hydrophobic casting-bed wall, and a casting-bed adjustment mechanism. The casting bed base unit (al) can include a removable/replaceable casting

bed top plate (a2) with an attached cellulose layer (a3). The cellulose layer can be about 0.5 mm in thickness. The vertically adjustable hydrophobic casting-bed wall (b) can be adjusted using the casting-bed depth adjustment mechanism, which can be comprised of lead-screw (c1) and level adjustment knob (c2). In the illustrated embodiment, a quarter turn of this knob can result in a 0.5 mm lift of the bed wall.

Initially, the adjustable casting bed wall can be set to height where the distance between the acrylic spreader and the cellulose layer of the bed is about 1 mm when the spreader is in position. A predefined volume *(e.g.,* about 0.1 ml/cm2) of the 12.5 % CMC-hydrogel can be added and layered. The layer can be evened or leveled by sliding the acrylic spreader (d) on the top surface of the adjustable casting wall to yield an even layer of about 1 mm of CMC-hydrogel. The layered CMC-hydrogel can be dried to a solid phase in the drying apparatus shown in FIG. 34 and described in more detail below.

The layering and drying steps can be repeated until the desired layered structure (sheet) is achieved. The casting bed wall can be raised by an appropriate amount during the addition of each layer. For example, after adding each layer, the bed wall can be raised or lifted by about 0.5 mm. Thus, the above-described cycle can deposit about 0.5 mm solid CMC layer. The process *(e.g.,* the layering of material, the raising of bed wall, *etc.)* can be repeated until the desired block thickness achieved.

The layered CMC-hydrogel polymer can be dried in various manners. For example, FIG. 34 illustrates a drying apparatus that can be used to dry the various deposited layers of the sheet material. It should be noted that FIG. 34 is not drawn to scale or otherwise shown with elements in their proper proportions. A fan can provide continuous gas flow *(e.g.,* air or other inert gas, such as nitrogen) over the CMC-hydrogel layered in the casting mold assembly. The gas flow will result in a gentle dehydration of the CMC-hydrogel layer. The drying speed can be adjusted to prevent or reduce gas enclosures *(e.g.,* air bubbles) in the solid CMC product. The humid air over the layer can be dried over desiccant *(e.g.,* an air dryer or dehumidifier), temperature adjusted, and returned over the hydrogel again by the speed-controlled fan. A hygrometer can be positioned on the humid side of the chamber to provide an indication of the status of the drying process. After a predetermined dryness has been achieved, as indicated by the hygrometer, the drying process can be ended.

Airflow can be adjusted to affect the drying speed. In the exemplary embodiment, the airflow is controlled to be between about 0.1-2.0 m/sec; the temperature is between ambient and about 50 degrees Celsius. Using these configurations, the drying time of a single layer CMC-hydrogel can be about 0.5-4 hours depend on the airflow and the set temperature.

The pure CMC based product can be transparent, light off white, or amber colored. Its specific gravity can be about 1.55-1.58 g/ml. The product is desirably free of micro-bubbles and otherwise suitable for fabricating micron scale objects. The physical characterization of the final block/sheet product (hardness, tensile strength, *etc.)* can vary, but should generally be able to resist physical stresses associated with micromilling.

As described above, the microneedle arrays disclosed herein are capable of providing reliable and accurate delivery methods for various bioactive components. The structural, manufacturing, and distribution advantages characteristic of the above-described microneedle arrays can be particularly applicable for use in delivering vaccines. Advantages of these microneedle arrays include (1) safety, obviating the use of needles or living vectors for vaccine delivery, (2) economy, due to inexpensive production, product stability, and ease of distribution, and 3) diversity, via a delivery platform compatible with diverse antigen and adjuvant formulations.

Moreover, cutaneous immunization by microneedle array has important advantages in immunogenicity. The skin is rich in readily accessible dendritic cells (DCs), and has long been regarded as a highly immunogenic target for vaccine delivery. These dendritic cell populations constitute the most powerful antigen presenting cells (APCs) identified thus far. For example, genetic immunization of skin results in transfection and activation of dendritic cells in murine and human skin, and these transfected dendritic cells synthesize transgenic antigens, migrate to skin draining lymph nodes, and efficiently present them through the MHC class I restricted pathway to stimulate CD8+ T-cells. The immune responses induced by skin derived DCs are remarkably potent and long-lasting compared to those induced by other immunization approaches. Recent clinical studies demonstrate that even conventional vaccines are significantly more potent when delivered intradermally, rather than by standard intramuscular needle injection. Thus, microneedle arrays can efficiently and simultaneously deliver both antigens and adjuvants, enabling both the targeting of DCs and adjuvant engineering of the immune response using the same delivery platform.

Cancer Therapy Applications

Bioactive components used with the microneedle arrays described herein can include one or more chemotherapeutic agents. Effective and specific delivery of chemotherapeutic agents to tumors, including skin tumors is a major goal of modern tumor therapy. However, systemic delivery of chemotherapeutic agents is limited by multiple well-established toxicities. In the case of cutaneous tumors, including skin derived tumors (such as basal cell, squamous cell, Merkel cell, and melanomas) and tumors metastatic to skin (such as breast cancer, melanoma), topical delivery can be effective. Current methods of topical delivery generally require the application of creams or

repeated local injections. The effectiveness of these approaches is currently limited by limited penetration of active agents into the skin, non-specificity, and unwanted side effects.

The microneedle arrays of the present disclosure can be used as an alternative to or in addition to traditional topical chemotherapy approaches. The microneedle arrays of the present disclosure can penetrate the outer layers of the skin and effectively deliver the active biologic to living cells in the dermis and epidermis. Delivery of a chemotherapeutic agents results in the apoptosis and death of skin cells.

Further, multiple bioactive agents can be delivered in a single microneedle array (patch). This enables an immunochemotherapeutic approach based on the co-delivery of a cytotoxic agent with and immune stimulant (adjuvants). In an immunogenic environment created by the adjuvant, tumor antigens releases from dying tumor cells will be presented to the immune system, inducing a local and systemic anti-tumor immune response capable of rejecting tumor cells at the site of the treatment and throughout the body.

In an exemplary embodiment, the delivery of a biologically active small molecule was studied. In particular, the activity of the chemotherapeutic agent Cytoxan® delivered to the skin with CMC microneedle arrays was studied. The use of Cytoxan® enables direct measurement of biologic activity (Cytoxan® induced apoptosis in the skin) with a representative of a class of agents with potential clinical utility for the localized treatment of a range of cutaneous malignancies.

To directly evaluate the immunogenicity of CMC microneedle array incorporated antigens, the well characterized model antigen ovalbumin was used. Pyramidal arrays were fabricated incorporating either soluble ovalbumin (sOVA), particulate ovalbumin (pOVA), or arrays containing both pOVA along with CpGs. The adjuvant effects of CpGs are well characterized in animal models, and their adjuvanticity in humans is currently being evaluated in clinical trials.

Immunization was achieved by applying antigen containing CMC-microneedle arrays to the ears of anesthetized mice using a spring-loaded applicator as described above, followed by removal of the arrays 5 minutes after application. These pyramidal microneedle arrays contained about 5 wt% OVA in CMC and about 0.075 wt % (20 μM) CpG. As a positive control, gene gun based genetic immunization strategy using plasmid DNA encoding OVA was used. Gene gun immunization is among the most potent and reproducible methods for the induction of CTL mediated immune responses in murine models, suggesting its use as a "gold standard" for comparison in these assays.

Mice were immunized, boosted one week later, and then assayed for OVA-specific CTL activity in vivo. Notably, immunization with arrays containing small quantities of OVA and CpG induced high levels of CTL activity, similar to those observed by gene gun immunization.

Significant OVA-specific CTL activity was elicited even in the absence of adjuvant, both with particulate and soluble array delivered OVA antigen. It is well established that similar responses require substantially higher doses of antigen when delivered by traditional needle injection.

To evaluate the stability of fabricated arrays, batches of arrays were fabricated, stored, and then used over an extended period of time. No significant deterioration of immunogenicity was observed over storage periods spanning up to 80 days (longest time point evaluated). Thus, the CMC microneedle arrays and this delivery technology can enable effective cutaneous delivery of antigen and adjuvants to elicit antigen specific immunity.

To evaluate the delivery of a biologically active small molecule, pyramidal CMC-microneedle arrays were fabricated with the low molecular weight chemotherapeutic agent Cytoxan® (cyclophosphamide), or with FluoresBrite green fluorescent particles as a control. Cytoxan® was integrated at a concentration of 5 mg/g of CMC, enabling delivery of approximately about 140 μg per array. This is a therapeutically relevant concentration based on the area of skin targeted, yet well below levels associated with systemic toxicities. Living human skin organ cultures were used to assess the cytotoxicty of Cytoxan®. Cytoxan® was delivered by application of arrays to skin explants as we previously described. Arrays and residual material were removed 5 minutes after application, and after 72 hours of exposure, culture living skin explants were cryo-sectioned and fixed. Apoptosis was evaluated using green fluorescent TUNEL assay (In Situ Cell Death Detection Kit, TMR Green, Roche, cat#: 11-684-795-910). Fluorescent microscopic image analysis of the human skin sections revealed extensive apoptosis of epidermal cells in Cytoxan® treated skin. No visible apoptosis was observed in fluorescent particle treated skin though these particles were evident, validating that the observed area was accurately targeted by the microneedle array.

In another embodiment, topical treatment of established tumors with doxorubicin and/or Poly(I:C) integrated into MNAs established tumor regression and durable immunity that can protect from subsequent lethal systemic tumor challenges.

Novel therapeutic approaches for treating established skin tumors were provided based on the combined effect of MNA delivered chemotherapy, MNA delivered immunostimulant therapy, and/or MNAs delivering combination chemo-immunotherapy. The B16 melanoma model was used as a model tumor to test these novel approaches. The B16 melanoma model is very well studied, and is one of the most aggressive murine skin cancers. Of all skin tumor models available, an established B16 tumor is among the most difficult to treat. Further, B16 has a very high metastatic potential, enabling a clinically relevant assessment of systemic tumor immunity.

B16 skin tumors were established in normal mice by injection. Visible established cutaneous tumors were treated once weekly for three weeks with MNAs containing either doxorubicin alone, Poly(I:C) alone, or doxorubicin and Poly(I:C) incorporated into the same MNA. The doxorubicin dose chosen corresponds to an MNA dose that induces apoptosis in human skin without causing necrosis. Tumor growth and survival were measured regularly for the duration of the study. Treatment with MNAs containing doxorubicin alone slowed tumor growth, and improved survival (30%) compared to that observed in untreated tumor bearing animals that had a 100% mortality rate. Further, treatment with MNAs containing Poly(I:C) alone slowed tumor growth, and improved survival (50%) compared to that observed in untreated tumor bearing animals that had a 100% mortality rate. Remarkably, treatment with containing both doxorubicin + Poly(I:C) substantially slowed tumor growth in all animals, and eradicated tumors completely in 8 out of 10 mice. This was reflected in 80% long term survival extending through day 70.

Surviving animals were evaluated to determine whether they developed long-term immunity against these same tumors. Specifically, systemic immunity was evaluated in these animals, including the durability of the immune response and the capacity of surviving animals to survive IV challenge. In particular, sixty days after the initial MNA treatment, mice were treated with a lethal dose of B16. Fourteen days later, mice were sacrificed and lung metastases were quantified microscopically. Treated mice demonstrated dramatically reduced numbers of lung lesions compared to naive controls. Taken together, these results demonstrate the capacity of MNAs to deliver chemotherapeutic agents, immune stimulants, and combinations of these agents to both induce regression of established skin tumors, and to simultaneously induce durable systemic tumor specific immune responses capable of protecting the subject from subsequent tumors.

In another embodiment, Poly-ICLC can be substituted for Poly(I:C), and MNAs can be formed, for example, with Poly-ICLC in combination with at least one other chemotherapeutic agent (e.g., doxorubicin).

As discussed above, the one or more chemotherapeutic agents can include one or more immunostimulants agents (specific and non-specific) known by those skilled in the art to stimulate the immune system to reject and destroy tumors, such as Poly(I:C) and Poly-ICLC. These immunostimulants can be integrated into the MNAs along with other chemotherapeutic agents, such as cytotoxic agents like doxorubicin. Immunostimulants that can be used in the manner described herein include adjuvants, toll-like receptors (TLRs), ribonucleotides and deoxyribonucleotides, double stranded RNAs (dsRNA), and derivatives of Poly(I:C).

Compositions Comprising Bioactive Components and Methods of Forming the Same

As discussed in detail above, dissolvable microneedle arrays can be used for transdermal delivery of drugs and biologies to human skin. Such microneedle arrays can include one or more bioactive components, including drugs, adjuvants, antigens, and chemotherapeutic agents such as Doxorubicin.

In some embodiments, one or more bioactive molecules can be linked to carboxymethylcellulose or similar biocompatible components. The methodology for chemically combining these agents can include methods that create a linkage designed to release one or more active components in target microenvironments by utilizing unique features of the microenvironment. This can include, for example, the acidic environment of a cellular compartment or vesicle, or the reducing environment of a tumor. In another embodiment of this invention this can include the combined delivery of carboxymethylcellulose conjugate and an agent facilitating cleavage of the conjugate that releases an active component. Delivery of the release facilitating agent can be simultaneous or sequential with delivery of the conjugate.

Advantages of providing cleavable bioactive components include the capability to deliver bioactive components in a protected fashion, limiting drug release to the target site thereby enhancing effective delivery concentrations while minimizing systemic or non-specific exposures. Further, in the event that the bioactive component is a targeting entity, drug release can be targeted to specific cell types or cells with certain metabolic features. A further advantage is the potential for protracted or sustained release delivery.

Carboxymethylcellulose or similar biocompatible components can be selected to enable fabrication into dissolvable microneedle arrays such as the arrays and methods of fabrication described herein. Alternatively, these conjugates can be delivered into the body by other means such as needle injection or ingestion.

As described herein, molecules of bioactive components, such as pharmaceutically active compounds, can be chemically conjugated to carboxymethylcellulose. In some embodiments, this is achieved using a cleavable bond capable of releasing the active chemical moiety in certain biologically natural or engineered environments. This technology can be useful for controlled and targeted drug delivery. Further, due to structural features of CMC, CMC-drug conjugates can be delivered by traditional methods including needle injection, and by novel delivery strategies by physically hardening the conjugate into solid structures that can be implanted, or that can serve as a combination drug/delivery device in the same entity. Examples of the latter would include CMC-drug conjugates fabricated into dissolvable microneedle arrays.

The example presented below includes a chemotherapeutic agent, Doxorubicin, which can be chemically linked to carboxymethylcellulose through a cleavable disulfide bond. As discussed below, this approach can be chemically compatible with a broad range of other bioactive components. Further, other known chemical linkage strategies could be utilized to conjugate a broad range of chemicals/drugs to CMC, including small molecule drugs, peptide and protein drugs. These drugs can be linked to a CMC substrate singly or in combinations, and in the presence or absence of one or more targeting molecules.

In this example, Doxorubicin is chemically linked to carboxymethylcellulose (CMC) through a cleavable disulfide bond. The synthesis strategy employed creates a sulfhydryl-bridged doxorubicin-CMC complex that is cleavable (i.e., able to release the drug) in a reductive environment such as cytosol and other cell-compartments, the extracellular space of the tumor microenvironment, or reducing environments created by cellular stress (redox). Further, the release of doxorubicin could also be triggered by targeted introduction of reducing agent such as dithiothreitol (DTT), beta-mercaptoethanol (MEA), Tris(2-carboxyethyl)phosphine hydrochloride (TCEP) or others, together with or subsequent to drug delivery.

In this example the synthesis process is composed of 3 major steps:

1) Highly purified Doxorubicin-SH preparation by 3' amin-conversion to sulfhydryl-group.

2) Animation of free HO-groups on dextrose units of CMC.

3) Crosslinking of Doxorubicin-SH to NH_2-CMC

Detailed approaches for achieving the three above steps are provided below.

(1) Highly purified Doxorubicin-SH preparation by 3' amin-conversion to sulfhydryl-group.

The process relies on linking doxorubicin to a solid support through sulfhydryl-bridge formation. After complete removal of the residual reactants the doxorubicin-SH is cleaved off of the support and released using a reductive agent (e.g., MEA). The eluted doxorubicin-SH is vacuum dried to remove the reducing agent and stored at -20°C or reconstructed for further use. The described process ensures that only pure modified sulfhydryl-doxorubicin is recovered as final product.

Methods:

a. Preparation of NH_2 *-cellulose for solid support using epichlorohdrin and ammonium hydroxide*

A two-step ammination of cellulose in alkaline environment was provided using epichlorohydrinand ammonium hydroxide.

-Rehydrate 25 g cellulose particles in 200 ml 2n NaOH.

-With continuous stirring bring it to 60°C.

-When the cellulose suspension reached 60°C 1.5 g of epichlorohdrin per g cellulose is added.

-Vigorously stir at 60°C for 2 hours.

-Wash the epoxide-cellulose 4x with 500 ml distilled water to obtain pH 7-8.

-Resuspend epoxide-cellulose particles in 200 ml O.ln NaOH.

-With continuous stirring bring it to 60°C.

-When the epoxide-cellulose suspension reached 60°C, 150 ml $ccNH_4$-OH is added.

-Vigorously stir at 60°C for 2 hours.

- Wash the aminated-cellulose 4x with 500 ml distilled water to obtain pH ~7.

-Store at 4 °C until used in (b) doxorubicin /NH2-cellulose crosslinking reaction.

b. Crosslinking Doxorubicin to aminated-cellulose using internally cleavable Dithiobis[succinimidyl propionate] (DSP) adapter

-Prepare 1 g NH2-cellulose in 10 ml PBS

-Prepare 8 ml doxorubicin solution in water at 1 mg/ml

-Prepare 80 mg DSP in 2 ml dry DMSO

-Mix all 3 reagents and incubate at RT for 30 min.

-Prepare sham reaction with DMSO only, no DSP.

-Wash doxorubicin-S-S-cellulose conjugate 4x with 50 ml water pH adjusted to 5 to remove unbound doxorubicin and other residual reactants.

-After final wash resuspend cleaned doxorubicin-cellulose in 10 ml PBS, store at 4 °C until desired cleavage of the S-S bonds and release of the doxorubicin-SH.

c. Elution and purification of clean doxorubicin-SH from cellulose support

The doxorubicin-SH (B) after elution was further purified by vacuum-drying and reconstructed in water.

-One ml samples of doxorubicin-S-S-cellulose slurry and the sham control were packed in chromatography-columns.

-Columns were washed with 1 ml distilled water.

-To cleave and elute the doxorubicin-SH 0.5 ml of 0.1 M 2-mercaptoethanol was added.

-Columns were incubated at 37 °C for 30 min and then eluted.

-The elution was repeated with an additional 0.5 ml 0.1 M 2-mercaptoethanol.

-The collected doxorubicin-SH was vacuum dried.

-Dried doxorubicin-SH was stored at -20 °C desiccated or reconstructed in H20 for further use.

(2) Animation of free HQ-groups on dextrose units of CMC.

The basic reactions of the amination of CMC are performed as described above but in solution. Therefore the residual reactants are removed by repeated precipitation with ethanol since CMC is generally insoluble in organic solvents.

A two-step ammination of CMC in alkaline environment was performed using epichlorohydrinand ammonium hydroxide.

Methods:

a. Prepare 5% CMC in H20

- dissolve 20 g in 400 ml
- On a heating/stirring plate bring it to 60°C
- Move it to an oven equipped with a stirring plate and set to 60°C
- Stir O/N, completely dissolve CMC.

*b. **NH2 -CMC** preparation using epichlorohdrin and ammonium hydroxide.*

-To 200 ml 5% CMC solution add NaOH to bring it to final concentration of 2.5 n.

-With continuous stirring bring it to 60°C.

-When the CMC solution reaches 60°C 1.5 g, epichlorohdrin per g CMC is added

-Vigorously stir at 60 °C for 2 hours.

-Add epichlorohydrin (18 mmol/g CMC that is 1.66 g/g CMC or 1.4 ml/g CMC). Temperature will rise to 65-70°C, let it cool down to 60°C.

-Reaction time is 2 h from the addition of epichlorohydrin.

-Precipitate Epoxide-CMC w/EtOH by adding 4 vol. (80% final cone.) O/N at 4 °C.

-Centrifuge at 2K rpm for 20 min., decant, air-dry briefly.

-Resolve Epoxide-CMC in 200 ml O.ln NaOH

-On a heating/stirring plate bring it to 60°C.

-Add 150 ml ccNH4-OH (29 % w/v)

-React for 2 h at 60°C.

-Precipitate as in steps above.

-Wash pelleted NH_2-CMC w/ 90% EtOH twice.

-Resolubilize in 100 ml H2O (get it in solution completely).

-Repeat precipitation step as before.

-Reconstruct in 100 ml H2O.

-Neutralize the residual NaOH and NH4-OH with 4 n HC1, get ~pH 6.5-8.5 range.

-Test for recovery efficiency of NH2-CMC. (Expected is 60-80%)

3) Cross-linking of Doxorubicin-SH to NH2-CMC.

The cross-linking of Doxorubicin-SH to NH2 -CMC utilizes a hetero-bi-functional adapter (N-Succinimidyl 3-(2-pyridyldithio)-propionate (SPDP)) to achieve a short extension at the 3'-NH2 of the doxorubicin upon release from the doxorubicin-S-S-CMC conjugate preserving the functionality of doxorubicin.

Methods:

-Prepare 1 g NH_2-CMC in 10 ml PBS

-Prepare 5 ml doxorubicin-SH solution in water at 0.5 mg/ml

-Prepare 40 mg SPDP in 1 ml dry DMSO

-Mix all 3 reagents and incubate at RT for 30 min.

-Prepare sham reaction with DMSO only, no SPDS.

-Precipitate doxorubicin-S-S-CMC conjugate 4x volume of ethanol pH adjusted to 5 with 1 n HC1 to remove unbound doxorubicin and other residual reactants.

-Resolve pelleted doxorubicin-S-S-CMC in 10 ml water.

-Dialyze doxorubicin-S-S-CMC solution using spectrapore dialysis tubing (MW cutoff 3,500 dalton) against 2 1distilled water changing the distilled water 2x in every 12 hours at 4 °C.

-Precipitate doxorubicin-S-S-CMC as above with ethanol

-Vacuum dry pelleted doxorubicin-S-S-CMC.

-Store at -20°C until use or reconstruct at the required concentration with water.

Conjugation and release were validated by quantification of the active epoxide group using titration according to equation:

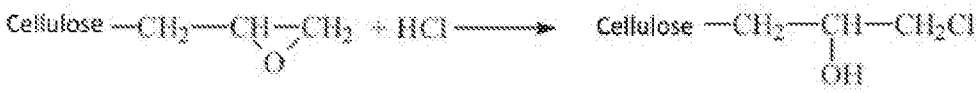

Other Linkable Bioactive Components

Although Doxorubicin is the bioactive component in the above-disclosed embodiment, other bioactive components can be used and be linked to a CMC or other biocompatible structural substrate. Suitable compounds that form the bioactive components may include, for instance, proteinaceous compounds, such as insulin, peptide antimicrobials (e.g., naturally occurring defensins, cathelicidins and other proteins with anti-bacterial and/or antiviral activity and synthetic derivatives of naturally occurring peptide antimicrobials including truncated or structurally modified variants), immunoglobulins (e.g., IgG, IgM, IgA, IgE), TNF-a, antiviral medications, etc.; polynucleotide agents, such as plasmids, siRNA, RNAi, nucleoside anticancer drugs, vaccines, etc.; small molecule agents, such as alkaloids, glycosides, phenols, etc.; anti-infection agents, hormones, drugs regulating cardiac action or blood flow, pain control; and so forth. Suitable compounds also

include electrophilic nitro-fatty acids (FA-NO2) such as nitro-oleic acid (OA- NO2) and nitro-linoleic acid (LN- NO2) and their derivatives. Suitable compounds also include redox cycling nitroxides such as TEMPOL, as well as targeted derivatives such JP4-039 and the related family of compounds, and XJB-5-131 and the related family of compounds. Suitable compounds also include the transcription factor XBPl, its derivative XBPls, and synthetic derivatives of XBPl including XBPl pathway stimulating factors. Suitable compounds also include neurokin 1 receptor (NK1R) agonists including tachykinins (e.g. substance P) and NKR1 such as aprepitant (Emend), their derivatives. A non-limiting listing of agents includes anti-Angiogenesis agents, anti-depressants, antidiabetic agents, antihistamines, anti-inflammatory agents, butorphanol, calcitonin and analogs, COX-II inhibitors, dermatological agents, dopamine agonists and antagonists, enkephalins and other opioid peptides, epidermal growth factors, erythropoietin and analogs, follicle stimulating hormone, glucagon, growth hormone and analogs (including growth hormone releasing hormone), growth hormone antagonists, heparin, hirudin and hirudin analogs such as hirulog, IgE suppressors and other protein inhibitors, immunosuppressives, insulin, insulinotropin and analogs, interferons, interleukins, leutenizing hormone, leutenizing hormone releasing hormone and analogs, monoclonal or polyclonal antibodies, motion sickness preparations, muscle relaxants, narcotic analgesics, nicotine, non-steroid anti-inflammatory agents, oligosaccharides, parathyroid hormone and analogs, parathyroid hormone antagonists, prostaglandin antagonists, prostaglandins, scopolamine, sedatives, serotonin agonists and antagonists, tissue plasminogen activators, tranquilizers, vaccines with or without carriers/adjuvants, vasodilators, major diagnostics such as tuberculin and other hypersensitivity agents. Vaccine formulations may include an antigen or antigenic composition capable of eliciting an immune response against a human pathogen or from other viral pathogens.

Other Linkage Strategies for Use with Bioactive Components and Substrates

A cleavable disulfide bond is just one chemical linkage strategy that can be used to link molecules of a bioactive component to a substrate, such as a CMC substrate. For example, in addition to disulfide bonds, other chemical linkage strategies that can be used, so long as they are cleavable in the intended environment, include crosslinking and chemical modification using primary amines ($-NH_2$), carboxyls (-COOH), and carbonyls (-CHO).

As discussed herein, in addition to CMC, other biocompatible structural substrate can be used. For example, in another embodiment, Poly-IC or Poly-ICLC can be substituted for CMC, and MNAs can be formed, for example, with Poly-IC or Poly-ICLC in combination with the bioactive materials disclosed herein, such as doxorubicin.

Controlled Release of Bioactive Components

In some embodiments, controlled multi-drug multi-kinetic drug delivery can be provided to utilize dissolvable MNAs for drug delivery and to control the diffusion phase of individual cargos, including, for example, the bioactive components discussed herein, to achieve the desired pharmacokinetics.

Overall release kinetics of encapsulated cargo depends on the molecular characteristics of the cargo, the polymer, and the molar ratio of the polymer to other MNA scaffold materials. Differences in the properties of various sustained release polymers in combination with the matrix component of an MNA can affect the desired delivery kinetics. Specific interactions between the drug, the sustained release copolymer, and the MNA scaffold component impact the unique delivery kinetics for MNA delivery of each drug. In the following example, MNAs are formulated with integrated layers made with varying molar ratios of a drug in a given polymer.

Example 6

MNAs were formulated using 0 % (FIG. 38A), 5 % (FIG. 38B) and 20 % (FIG. 38C) of sustained release polymer co-solubilized with Sudan I as a marker dye (as an identifiable surrogate drug). The representative images of these MNAs shown in FIGS. 38A-C demonstrate that an active component can be encapsulated and integrated into the MNA scaffold through the 0-20 % polymer concentration range, with varying release kinetic for each. In FIGS. 38A-C the arrows indicate the deposition of the dye in representative microneedles.

To illustrate the delivery of multiple drugs with distinct release kinetics, MNAs were fabricated to delivery two distinct cargos by distinct release kinetics. Specifically, MNAs were fabricated to release the marker Toluidine Blue in an initial burst, followed by a sustained release of the marker FD&C Red40. Dyes were directly loaded in the MNA scaffold matrix (in this case CMC) of the needle tips and in some cases a second dye, encapsulated in a sustained release polymer was layer directly below. MNAs were inserted into 4% agar test-gels and removed after 1 min.

Images of dye diffusion were collected at the indicated time points (FIG. 39A). As shown in FIGS. 39A-C, FD&C Red40 (FIG. 39A) and toluidine blue (FIG. 39B), tracer dyes were tip-loaded in MNAs for immediate release. Alternatively, MNAs were fabricated with toluidine blue tip-loaded and FD&C Red40 encapsulated in a sustained release polymer (FIG. 39C). MNAs were inserted into 4% agar test-gel and removed after 1 min. Images were collected at the indicated time-points. Tip-loaded cargos were rapidly released from the MNAs and dispersed progressively in the gel (FIG. 39A and B). Dually loaded MNAs released tip loaded toluidine blue in an initial burst,

while encapsulated Red40 dye (FIG. 39C) was released slowly over an extended time period. Upper panels depict images of microneedles from MNAs before application. The middle images are the imprints of the arrays 1 minute after application and MNA removal. Lower panels depicted the indicated representative magnified images at the indicated time points.

As expected, when MNAs were fabricated with either FD&C Red40 (FIG. 39A) or Toluidine Blue (FIG. 39B) alone in the CMC matrix of the needle tip, release began rapidly (within 1 min) and diffusion was essentially complete within 2h. When using MNAs fabricated with Toluidine Blue in CMC in the needle tip, and sustained FD&C Red40 in an underlying layer of sustained release polymer, toluidine blue was again released in an initial burst while FD&C Red40 was released from its depot over an extended period of time spanning 10 days (FIG. 39C).

Exemplary polymers for controlling and/or triggering the release of cargo

Kinetics of the cargo release from applied MNAs controlled by the solubility and biodegradation of cargo-encapsulating polymers. In the absent of these polymers the release is immediate with burst like kinetics as the rehydration of the needle-materials occur. With reference to FIG. 40, in the presence of control-polymers the release of the cargo can be:

(A) Sustained Release - cargo release is temporally extended, resulting in a sustained release where the rate of release is dependent on the dissolution and/or biodegradation of the control-polymer;

(B and C) Triggered Release - (B) the release of the cargo requires an external trigger which initiate a phase shift, conformational or chemical change in the control-polymer resulting in sustained or single burst like kinetics of the cargo release. Burst type repeated partial release of the bioactive payload can be achieved with the repeated application of the trigger-signal (C).

Examples of structural embedding-polymers for sustained release with different release time kinetics include:

- Poly(D,L lactide-co-glycolide), [PLGA]
- Poly(L-lactide), [P(L)LA]
- Poly(D,L-lactide), [P(D,L)LA]
- Poly(caprolactone), [PCL]
- Poly(lactide)-co-(caprolactone), [PLCL]

Examples of Trigger Signals for complex release kinetics can include:

-Thermal trigger (e.g. temperature sensitive phase transition)

Tetradecanol (phase shifting temperature: 38-39 °C)

Hexadecanol (Cetyl alcohol, phase shifting temperature: 48-50 °C)

Octadecanol (Stearyl alcohol, phase shifting temperature: 56-60 °C)

Dodecanoic acid (phase shifting temperature: 43-46 °C)

Tridecanecarboxilic acid (Myristic acid, phase shifting temperature: 52-54 °C)

Pentadecanecarboxilic acid (Palmitic acid, phase shifting temperature: 60-63 °C)

Block polymers:

PEG-PCL, Poly(ethylene glycol)-b-poly(caprolactone),

PEG-PLGA, Poly(ethylene glycol)-b-poly(lactide-co-glycolide),

PEG-PLLA, Polyethylene glycol)-b-poly(L-lactide),

PEG-PDLLA, Poly(ethylene glycol)-b-poly(D,L-lactide),

PLGA-PEG-PLGA, Poly(lactide-co-glycolide)-b-poly(ethylene glycol)-b-poly(lactide-co-glycolide),

-Electric-field

Polypyrrole (PPy)

-Light/NIR light

Gold-PEG-block polymer composites

Gold-Tetradecanol/ Hexadecanol /Octadecanol composites

Gold-Dodecanoic/Tridecanecarboxilic/Pentadecanecarboxilic acid composites

-Ultrasound

Gold-Tetradecanol/ Hexadecanol /Octadecanol composites

Gold-Dodecanoic/Tridecanecarboxilic/Pentadecanecarboxilic acid composites

FIG. 40 illustrates release profiles consisting of different phases with or without trigger. Referring to that figure, the open triangles show a burst followed by a rapid diffusion phase; the open squares show a tri-phasic release, initial burst followed by a very slow diffusion phase and the fast accelerated release during the triggered degradation phase; and the open circles show a bi-phasic release with multiple triggering signals (similar to tri-phasic but without the burst release).

These technologies are compatible with delivery of a wider range of cargos in terms of both cargo structure and cargo function, and disparet cargos can readily be combined in single MNAs for coordinated kinetic and spatial co-delivery.

Examples of bioactive materials that can be delivered using the delivery systems discussed herein (including, but not limited to, controlled release delivery) include:

Small molecules, organics: Calcipotriol (vitamin D3 derivate/analog), Daunorubicin, Doxorubicin, Cumarin (chemo therapeutics, antibiotic), Rapamycin (mTOR inhibitor, immune suppressor, antibiotic), Dexamethasone (anti-inflammatory/allergic agent), POM-1 (ecto-NTPDase

inhibitor), BzATP (purinergic receptor agonist), DMXAA (tumor VDA), L733-060 (NK-IR ligand, NK-1 antagonist), R848 (TLR7/TLR8 agonist), Imidazoquinoline (TLR7 agonist), 2,4-Dinitrochlorobenzene, DNCB (irritant, immune stimulant), 2,4-Dinitrobenzenesulfonic acid, DNSB (irritant, immune stimulant), 5-fluorouracil, 5-FU thymidylate synthase inhibitor, Folinic acid, synergetic to 5-FU, Irinotecan, Camptothecin (CPT) analog, DNA topoisomerase 1 inhibitor, Cyclophosphamide (Cytoxan), synthetic antineoplastic drug, JP4-39, and Necrotin.

Antibiotics, topicals, alone and in combinations: Na-sulfacetamide, Erythromycin, Bacitracin, Neomycin, Polymyxin b, Gentamicin, Tetracycline.

Antioxidants, vitamins, topicals: Polyphenols, e.g. silymarin, proanthocyanidins, tannins, Vitamin C, Vitamin E, Nicotinamide, Coenzyme Q10 (CoQIO) and analoges, Resveratrol, 3,5,4'-trihydroxy-trans-stilbene, Lycopine, Genistein, Tempol and Tempol derivatives (including mitochondria-targeted Tempol), and other nitroxides.

Nucleic acid drugs: Aptamers (Target specific ligands to inorganic or organic molecules, protein or specific to cells of interest, small single strand DNA or RNA oligonucleotides, can serve as carriers of chemotherapeutics in guided/targeted delivery), Poly(I:C), Oligo-dG, CpG1668, CpG2006, siRNA.

Small peptide antigens, epitopes, and ligands: Substance-Pi, neurokinin 1 receptor agonist, neurotransmitter, NK1R peptide, neurokinin 1 receptor agonist, TRP-2, tyrosinase-related protein 2, residues 180-188 aa, EpHA2, ADH-1, N-cadherin inhibitor, antiangiogenic cyclic pentapeptide.

Large peptides, peptides, recombinant-peptide antigens, alone or in combination with modulators/suppressors simultaneous or separate triggers for the release: DPPD (to diagnose tuberculosis, recombinant protein of M. tuberculosis), Sl-MRSA, rEBOV-Gp Ebola, Trypsin (debridement of skin tissues), Papain (debridement of skin tissues), Hyaluronidase (drug dispersion in skin, opposite effects to hyaluronic acid), anti-TNFa (several versions are approved or in progress of approval), anti-IL-lbR, anti-IL22, Fezakinumab, anti-IL23, Guselkumab, anti-IL22 and 23, Briakinumab, anti-CD4, Zanolimumab, anti-CD152, Ipilimumab, anti-VEGF-A, Bevacizumab, anti-Integrin $\alpha v\beta 3$, Etaracizumab, rHBsAg, Exbivirumab (recombinant hepatitis B surface antigen), anti-TyRPl, Flanvotumab, anti- GPNMB, Transmembrane glycoprotein NMB, Glembatumumab vedotin, BSA, OVA and other model antigens.

Radiation agents: radiation mitigating agents and radiation protection agents including, for example, GS-nitroxides (JP4-039 and XJB-5-131), the bifunctional sulfoxide MMS-350, the phosphoinositol-3 -kinase inhibitor LY29400, triphenylphosphonium-imidazole fatty acid, the nitric oxide synthase inhibitor (MCF-201-89), the p53/mdm2/mdm4 inhibitor (BEB55), methoxamine,

isoproterenol, propranolol, and the adenosine triphosphate-sensitive potassium channel blocker (glyburide).

Integration of antigens and immune-adjuvant molecules in MNAs for immunization

The systems and methods described herein include carboxymethyl-cellulose (CMC) biodegradable Micro-Needle Arrays (MNA) which integrate antigens and adjuvants for immunization to prevent and treat of infectious and neoplastic diseases. As discussed below, for example, in one embodiment the integration involves of members of the class of proinflammatory tachykinins in MNAs with antigen or antigens, and with or without other known adjuvants.

Mouse and human skin dendritic cells (DC) express functional NKIR. As shown in FIGS. 41A and 41B, mouse skin CD11c^{+} epidermal and dermal DCs, keratinocytes, and other non-dendritic dermal cells (likely mast cells (MC) and endothelial cells), express the C-terminus motif of the NKIR functional variant. FIG. 41A shows NKIR expression in CDllc^{+} DC (by FACS) and FIG. 41B shows NKIR expression in keratinocytes, with CDllc^{+} epidermal LC shown by the arrowheads and dermal DC shown by the arrows in the image taken using fluorescence microscopy (X200).

The role of NKIR in the skin immune function is demonstrated in FIG. 41C by significantly increased DTH reactions in C57BL/6 (B6) mice sensitized with DNCB in the presence of the NKIR agonist Sar^{9} Met(O$_2$)^{11}-SP (SarSP) (10^{-9} M). Conversely DTH was completely abrogated when the same sensitization approach was applied to NKlR$^{-/-}$ mice as shown in FIG. 41D.

FIGS. 42A and 42B show human skin DCs express functional NKIR. FIGS. 42A shows NKIR expression by human skin DC by FACS and FIG. 42B shows expression of NKIR in epidermal (CD207+) LC and (CD86+) dermal DC by fluorescence microscopy (X200). As shown in FIGS. 43C and 43D, adding SarSP to human mixed leukocyte cultures (MLC) using skin DC as stimulators of allogeneic naive CD4 T cells, significantly augmented Tcell proliferation (FIG. 42C) and IFN-γ secretion (FIG. 42D).

Conventional rigid MNA with pyramid geometry can suffer from limited skin penetration, and poor and unreliable cargo delivery capacity compared to the novel microneedle structures disclosed herein. For example, in some embodiments, the delivery systems disclosed herein integrate biologies into dissolvable carboxymethyl-cellulose (CMC) microneedles with obelisk geometries. As shown in the table of FIG. 43, obelisk-shaped microneedles can be significantly more efficient than conventional-shaped pyramid microneedles.

In some embodiments, each MNA can be composed of an array of 10 x 10 microneedles, arranged in about a 6 x 6 mm area (FIG. 3A). In this example, individual needles can be about 700 μιη high, have an apex angle of about 30°, and base of about 200 μιη. This design, and other novel

designs disclosed herein can provide better cutaneous penetration and more accurate cargo delivery into the skin. When the MNAs are applied to the skin, the microneedles efficiently pierce the epidermis and dermis, allowing the penetrating needles to dissolve (e.g., within about 5 min after application in some embodiments) and release with high reproducible efficiency their cargo that diffuses throughout the skin treated area.

Using the systems and methods disclosed herein, the advantages of dissolvable CMC and micro milling can produce optimized MNA geometries that uniquely enables efficient integration of multiple bioactive drugs, and their precise and reproducible delivery to skin strata. The efficiency and reproducibility of the MNAs is visually demonstrated by the delivery of MNA integrated-green fluorescent beads into mouse skin (FIGS. 44A and 44B), and integrated-toluidine blue or fluorescent beads into human skin (FIGS. 44C and 44D) dye into MNAs that were used to deliver this cargo to mouse and human skin. Planimetric and mouse skin sections show efficient penetration and delivery of green fluorescent beads in the epidermis and dermis in FIGS. 44A and 44B. The planimetric image of human skin in FIG. 44C shows efficient penetration and delivery of toluidine blue, and the human skin section in FIG. 44D shows efficient penetration and delivery of green fluorescent beads in the epidermis and dermis.

A quantitative comparison of MNA cargo delivery into human skin was determined using ^{3}H TdR-OVA loaded MNAs applied to human skin organ cultures. As shown in FIG. 43, an improved reproducibility in cargo loading and a 3.89 fold higher drug delivery was achieved by using obelisk MNA compared to pyramidal MNAs.

FIGS. 45A-45D illustrate inflammatory responses observed in cross sections of abdominal skin and skin draining lymph nodes of B6-WT mice sensitized or not (controls) with DNCB in the presence or not of the NK1R agonist SarSP. FIG. 45A shows Hematoxylin & Eosin staining of ear sections. Mice treated with DNCB illustrate moderate skin inflammation composed of PMN cells (inset) distributed mainly in the papillary dermis (arrows). Coadministration of SarSP significantly increased the number of inflammatory cells distributed throughout the epidermis and dermis (arrows) and the severity of skin damage.

FIG. 45B illustrates staining of skin sections with TB increased inflammatory infiltrate correlates with the degree of MC degranulation, insets. FIG. 45C shows skin draining lymph nodes of mice treated with DNCB present the characteristic histology of acute inflammation with recruitment of PMN cells, and mononuclear cells including macrophages and DCs (insets). Co-administration of SarSP significantly increases the inflammatory infiltrate in the paracortical area of the draining lymph node (arrows).

FIG. 45D shows staining of lymph node sections with Toluidin Blue and illustrates that increased inflammatory infiltrate correlates with increased number of MC and a higher degree of MC degranulation (insets). (A & C: H and E, 200X; Insets, 1,000X; B & D: TB, 200X; Insets 1,000X; NT refers to non-treated mice.)

Agonistic signaling via NK1R significantly increases innate and adaptive immunity to DNCB Ag. The effect of different treatments in B6-WT mice was compared with n=6/experimental group. Priming with DNCB induced moderate inflammation of the epidermis and dermis and, as shown in FIG. 45A co-administration of SarSP dramatically increased the magnitude of the inflammatory response and tissue damage. The inflammatory infiltrate was composed of leukocytes including polimorphonuclear neutrophils (PMN) and eosinophils as shown in the inset of FIG> 45A. Administration of SarSP alone did not induce inflammatory response. In addition, administration of DNCB and SarSP alone or in combination triggered MC activation and degranulation as shown in the insets of FIG. 45B.

Administration of DNCB in the epidermis, induced inflammation in local draining lymph nodes, as determined by the presence of polimorphonuclear, mononuclear and MC (FIG 45C). Similar to what was observed in the skin, DNCB and SarSP alone or in combination, induced an increased number of MC (FIG 45D), with characteristic signs of degranulation (FIG 45D insets). Evaluation of effector cellular immunity recall to the skin following elicitation of DTH, demonstrated a significant thickness increase of elicited ears vs. controls and that effect was further increased by coadministration of DNCB and SarSP. Together these results show that endogenous NK1R agonists released during sensitization and elicitation of CHS, play a relevant role in the priming of hapten specific effector immunity and demonstrate that administration of the exogenous NK1R agonist SarSP promotes a further increase in the inflammatory (innate) and adaptive immune responses that account for the onset of CD (FIG 46E).

FIG. 46 shows DTH effector response expressed as percent of ear thickness increase and analyzed up to 8d following elicitation. Means ± 1SD of 6 mice / experimental group are illustrated, with three independent experiments performed.

Accordingly, methods and systems for reducing or desensitizing an immune response by deliver of sub-immunogenic doses of an allergen to the cutaneous microenvironment are provided. These methods can include delivery of such materials using the novel microneedle arrays described herein, or by other means.

Various allergens can be delivered using the methods and systems disclosed herein. For example, the following is a non-exhaustive list of possible allergens that can be delivered using the microneedle arrays described herein:

Allergen: As described above, allergens are substances that can induce an allergic or asthmatic response in a susceptible subject. The list of allergens is enormous and can include pollens, insect allergens, animal dander dust, fungal spores, food allergens, environmental allergens, and drugs (e.g. penicillin).

Examples of natural, animal and plant allergens include proteins specific to the following genera: Canine (Canis familiaris); Dermatophagoides (e.g. Dermatophagoides farinae); Felis (Felis domesticus); Ambrosia (Ambrosia artemiisfolia); Lolium (e.g. Lolium perenne or Lolium multiflorum); Cryptomeria (Cryptomeria japonica); Alternaria (Alternaria alternata); Alder; Alnus (Alnus gultinosa); Betula (Betula verrucosa); Quercus (Quercus alba); Olea (Olea europa); Artemisia (Artemisia vulgaris); Plantago (e.g. Plantago lanceolata); Parietaria (e.g. Parietaria officinalis or Parietaria judaica); Blattella (e.g. Blattella germanica); Apis (e.g. Apis multiflorum); Cupressus (e.g. Cupressus sempervirens, Cupressus arizonica and Cupressus macrocarpa); Juniperus (e.g. Juniperus sabinoides, Juniperus virginiana, Juniperus communis and Juniperus ashei); Thuya (e.g. Thuya orientalis); Chamaecyparis (e.g. Chamaecyparis obtusa); Periplaneta (e.g. Periplaneta americana); Agropyron (e.g. Agropyron repens); Secale (e.g. Secale cereale); Triticum (e.g. Triticum aestivum); Dactylis (e.g. Dactylis glomerata); Festuca (e.g. Festuca elatior); Poa (e.g. Poa pratensis or Poa compressa); Avena (e.g. Avena sativa); Holcus (e.g. Holcus lanatus); Anthoxanthum (e.g. Anthoxanthum odoratum); Arrhenatherum (e.g. Arrhenatherum elatius); Agrostis (e.g. Agrostis alba); Phleum (e.g. Phleum pratense); Phalaris (e.g. Phalaris arundinacea); Paspalum (e.g. Paspalum notatum); Sorghum (e.g. Sorghum halepensis); and Bromus (e.g. Bromus inermis).

Examples of insect allergens include bee, wasp, or hornet venoms (such as Myrmecia pilosula; Apis mellifera bee venom phospholipase A2 (PLA2) and antigen 5S, phospholipases from the yellow jacket Vespula maculifrons and white faced hornet Dolichovespula maculate, etc.), spider venom, etc. Examples of food allergens include fish, shellfish (shrimp, crab, lobster, oyster, scallops), soy, strawberries, tree nuts (walnut, hazel/filbert, cashew, pistachio, Brazil, pine nut, almond), peanuts, milk, egg protein, etc.

Allergens can include those known to be associated with anaphylaxis include food allergens (peanuts, tree nuts, fish, shellfish, cow's milk, soy, and eggs), insect allergens, particularly from stinging insects (e.g. honeybees, fire ants, yellow jackets, yellow hornets and paper wasps), drugs (e.g., β-lactams; nonsteroidal anti-inflammatory drugs (NSAIDs)), and biologic modifiers (e.g. cetuximab, infliximab and omalizumab).

Allergens can also include those responsible for allergic dermatitis caused by various arthropods, e.g. Diptera, including mosquitos (Anopheles sp., Aedes sp., Culiseta sp., Culex sp.);

flies (Phlebotomus sp., Culicoides sp.) particularly black flies, deer flies and biting midges; ticks (Dermacenter sp., Ornithodoros sp., Otobius sp.); fleas, e.g. the order Siphonaptera, including the genera Xenopsylla, Pulex and Ctenocephalides felis felis.

Allergens can also include wheat and soy proteins. Wheat allergens can include, for example, Profilin (Tri a 12); Tri a 12.0101 accession P49232; Tri a 12.0102 accession P49233; Tri a 12.0103 accession P49234; Tri a 12.0104 accession B6EF35; Tri a 14.0201 accession D2T2K2; Tri a 15.0101 accession D2TGC3; Tri a 18.0101 accession P10968; Tri a 19.0101; Tri a 21.0101 accession D2T2K3; Tri a 25.0101 accession Q9LDX4; Tri a 26.0101 accession P10388; Tri a 26.0201 accession Q45R38; Tri a 27.0101 accession Q7Y1Z2; Tri a 28.0101 accession Q4W0V7; Tri a 29.0101 accession C7C4X0; Tri a 29.0201 accession D2TGC2; Tri a 30.0101 accession P17314; Tri a 31.0101 accession Q9FS79; Tri a 32.0101 accession Q6W8Q2; Tri a 33.0101 accession Q9ST57; Tri a 34.0101 accession C7C4X1; Tri a 35.0101 accession D2TE72; Tri a 36.0101 accession 335331566; Tri a 37.0101 accession Q9T0P1; Tri a 39.0101 accession J7QW61. Soy allergens can include, for example, Gly m 5 Glycine Beta- conglycinin accession CAA35691.1; Gly m 5 Glycine Beta-conglycinin accession AAA33947.1; Gly m 5 Glycine Beta-conglycinin accession AAB01374.1 ; Gly m 5 Glycine Beta-conglycinin accession AAB23463.1 ; Glycine Gly m 1 accession AAB34755.1; Glycine Gly m 1 accession ABA54898.1; Glycine Gly m 3 accession CAA1 1755.1; Glycine Gly m 3 accession 065809.1; Glycine Gly m 3 accession ABU97472.1; Glycine Gly m 4 accession P26987.1; Glycine Gly m 8 2s albumin accession AAD09630.1; Glycine Gly m Bd 28K accession BAB21619.1; Glycine Gly m Bd 28K accession ACD36976.1; Glycine Gly m Bd 28K accession ACD36975.1; Glycine Gly m Bd 28K accession ACD36974.1; Glycine Gly m Bd 28K accession ACD36978.1; Glycine Gly m Bd accession P22895.1; Glycine Gly m Bd accession AAB09252.1; Glycine Gly m Bd accession BAA25 899.1; Glycine Glycinin G1 accession CAA26723.1; Glycine Glycinin G1 accession CAA33215.1; Glycine Glycinin G2 accession CAA26575.1; Glycine Glycinin G2 accession CAA33216.1; Glycine Glycinin G3 accession CAA33217.1; Glycine Glycinin G4 accession CAA37044.1; Glycine Glycinin G5 accession AAA33964.1 ; Glycine Glycinin G5 accession AAA33965.1; Glycine Major Gly 50 kDa allergen accession P82947.1; Glycine Trypsin inhibitor accession AAB23464.1; Glycine Trypsin inhibitor accession AAB23482.1; Glycine Trypsin inhibitor accession AAB23483.1; Glycine Trypsin inhibitor accession CAA56343.1; Glycine Glycinin G4 accession CAA60533.1; Glycine Glycinin G5 accession CAA55977.1.

In some embodiments, the allergen can be delivered in combination with one or more immune suppressant or tolerizing agent to the cutaneous environment. Such suppressants or tolerizing agents can include, for example, NKR antagonists, Fbxo3 inhibitors, anti-TNF Ab, or

other suitable agents. Various combinations of allergens, suppressants, or tolerizing agents can be used. For example, two different suppressants or tolerizing agents can be used in combination with a single allergen, multiple allergens can be used with a single suppressant or tolerizing agent, or multiple allergens can be delivered in combination with multiple suppressants or tolerizing agents.

In some embodiments, the allergen and one or more immune suppressants/tolerizing agents can be delivered to the cutaneous microenvironment to treat patients with various skin conditions, disorders, or diseases, such as contact dermatitis, atopic dermatitis, psoriasis, immunobullous diseases, or inflammatory skin disorders. In other embodiments, various autoimmune disorders can be treated using the systems and methods described herein, including lupus or arthritis. In some embodiments, the allergen and one or more immune suppressants/tolerizing agents can be delivered to the skin draining lymph nodes of a patient.

Thus, as discussed above, the present application discloses many novel systems and methods, including the novel integration of biologic molecules into dissolvable MNAs, including, for example, proinflammatory tachykinins, to deliver vaccines to specific skin strata is entirely novel. The release neural mediators in the skin, such as tachykinins, creates a skin proinflammatory microenvironment that is highly effective in generating both local and systemic immune responses. In this way localized delivery of antigen and adjuvant engineers the skin microenvironment to become highly proinflammatory. In addition, skin immunization using the systems and methods disclosed herein can lead to the generation of a novel population of memory T-cells that traffic to and specifically localize in the skin, providing skin specific immune protection.

Down Regulation and/or Suppression of Inflammatory or Immune Responses

Regulation of immune responses in an antigen specific manner using the systems and methods disclosed herein can be achieved by the simultaneously delivery of one or more antigens and one or more immune-regulatory molecules as a "negative immunization." This strategy can down-regulate unwanted (pathologic) acute and chronic inflammatory responses and adaptive immune responses accounting for a broad number of inflammatory and immune mediated diseases. In some embodiments, the negative immunization is applied through the skin, in which down regulatory modulators are introduced into the cutaneous environment with a target antigen, or into an environment containing an endogenous antigen (auto-antigen).

In one embodiment, skin "negative immunization" involves utilization of a delivery system capable of achieving a simultaneous, efficient, and controlled, release of biologicals in the skin-confined area. For example, one method of achieving this delivery is using the systems and methods disclosed herein, such as carboxymethyl-cellulose (CMC) biodegradable MNAs that

integrate both antigen and anti-inflammatory anti-immune molecules. The MNAs can be configured, as disclosed herein, to co-deliver the various components into the epidermis and superficial dermis, which are the skin strata where inflammatory and immune responses can be initiated or abrogated. Such MNAs can integrate those biologicals individually and in combination, in a way that one or more antigen combinations can be associated with one or more anti-inflammatory and/or anti-immune molecules to achieve the desired effect.

Since a potential unwanted immune-stimulatory effect exerted by the MNA components represents a drawback for the purpose of the negative immunization proposed in this application, the potential pro-inflammatory effect of empty MNAs was analyzed. Empty MNAs or DNCB-loaded MNAs were applied to B6 wt mouse skin and inflammation was analyzed (24 h after sensitization) and, effector DTH (following elicitation 7 days after sensitization). As shown in FIGS. 47A and 47B, empty MNAs did not increase the DNCB-irritant effect or the DNCB-DTH response. FIG. 47A illustrates mouse skin histology 24 hours after application of blank or DNCB-MNA, with the arrows indicating skin thickness (H&E; X200). FIG. 47B shows that the MNA application also did not increase the DTH response to DNCB (S: sensitization; E: elicitation; N=3).

An example of the negative immunization approach described herein was performed using MNAs to abrogate DNCB-DTH by efficient co-delivery of DNCB and NK1R antagonists into mouse skin. FIG. 48 illustrates DNCB-MNA inducing enhanced DTH vs. topical DNCB ($p<0.01$) and DNCBL733,060-MNA promoting more potent DTH inhibition than topical DNCB + i.d. i L733,060 ($p<0.01$). For DTH induction DNCB (50 μg) and the NK1R antagonist L733, 060 (25 nM) integrated in one MNA, were co-delivered to wt. B6 mouse ear skin followed by elicitation by topical DNCB (10 μg/ml) performed 7 days after sensitization. In the absence of NK1R antagonist MNA-DNCB induced a significant DTH and MNA co-delivery of DNCB + L733,060 abrogated the DTH response to DNCB. The data shows that MNAs are effective for the delivery of functional DNCB and NK1R antagonists to the skin, a property that is needed for a successful desensitization strategy and consequently prevented DTH sensitization.

In some embodiments, the simultaneous co-delivery of DNCB and L733, 060 MNA can be administered to prevent contact dermatitis (CD) relapses locally and systemically. The effects of negative immunization in the prevention of contact dermatitis relapses were studied in wt-B6 mice. As indicated in FIG. 49A, mice were induced by sensitization and elicitation with DNCB applied topically to one ear. Mice were rested during weeks 2 and 3, and they were vaccinated on week 4 with DNCB-MNA (positive control), or with DNCB-L733, 060-MNA (negative immunization). On week 5 mice were challenged with DNCB applied topically to the previously sensitized and vaccinated ear (to evaluate the local effect of negative immunization) or in the contralateral ear (to

evaluate the systemic effect of negative immunization). Abrogation of contact dermatitis relapse was evaluated on week 5 by DTH. As shown in FIGS. 49B and 49C, negative immunization with DNCB-L733, 060-MNA was able to prevent local and systemic contact dermatitis relapses in DNCB sensitized mice. Mice vaccinated with DNCB-MNA in the absence of NK1R antagonist developed a significant DNCBDTH response in the equally sensitized mouse group. These results show that negative immunizations applied during contact dermatitis remission prevent and/or reduce contact dermatitis relapses.

NK1R blockade can provide additional beneficial effects in human skin samples. The NKlR-antagonist L733, 060 affects migration, and T-cell stimulatory function of human skin dendritic cells (DCs). To show these additional effects, DNCB ± L733, 060-MNA was applied to human skin explants (2 cm2 surface) (10 explants per variable). Negative controls included untreated skin, application of empty MNA, or L733, 060-MNA. Skin migratory DCs were quantified 24h later, and their T cell stimulatory function was analyzed in 5d MLC. As shown in FIG. 50A, L733, 060-MNA significantly reduced DC numbers, and DNCB-L733, 060-MNA reduce significantly the number of skin-migrating DCs induced by DNCB-MNA alone. As shown in FIG. 50B, DCs from DNCBL733,060-MNA treated skin also induced significant lower T cell proliferation compared to DC from DNCB-MNA treated skin.

Accordingly, the methods and systems discussed herein can promote pro-inflammatory and/or adaptive immune responses for the purpose of positive immunization for tumors and infectious diseases by delivery of antigen and selected adjuvants in the cutaneous microenvironment. These methods can include delivery of such materials using the novel microneedle arrays described herein, or by other means.

The immune response can be promoted by delivery of adjuvants or other immune response promoting agents described herein, in this section and in others, including, for example,

- Proinflammatory tachykinins, including substance-P and their analogs, Hemokinin-A and analogs, Neurokinin-B and analogs, bradykinin and analogs, Vascular Intestinal Peptide and analogs, calcitonin-gene-related peptide (CGRP) and analogs;
- Toll-like Receptor-Ligands (TLR-s);
- Pro-inflammatory cytokines including but not limited to: TNF-a, IL-Iβ, IL-6, IL-17 family of proteins, IL-12, IL-18, IL-33.

Microneedle arrays of the type described herein can be used to deliver the immunogenic doses of one or more antigens and/or one or more immune adjuvants and/or other stimulating agents to the cutaneous microenvironment. Any number of different combinations are possible. For example, the microneedle arrays may contain:

- one antigen and one immune adjuvant or other stimulating agent,
- one antigen and two or more immune adjuvants or other stimulating agents,
- more than one antigen and one adjuvant or other stimulating agent, or
- more than one antigen and more than one adjuvant or other stimulating agent.

In some embodiments, the one or more antigens and/or one or more immune adjuvants and/or other stimulating agents to the cutaneous microenvironment is administered to the cutaneous microenvironment to treat patients with various tumors, and/or various viral, bacterial, parasitic, or fungus-based conditions. For example, in some embodiments, the immunizing treatments can be administered to the cutaneous microenvironment to treat patients with solid primary tumors, circulatory tumors (e.g., leukemias), solid tumor metastasis, or circulatory tumor megastasis. In other embodiments, the immunizing treatments can be administered to the cutaneous microenvironment to prevent and/or provide treatment for infectious diseases caused by viruses, bacteria and their toxins, parasites, and/or fungi. In some embodiments, the cutaneous delivery of these treatments is achieved by preparing and administering the microneedle arrays discussed herein.

As used herein, immuno-suppression means as any intervention with the purpose to downregulate the innate (inflammation) and adaptive immune responses. Thus, as discussed above, the present application discloses novel systems and methods of antigen-specific immune suppression or tolerance induction, which may reduce the occurrence of off-target adverse events resulting from generalized immunosupression and general anti-inflammatory treatments such as steroids, FK-506 and others. In addition, as discussed above, such treatments are applicable to a broad range of inflammatory and autoimmune diseases from allergy desensitization to the treatment of psoriasis, eczema, asthma, and potentially transplant rejection.

Other immunosuppressive agents that can be embodied and/or delivered in the manners described herein, include:

Modulators of pro-inflammatory cytokine function including cytokine receptor blockade (i.e.: anti -TNF-a receptor, anti- IL-1B receptor, anti-IL-6 receptors, anti-IL 12 receptors, anti-IL-13 receptor, anti-IL-17 receptor, anti-IL-18 receptor, anti-IL23 receptors, anti-IL-33 receptor) and or inflammatory cytokine neutralizers (i.e: soluble receptors, decoy receptors (IL-ipRA).

Inhibitors of Toll-like receptor ligands, including but not limited to TLR-L antagonists, soluble TLRs, agents blocking intracellular pathways activated by TTLR signaling.

Other embodiments can use **Anti-inflammatory molecules** including but not limited to IL-10, TGF Bl, indoleamine 2,3-dioxygenase (IDO), l,a25-dihydroxy vitamin D3 (Vitamin D3),

vascular endothelial growth factor (VEGF), Proopiomelanocortin (POMC) and derivatives including the Melanocyte stimulating hormone (MSH).

Other embodiments can use **molecules interfering with the DC-T cell synapse, inducers of T cell death and calcineurin** including but not limited to: Galectin-1 and 3, CD200, CD152 (CTLA-4) CD160 and CD244, Rapamycin, Programmed cell death ligand 1 and 2, (PD-L1 and PD-L2), Cyclosporine A, Tacrolimus, pimecrolimus.

Still other embodiments can use **agents blocking intracellular signaling pathways blockade,** including but not limited to: PI3K, AKT, mTOR, p38 inhibitors. Nuclear Factor κB (NFkB) inhibitors, Inhibitor of cytokine signaling 1 and 3 (SOCS1 SOCS 3), inhibitors of tyrosine phosphatase involved in TCR signaling (SHP-1)
STAT3, inhibitors of E3 ubiquitin ligase involved in TCR degradation (Cbl-b),
inhibitors of RELB IL-12., NFATcl and NFATc2.

Still other embodiments can use inhibitors of **B cell survival and function,** including but not limited to: soluble CD40L, anti-CD20, anti-Immunoglobulins.

Additional results relating to MNA delivery for immunization

Various additional results are discussed below and illustrated in FIGS. 51-56, which disclose the results of testing using both mouse and human skin models for positive and negative immunization.

With regard to an exemplary positive immunization MNA delivery system, FIGS. 51A and 5IB demonstrate the immunogenicity of skin microenvironment targeted delivery of a representative hapten antigen, and characterizes the contact hypersensitivity response generated. These figures illustrate an exemplary MNA-DNSB dose response, by indicating an optimal lowest dose of hapten contained in MNAs capable of inducing effective skin acute and chronic inflammation. In particular, FIG. 51A charts MNA-DNSB doses as a percentage of ear thickness increase. FIG. 5IB provides histological detail of treated ear skin following the application of MNAs with the three different doses of DNSB (25 ng, 50 ng, and 100 ng). The results demonstrate an optimal, lowest dose of 50 ng DNSB, since doses of 50 ng DNSB and 100 ng DNSB were not significantly different (NS).

With regard to an exemplary negative immunization MNA delivery system, FIGS. 52A, 52B, and 52C demonstrate that skin microenvironment targeted delivery of a hapten antigen with a potent NK1R antagonist, prevents an acute inflammatory response against that same hapten. This demonstrates, in this well-established animal model, the ability of the system described herein to treat inflammatory skin. FIG. 52A illustrates a percent of mouse ear thickness increase 24h and

48h following one application of DNSB ± NKIR antagonists MNAs. FIG. 52B illustrates histological detail of the treated ear reflected in FIG. 52A. FIG. 52C shows the draining of lymph node from MNA treated skin showing abrogation of inflammation in mouse lymph nodes treated with NKIR antagonists MNA. Accordingly, FIGS. 52A-C demonstrate a reduction of inflammation in both the skin and the draining lymph nodes.

FIGS. 53A and 53B illustrate additional exemplary results from negative immunization MNA systems, demonstrating that skin microenvironment targeted delivery of a hapten antigen with a potent NKIR antagonist can similarly reduce an established chronic inflammatory response via a similar mechanism. FIG. 53A illustrate a percent of mouse ear thickness increase 24h, 48h, and 72h following sensitization (priming) and elicitation (challenge) seven days apart with DNSB ± NKIR antagonists MNAs. FIG. 53B illustrates histological detail of the treated ear reflected in FIGS. 53A.

FIGS. 54A, 54B, and 54C illustrate additional exemplary results from negative immunization MNA systems. These figures illustrate the role of the NKIR in the mechanism of immune suppression by demonstrating that NKIR improves T-cell survival. FIG. 54A provides an exemplary flow cytometry analysis and FIG. 54B provides a quantitative comparison of six independent experiments, showing that NKIR greatly improves the survival of activated T cells. FIG. 54C illustrates that NKIR improves IL-2 secretion by activated T cells, which is necessary to support the viability of activated T cells.

FIGS. 55A, 55B, 55C, and 55D illustrate the activation and migration of human skin dendritic cell subsets. As shown in these figures, for negative immunization, the skin microenvironment targeted delivery in human skin results in the same mechanistic effects as those observed in animal studies. Specifically, the NKIR blockade affects the migration, phenotype and T cell stimulatory function of human skin dendritic cells. FIG. 55A illustrates a number of total dendritic cells (DC) from human skin samples quantified following spontaneous migration or following sking treatment with MNA alone (negative control), MNA-DNCB, MNA-L733,060, or MNA-DNCB-L733,060. FIG. 55B and 55C demonstrates that an administration of NKIR antagonists modifies the relative number of different DC subsets (FIG. 55B) and decreases the expression of Ag presenting and co-stimulatory molecules (FIG. 55C). A mean ± 1 SD of DC number from 10 independent samples are shown in FIGS. 55A-C. FIG. 55D demonstrates that the addition of L733,060 in MLC cultures significantly reduces allogeneic T cell proliferation in response to DC stimulation.

FIGS. 56A and 56B illustrate additional exemplary results from negative immunization MNA systems. These figures demonstrate that NKIR improves T-cell survival of activated human

T cells. FIGS. 56A and 56B provide exemplary flow cytometry analyses indicating that NK1R greatly improves the survival of activated T cells following signally via CD3 and CD28 by artificial Ag presenting cells.

In view of the many possible embodiments to which the principles of the disclosed embodiments may be applied, it should be recognized that the illustrated embodiments are only preferred examples and should not be taken as limiting the scope of protection. Rather, the scope of the protection is defined by the following claims. We therefore claim all that comes within the scope and spirit of these claims.

We claim:

1. A method for reducing or desensitizing an immune response of a subject in need thereof, the method comprising:

administering one or more sub-immunogenic or non-immunogenic doses of an allergen/antigen to a cutaneous microenvironment of the subject, and thereby reducing or desensitizing the immune response of the subject.

2. The method of claim 1, wherein administering the one or more sub-immunogenic or non-immunogenic doses of the allergen comprises the use of one or more microneedle arrays containing the allergen/antigen therein.

3. The method of claim 1, further comprising:

administering one or more immune suppressants and/or tolerizing agents to the cutaneous microenvironment.

4. The method of claim 3, wherein administering the one or more sub-immunogenic or non-immunogenic doses of the allergen/antigen and the one or more immune suppressants and/or tolerizing agents comprises the use of one or more microneedle arrays containing the allergen/antigen and the one or more immune suppressants and/or tolerizing agents therein.

5. The method of claim 3 or 4, wherein the one or more immune suppressants and/or tolerizing agents comprises at least one selected from the group of NKR antagonists, Foxo3 inhibitors, and Anti-TNF Ab.

6. The method of claims of any of 3-5, wherein at least two immune suppressants and/or tolerizing agents are administered.

7. The method of any of the preceding claims, wherein the subject is at risk of acquiring or having at least one of the following conditions or disorders: contact dermatitis, atopic dermatitis, psoriasis, immunobullous diseases, inflammatory skin disorders, Type I-V hypersensitivity reactions, and systemic autoimmune disorders.

8. The method of any of the preceding claims, further comprising:

identifying a subject at risk of acquiring or having at least one of the following conditions or disorders: contact dermatitis, atopic dermatitis, psoriasis, immunobullous diseases, inflammatory skin disorders, Type I-V hypersensitivity reactions, and systemic autoimmune disorders.

9. The method of any of the preceding claims, wherein the one or more sub-immunogenic or non-immunogenic doses are administered to the skin or skin draining lymph nodes by needle or other methods of drug delivery.

10. A method for promoting a pro-inflammatory and an adaptive immune response to provide a positive immunization against tumors and infectious diseases to a subject in need thereof, the method comprising:

administering an antigen and at least one adjuvant in a cutaneous microenvironment of the subject, thereby promoting the pro-inflammatory and adaptive immune response in the subject.

11. The method of claim 10, wherein administering the antigen and at least one adjuvant comprises the use of one or more microneedle arrays containing the antigen and the at least one adjuvant therein.

12. The method of claim 10 or 11, wherein the one or more adjuvants comprise proinflammatory tachykinins.

13. The method of claim 12, wherein the proinflammatory tachykinins comprise at least one selected from the group consisting of substance-P and analogs, Hemokinin-A and analogs, Neurokinin-B and analogs, bradykinin and analogs, vascular intestinal peptide and analogs, and calcitonin-gene-related peptide (CGRP) and analogs.

14. The method of claim 10 or 11, wherein the one or more adjuvants comprise toll-like receptor-ligands (TLRs).

15. The method of claim 10 or 11, wherein the one or more adjuvants comprise pro-inflammatory cytokines.

16. The method of claim 15, wherein the pro-inflammatory cytokines comprise at least one selected from the group consisting of TNF-a, IL-Iβ, IL-6, IL-17 family of proteins, IL-12, IL-18, and IL-33.

17. The method of any of claims 12-16, wherein administering the antigen and at least one adjuvant comprises the use of one or more microneedle arrays containing the antigen and the at least one adjuvant therein.

18. A method for promoting an immune response to a subject in need thereof, the method comprising:

administering an antigen and at least one adjuvant in a cutaneous microenvironment of the subject, thereby promoting the immune response in the subject.

19. The method of claim 18, wherein the at least one adjuvant is selected from the group consisting of proinflammatory tachykinins, toll-like receptor-ligands (TLR-s), and pro-inflammatory cytokines.

20. The method of claim 19, wherein the at least one adjuvant comprises at least one proinflammatory tachykinin selected from the group consisting of substance-P and analogs, Hemokinin-A and analogs, Neurokinin-B and analogs, bradykinin and analogs, vascular intestinal peptide and analogs, and calcitonin-gene-related peptide (CGRP) and analogs.

21. The method of claim 19, wherein the at least one adjuvant comprises pro-inflammatory cytokines selected from the group consisting of TNF-a, IL-Iβ, IL-6, IL-17 family of proteins, IL-12, IL-18, and IL-33.

22. The method of any of claims 18-21, wherein administering the antigen and the at least one adjuvant comprises the use of one or more microneedle arrays containing the antigen and the at least one adjuvant therein.

23. A method for promoting an immune response to a subject in need thereof, the method comprising:

administering an antigen and at least two adjuvants in a cutaneous microenvironment of the subject, thereby promoting the immune response in the subject.

24. The method of claim 23, wherein the at least two adjuvants are selected from the group consisting of proinflammatory tachykinins, toll-like receptor-ligands (TLR-s), and pro-inflammatory cytokines.

25. The method of claim 24, wherein the at least two adjuvants comprise at least one proinflammatory tachykinins selected from the group consisting of substance-P and analogs, Hemokinin-A and analogs, Neurokinin-B and analogs, bradykinin and analogs, vascular intestinal peptide and analogs, and calcitonin-gene-related peptide (CGRP) and analogs.

26. The method of claim 24, wherein the at least two adjuvants comprise pro-inflammatory cytokines selected from the group consisting of TNF-a, IL-1β, IL-6, IL-17 family of proteins, IL-12, IL-18, and IL-33.

27. The method of any of claims 23-26, wherein administering the antigen and two or more adjuvants comprises the use of one or more microneedle arrays containing the antigen and the two or more adjuvants therein.

28. The method of any of claims 10-27, wherein the subject is at risk of acquiring or having one or more of a solid primary tumor, a circulatory tumor, or a condition of solid tumor or circulatory tumor metastasis.

29. The method of any of claims 10-27, wherein the subject is at risk of acquiring or having one or more infectious diseases caused by a virus, a bacteria and/or its toxin, a parasite, or a fungi.

30. A dissolvable microneedle array for transdermal insertion into a patient for reducing or desensitizing an immune response in a subject in need thereof, the array comprising:

a base portion; and

a plurality of microneedles extending from the base portion and containing a sub-immunogenic dose of an allergen/antigen.

31. The microneedle array of claim 30, wherein the plurality of microneedles further comprise one or more immune suppressants and/or tolerizing agents.

32. The microneedle array of claim 30, wherein the one or more immune suppressants and/or tolerizing agents comprises at least one selected from the group of NKR antagonists, Fbxo3 inhibitors, and Anti-TNF Ab.

33. The microneedle array of claim 30, wherein the plurality of microneedles comprise at least two immune suppressants and/or tolerizing agents.

34. A dissolvable microneedle array for transdermal insertion into a patient for promoting an immune response in a subject in need thereof, the array comprising:

a base portion; and

a plurality of microneedles extending from the base portion and containing a an antigen and at least one adjuvant.

35. The microneedle array of claim 34, wherein the one or more adjuvant comprises proinflammatory tachykinins.

36. The microneedle array of claim 35, wherein the proinflammatory tachykinins comprise at least one selected from the group consisting of substance-P and analogs, Hemokinin-A and analogs, Neurokinin-B and analogs, bradykinin and analogs, vascular intestinal peptide and analogs, and calcitonin-gene-related peptide (CGRP) and analogs.

37. The microneedle array of claim 34, wherein the one or more adjuvants comprise toll-like receptor-ligands (TLR-s).

38. The microneedle array of claim 34, wherein the one or more adjuvants comprise pro-inflammatory cytokines.

39. The microneedle array of claim 38, wherein the pro-inflammatory cytokines comprise at least one selected from the group consisting of TNF-a, IL-Iβ, IL-6, IL-17 family of proteins, IL-12, IL-18, and IL-33.

40. The microneedle array of any of claims 30-39, wherein the plurality of microneedles are obelisk in shape.

41. The microneedle array of any of claims 30-39, wherein the plurality of microneedles are pre-formed to have a shape that comprises a first cross-sectional dimension at a top portion, a second cross-sectional dimension at a bottom portion, and a third cross-sectional dimension at an intermediate portion, wherein the intermediate portion is located between the top portion and the bottom portion, and the third cross-sectional dimension is greater than the first and second cross-sectional dimensions.

42. The microneedle array of any of claims 30-41, wherein each microneedle comprises a plurality of layers of dissoluble biocompatible material.

43. The microneedle array of claim 42, wherein the dissoluble biocompatible material is carboxymethylcellulose.

FIG. 1

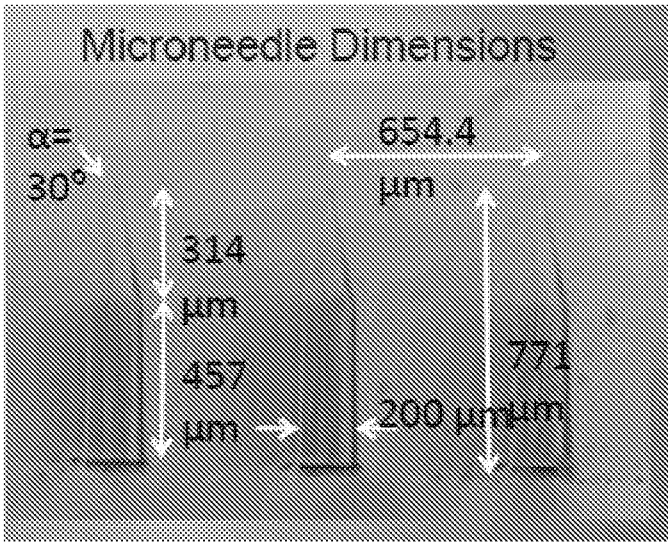
Microneedle Dimensions
α=
30°
654.4
μm
314
μm
457
μm
200 μm
771
μm

FIG. 2

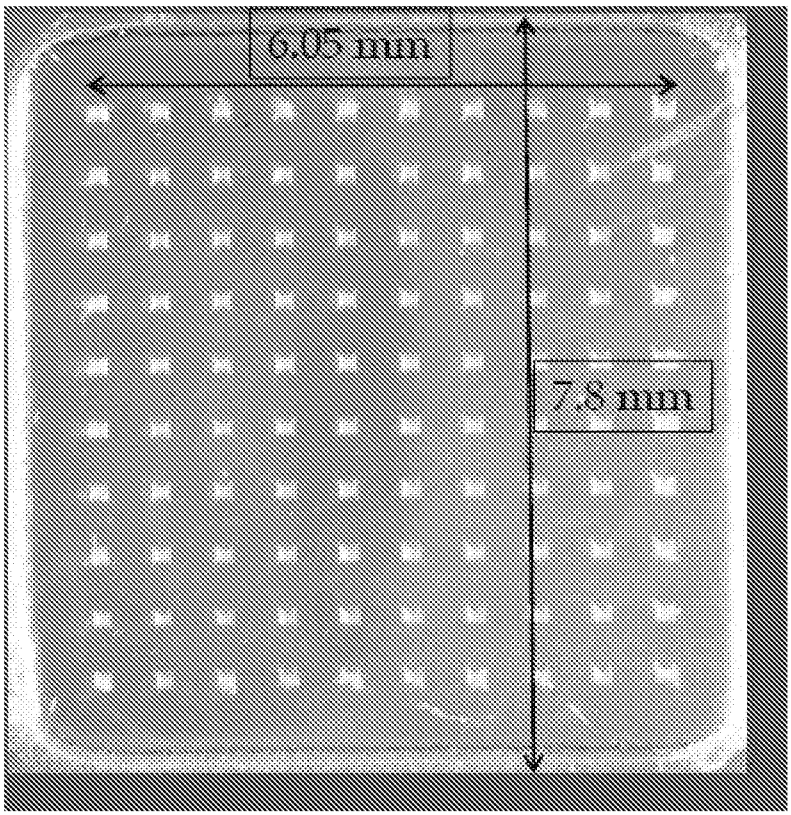
9.05 mm
7.8 mm

FIG. 3A

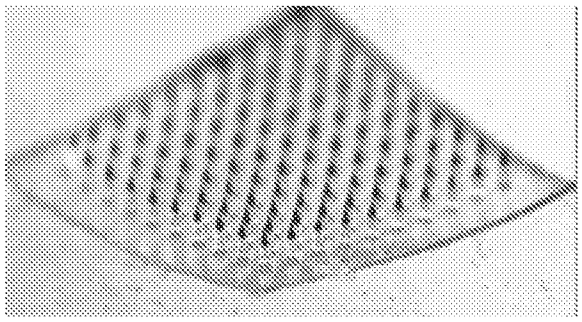

FIG. 3B

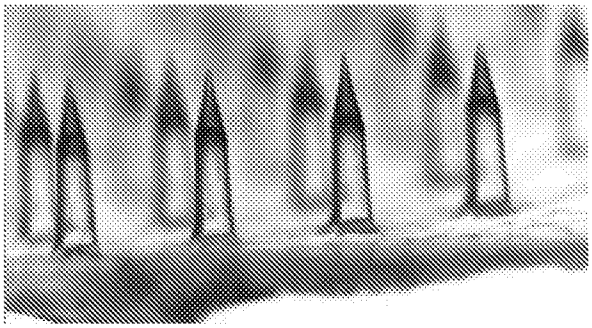

FIG. 4A

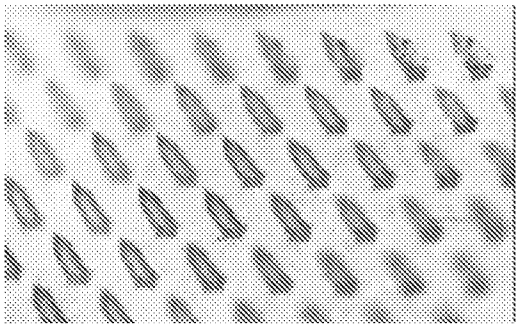

FIG. 4B

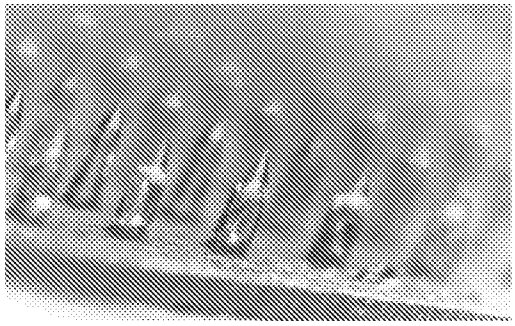

FIG. 5A

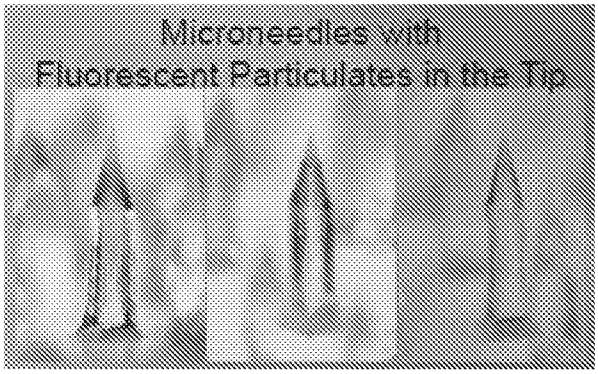

FIG. 5B

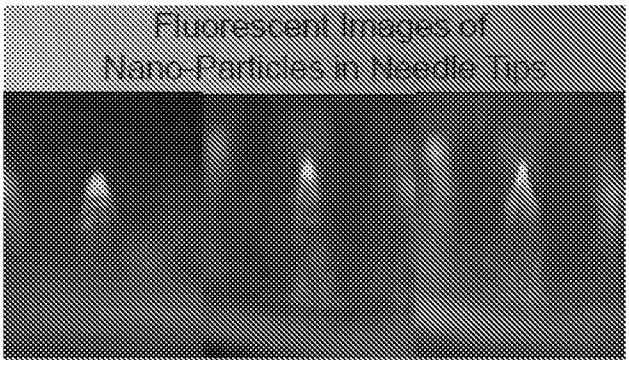

FIG. 6A

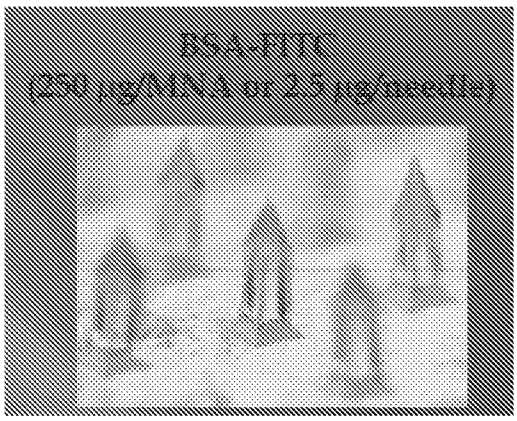

FIG. 6B

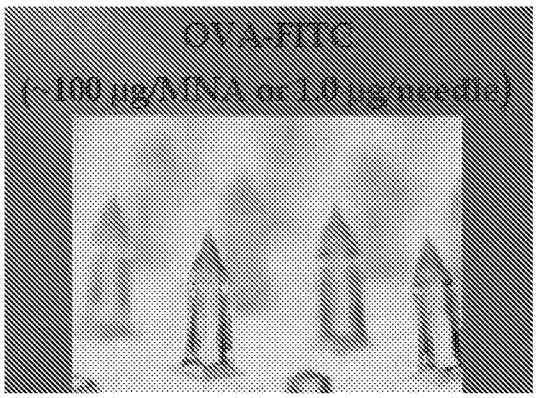

FIG. 7

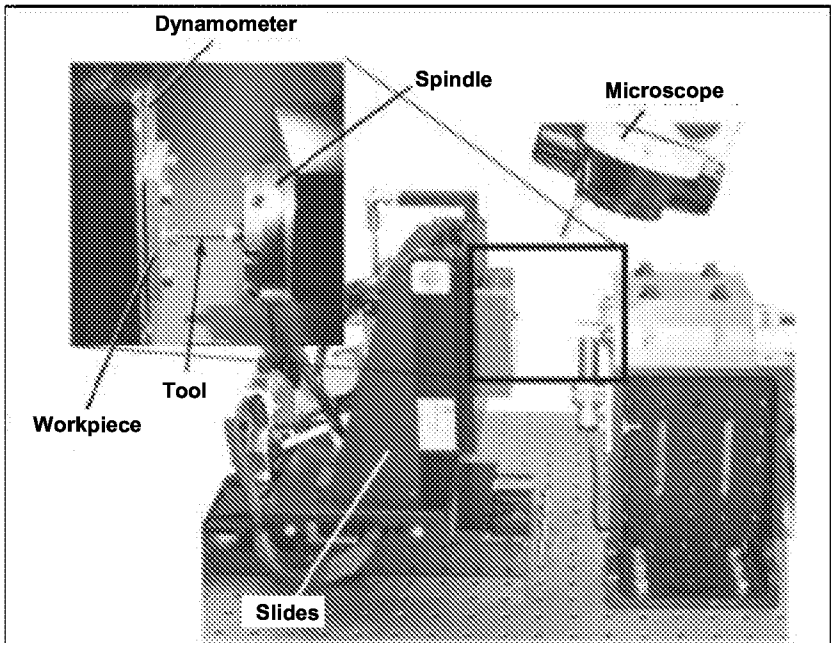
Dynamometer
Spindle
Microscope
Tool
Workpiece
Slides

FIG. 8

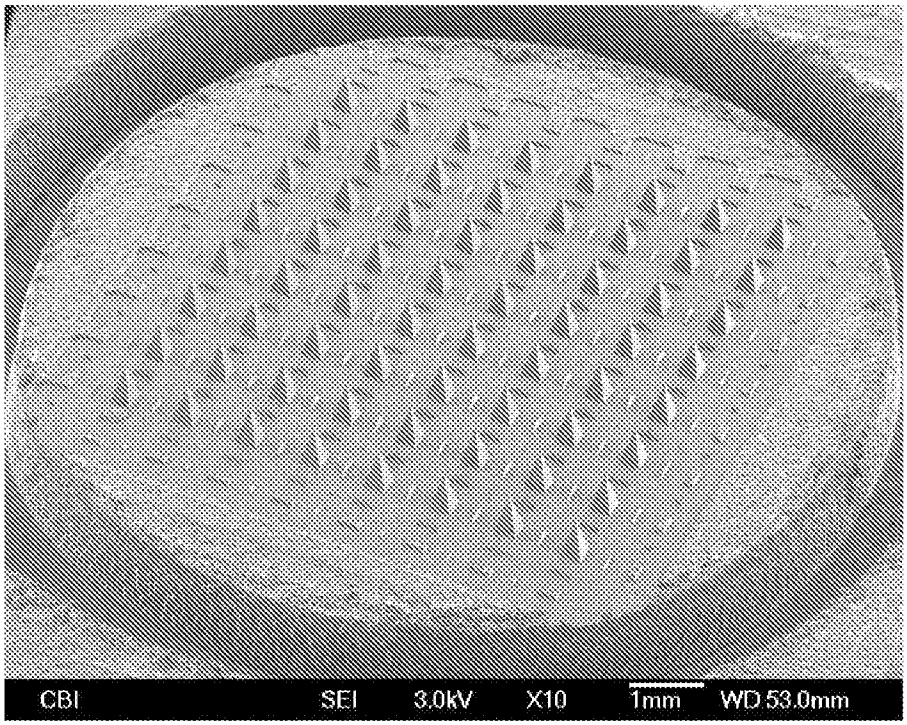
CBI
SEI
3.0kV
X10
1mm
WD 53.0mm

FIG. 9

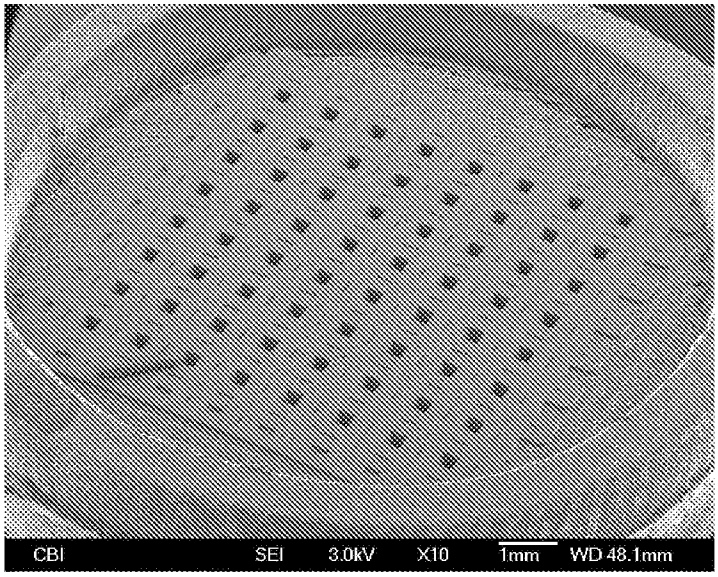

FIG. 10

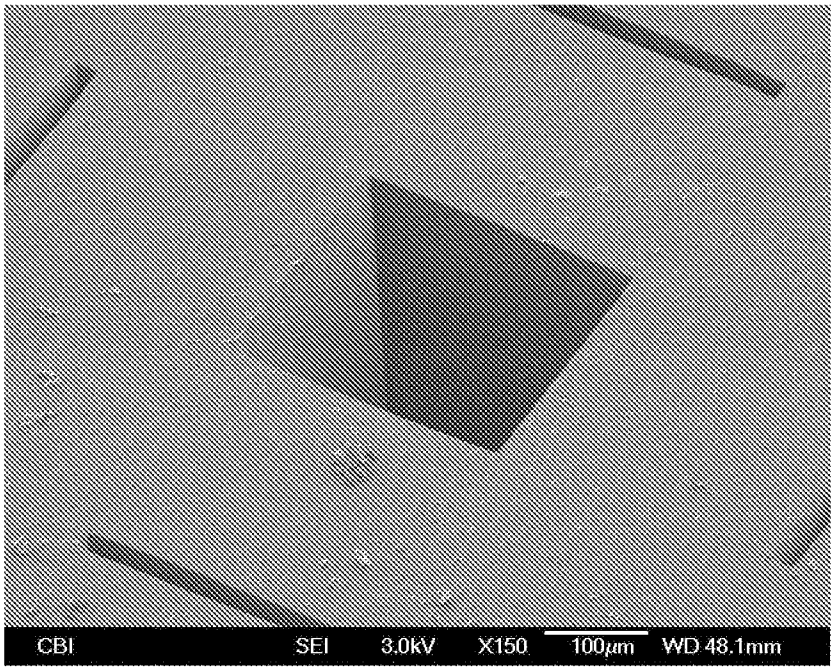

FIG. 11A

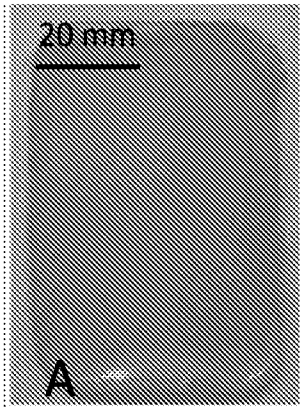

FIG. 11B

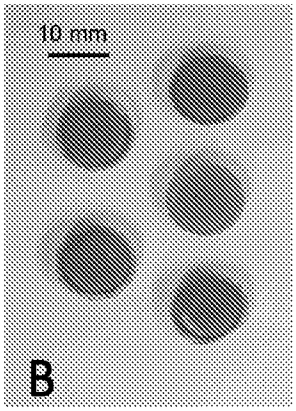

FIG. 11C

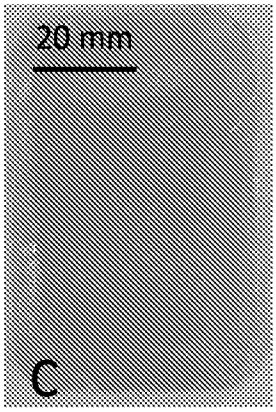

FIG. 11D

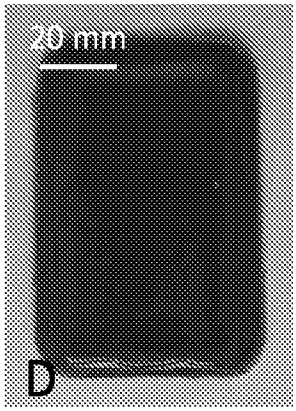

FIG. 12A

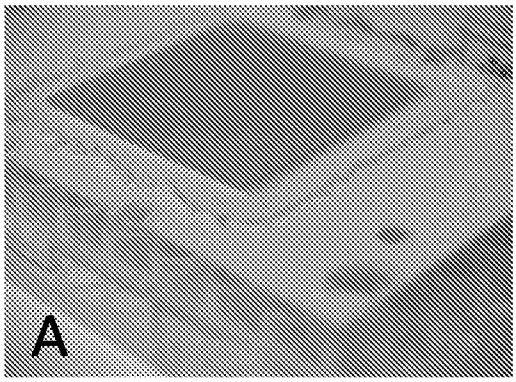

FIG. 12B

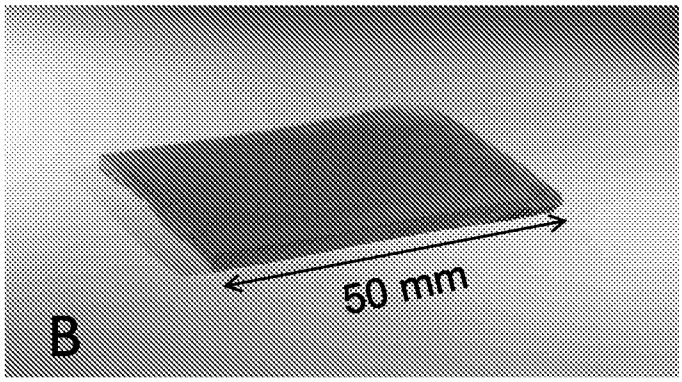

FIG. 13

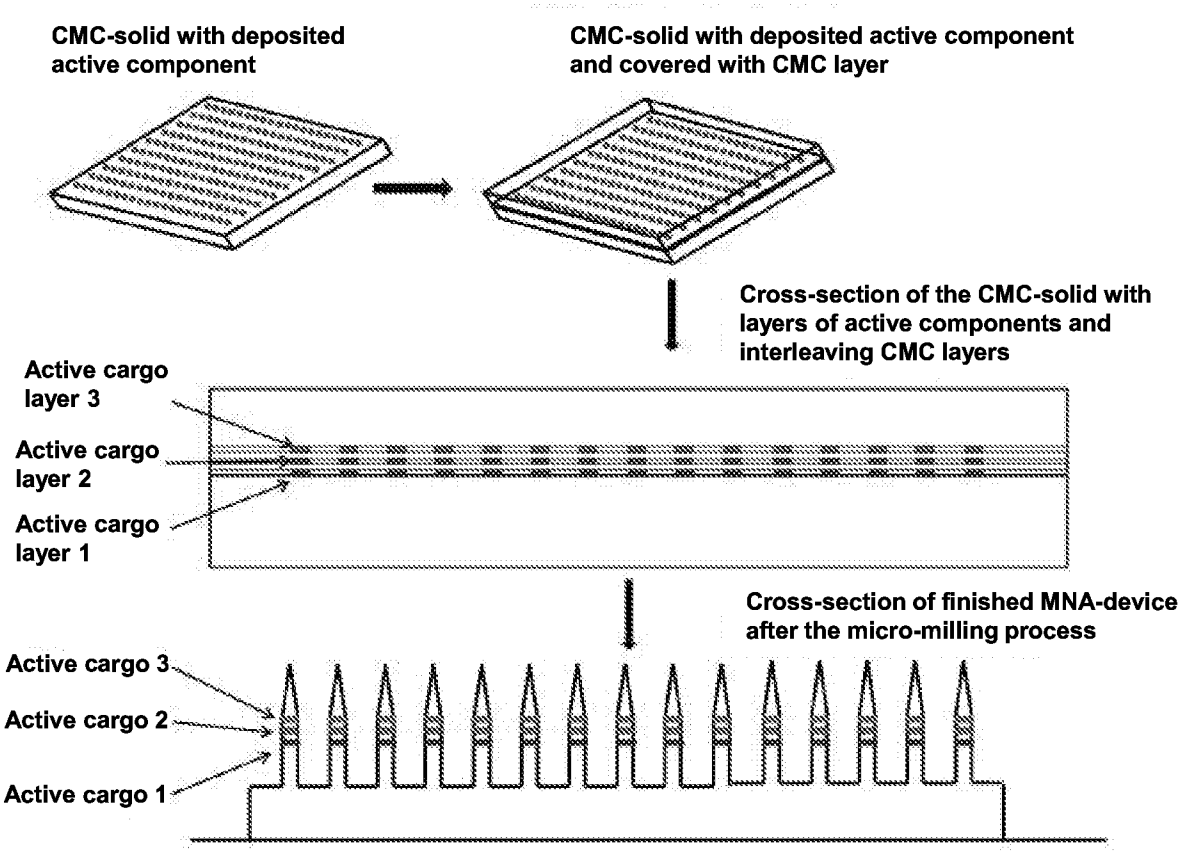
CMC-solid with deposited active component
CMC-solid with deposited active component and covered with CMC layer
Cross-section of the CMC-solid with layers of active components and interleaving CMC layers
Active cargo layer 3
Active cargo layer 2
Active cargo layer 1
Cross-section of finished MNA-device after the micro-milling process
Active cargo 3
Active cargo 2
Active cargo 1

FIG. 14

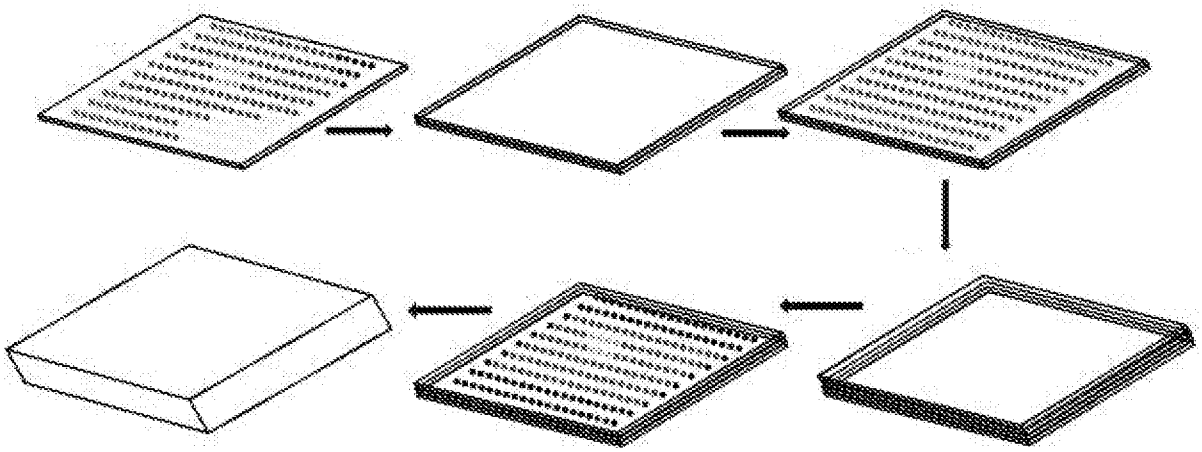

FIG. 15

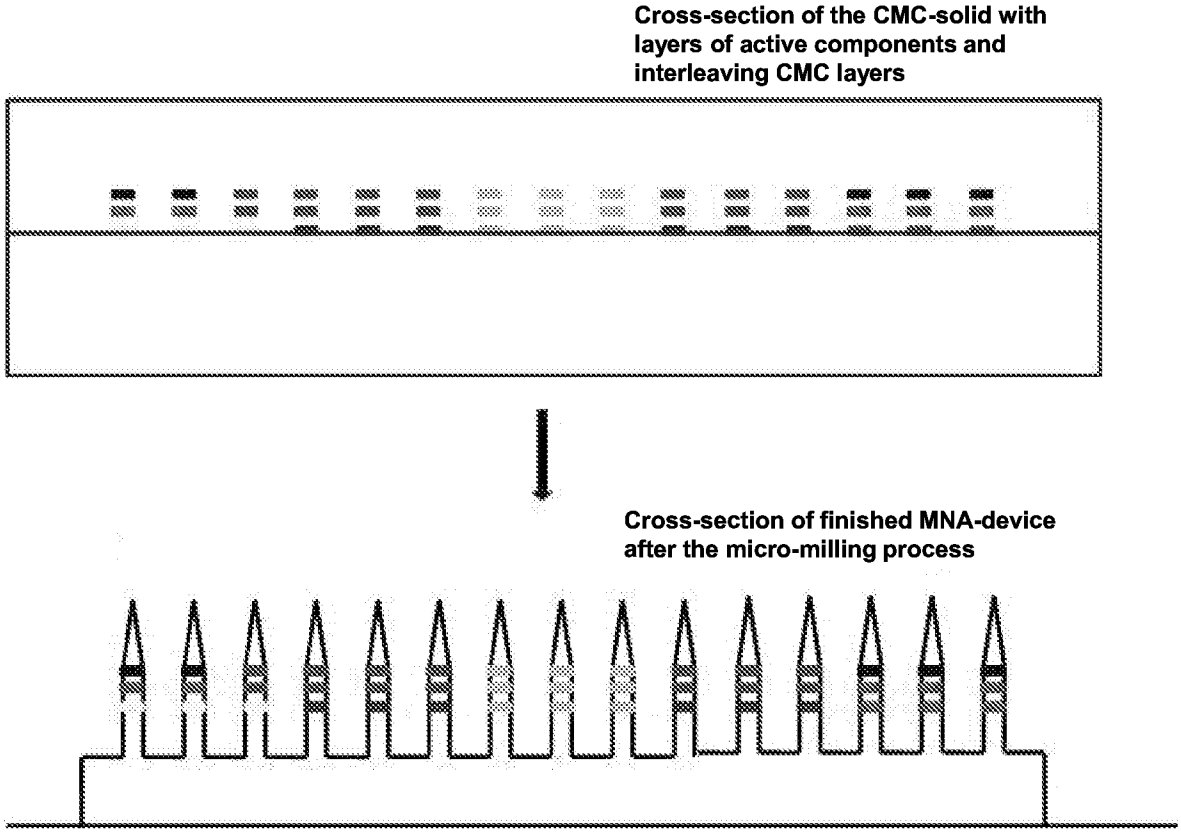
Cross-section of the CMC-solid with layers of active components and interleaving CMC layers
Cross-section of finished MNA-device after the micro-milling process

FIG. 16A

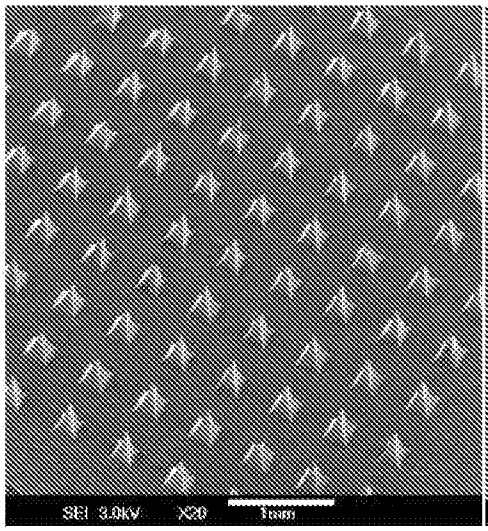

FIG. 16B

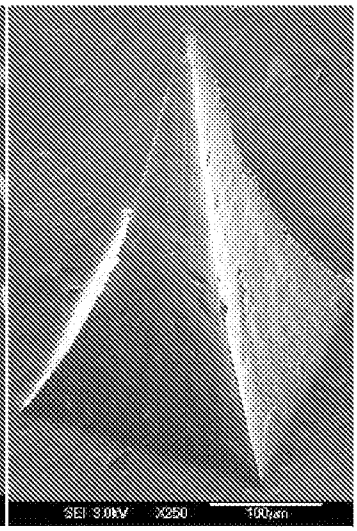

FIG. 17

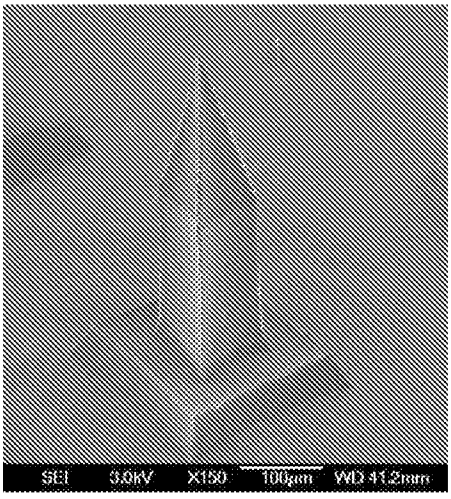

FIG. 18

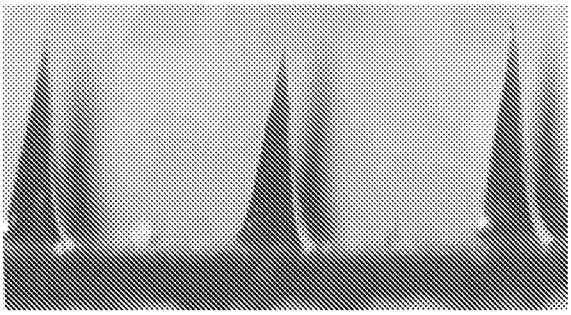

FIG. 19

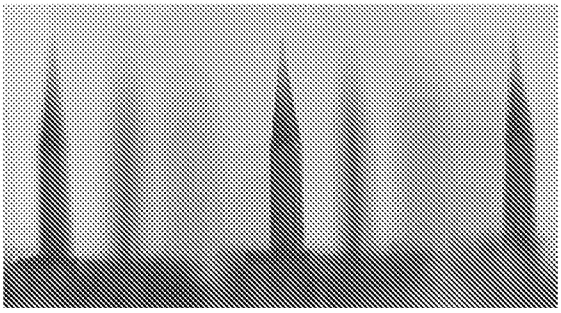

FIG. 20

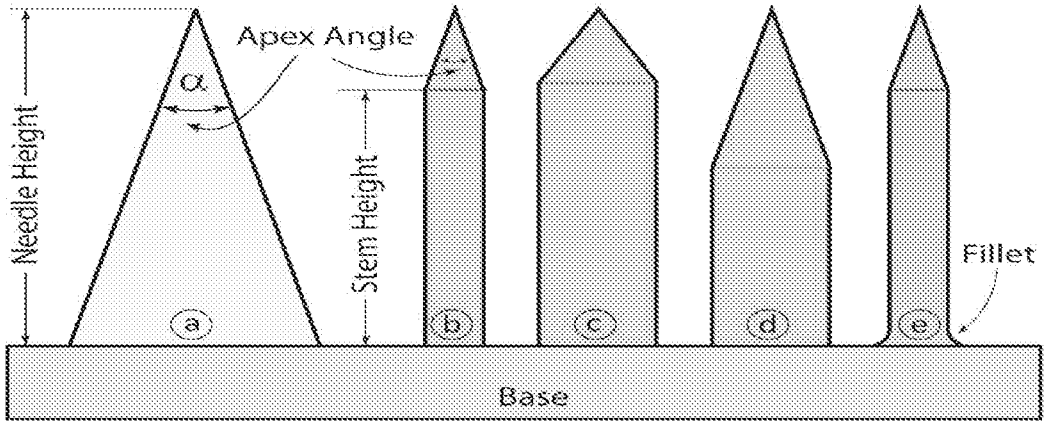

FIG. 21

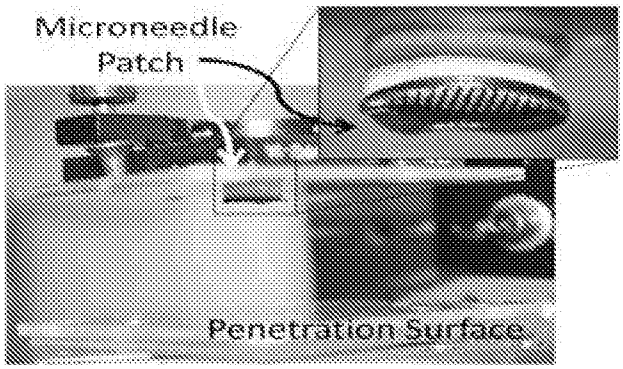
Microneedle
Patch
Penetration Surface

FIG. 22

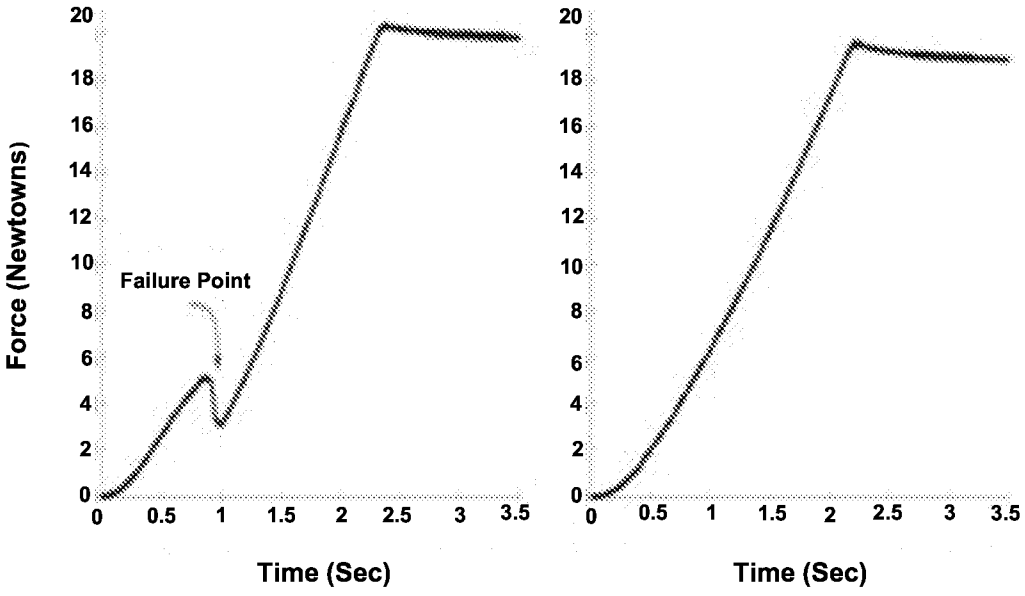
Force (Newtowns)
Failure Point
Time (Sec)
Time (Sec)

FIG. 23

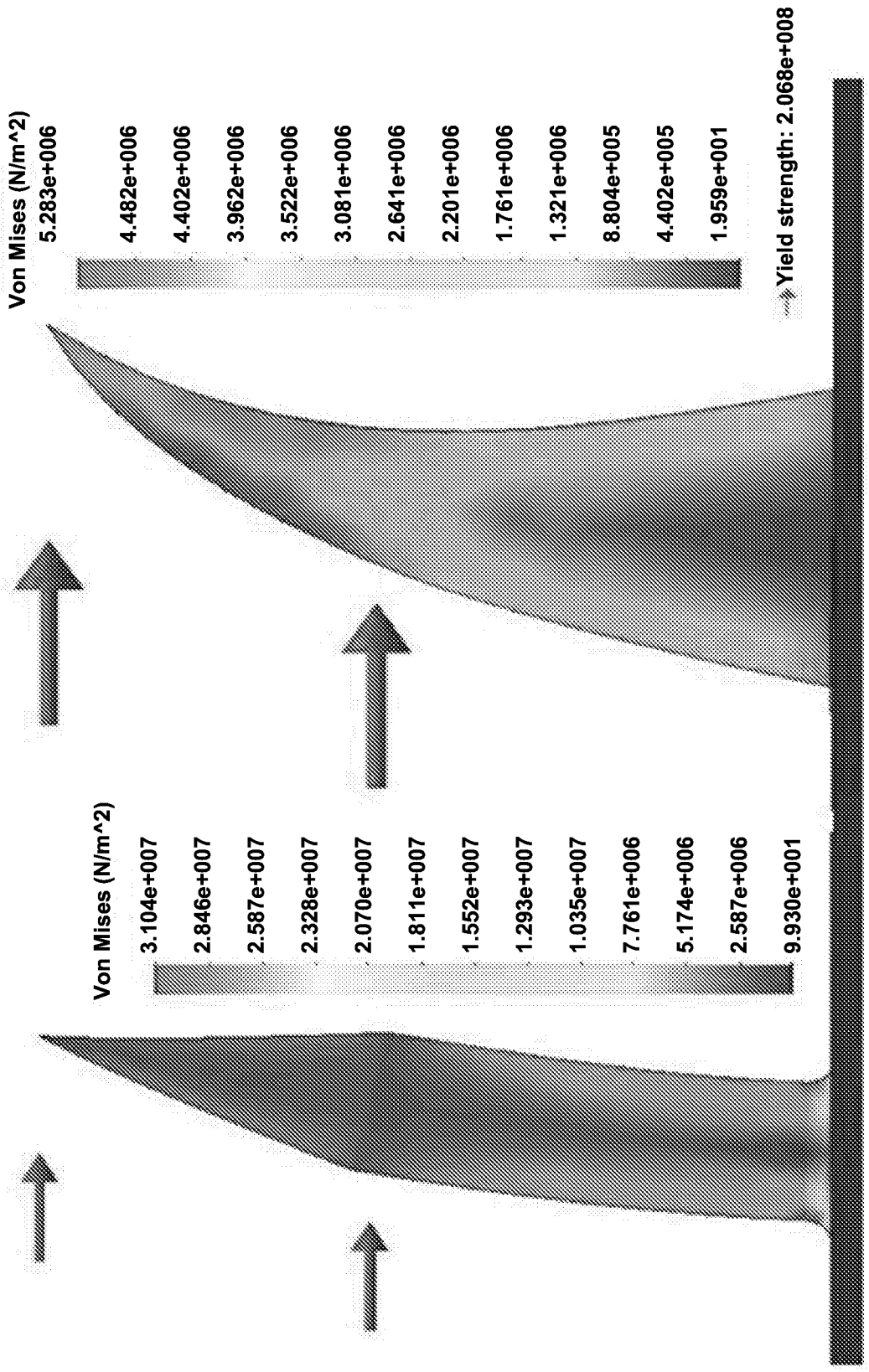
Von Mises (N/m^2)
3.104e+007
2.846e+007
2.587e+007
2.328e+007
2.070e+007
1.811e+007
1.552e+007
1.293e+007
1.035e+007
7.761e+006
5.174e+006
2.587e+006
9.930e+001
Von Mises (N/m^2)
5.283e+006
4.482e+006
4.402e+006
3.962e+006
3.522e+006
3.081e+006
2.641e+006
2.201e+006
1.761e+006
1.321e+006
8.804e+005
4.402e+005
1.959e+001
Yield strength: 2.068e+008

FIG. 24A

FIG. 24B

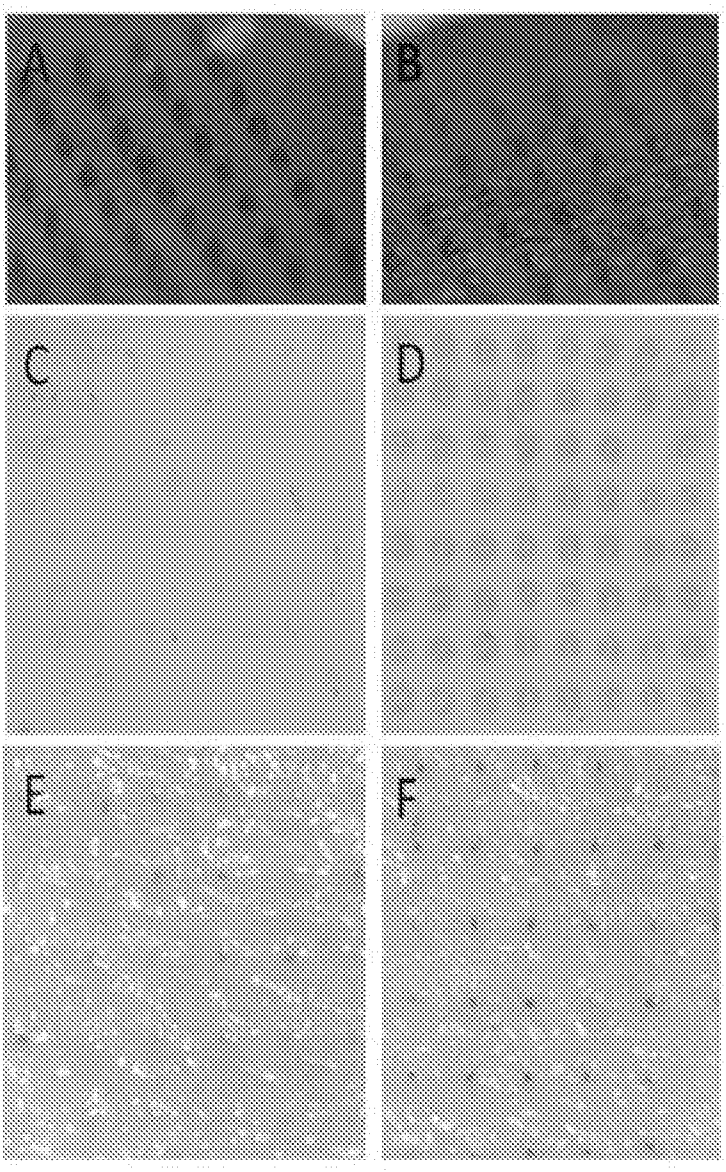

FIG. 24C

FIG. 24D

FIG. 24E

FIG. 24F

FIG. 25A

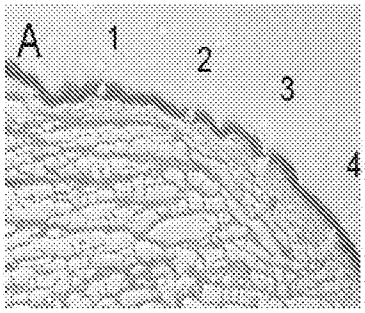

FIG. 25B

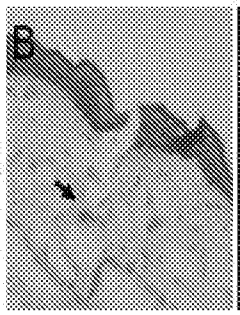

FIG. 25C

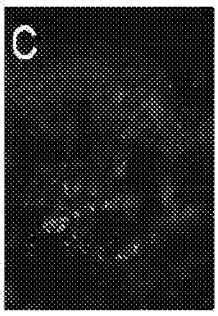

FIG. 26A

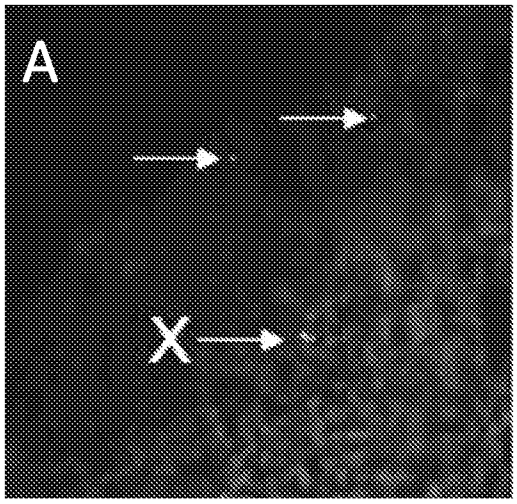

FIG. 26B

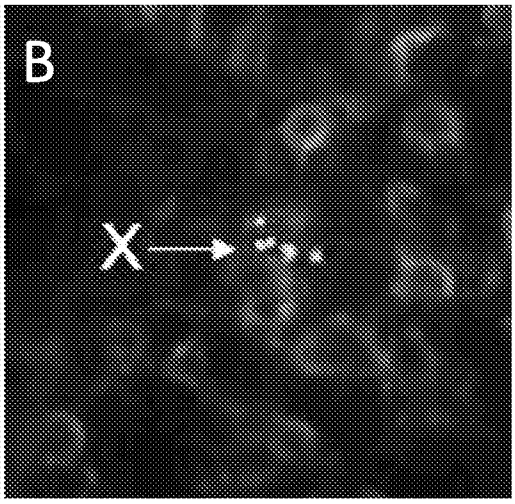

FIG. 27

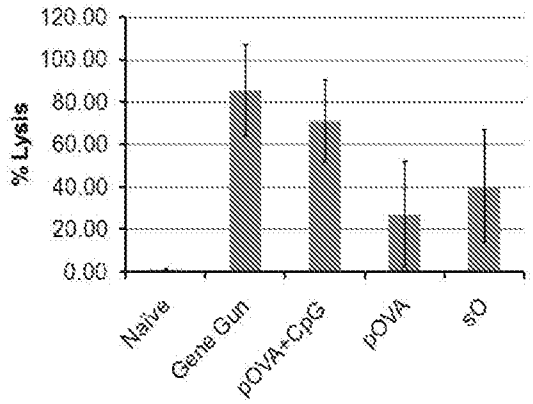

FIG. 28

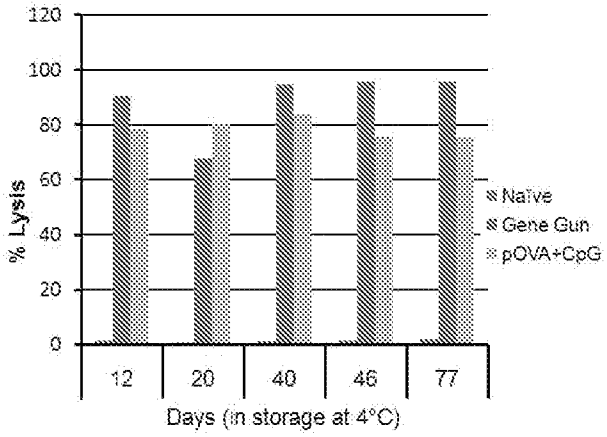

FIG. 29A

FIG. 29B

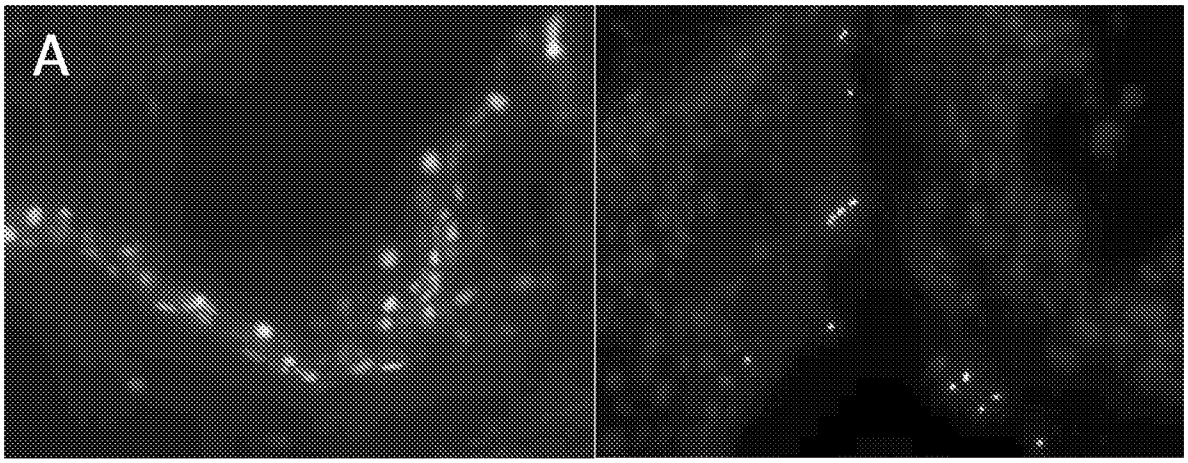

FIG. 30

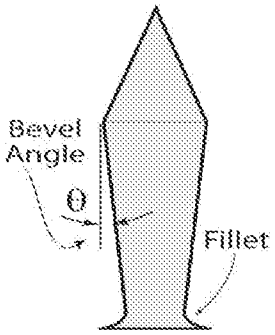

FIG. 31

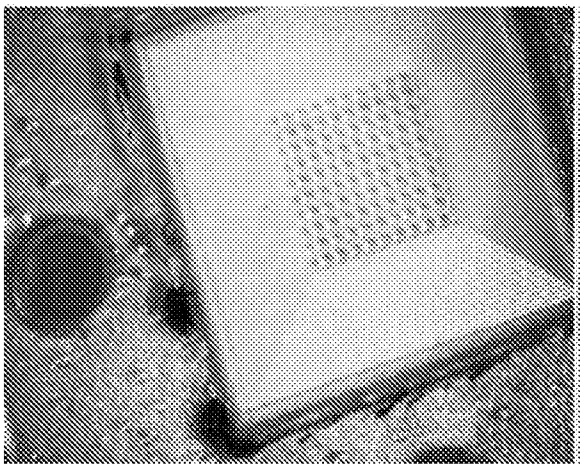

FIG. 32

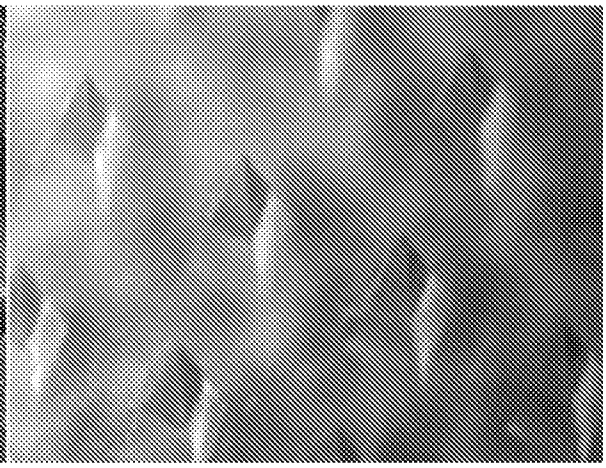

FIG. 33

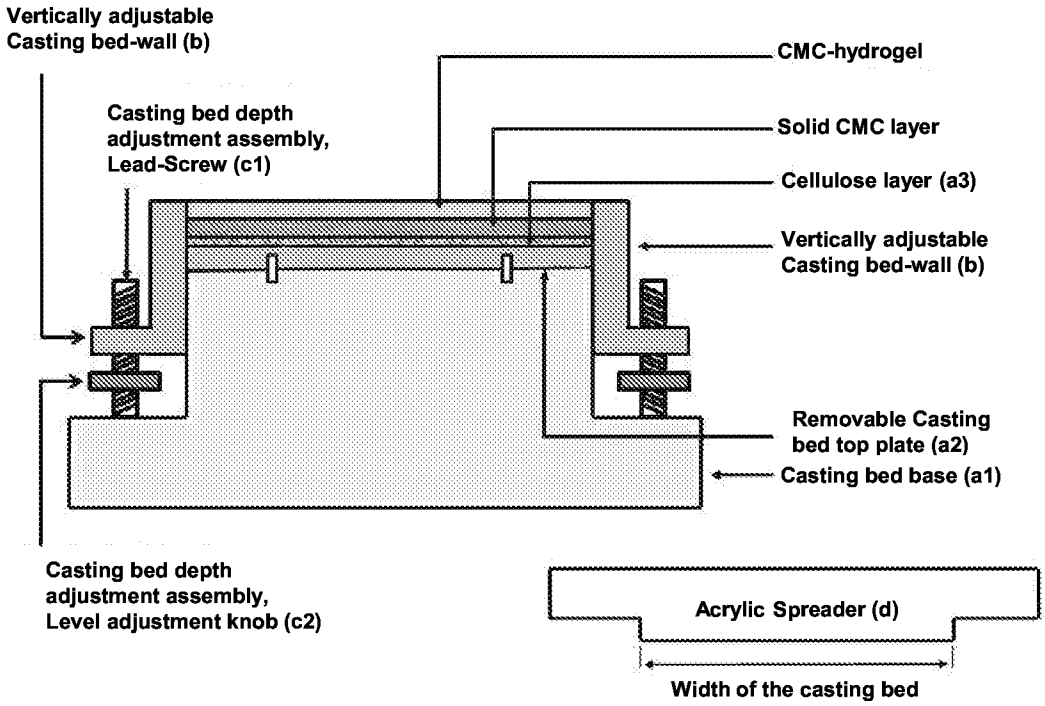
Vertically adjustable
Casting bed-wall (b)
CMC-hydrogel
Casting bed depth
adjustment assembly,
Lead-Screw (c1)
Solid CMC layer
Cellulose layer (a3)
Vertically adjustable
Casting bed-wall (b)
Removable Casting
bed top plate (a2)
Casting bed base (a1)
Casting bed depth
adjustment assembly,
Level adjustment knob (c2)
Acrylic Spreader (d)
Width of the casting bed

FIG. 34

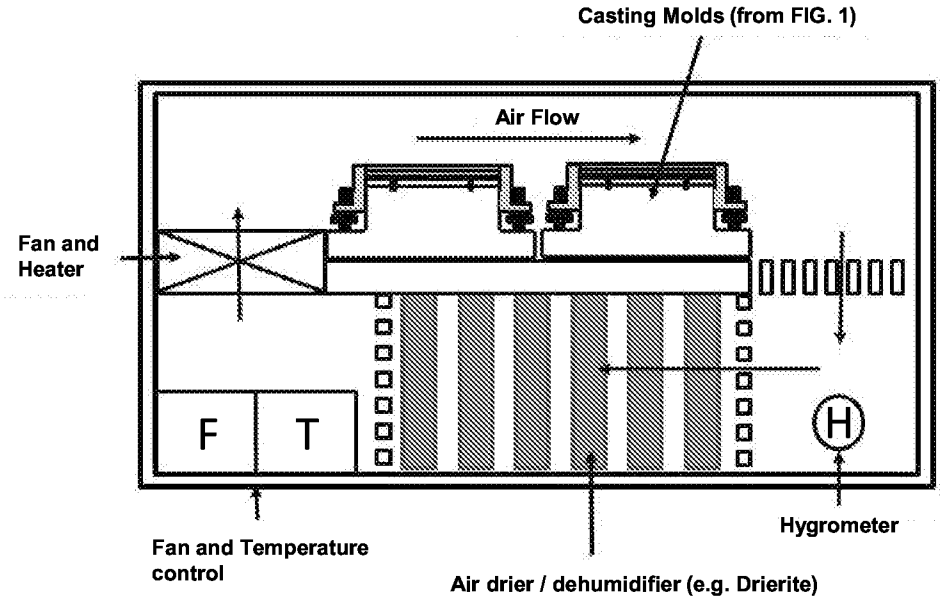
Casting Molds (from FIG. 1)
Air Flow
Fan and
Heater
F
T
H
Hygrometer
Fan and Temperature
control
Air drier / dehumidifier (e.g. Drierite)

FIG. 35

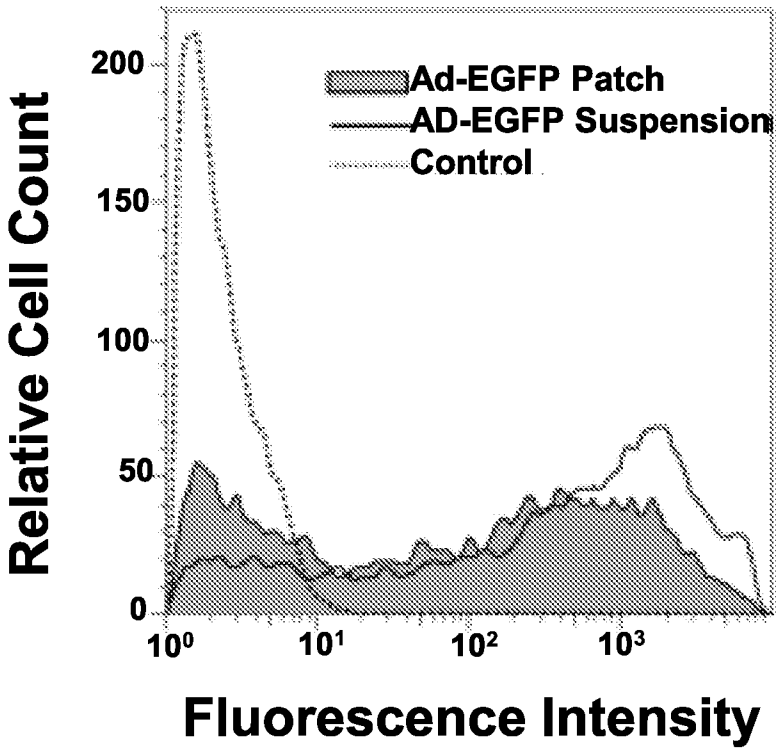
Relative Cell Count
200
150
100
50
0
Ad-EGFP Patch
AD-EGFP Suspension
Control
10^0
10^1
10^2
10^3
Fluorescence Intensity

FIG. 36

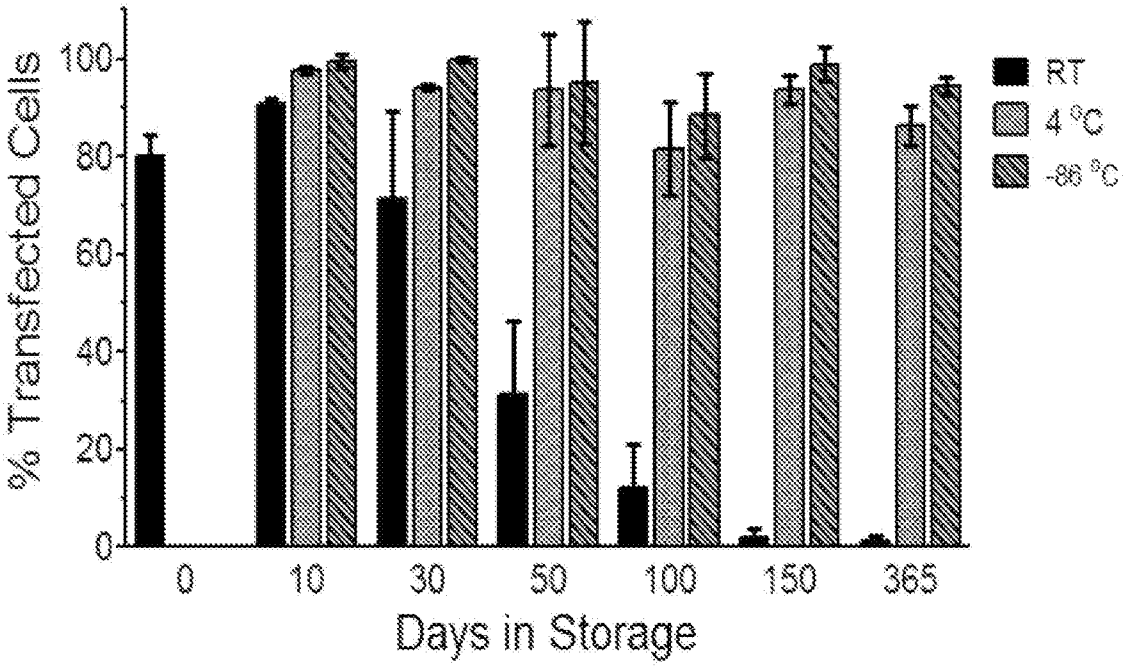
% Transfected Cells
100
80
60
40
20
0
RT
4 °C
-86 °C
0
10
30
50
100
150
365
Days in Storage

FIG. 37

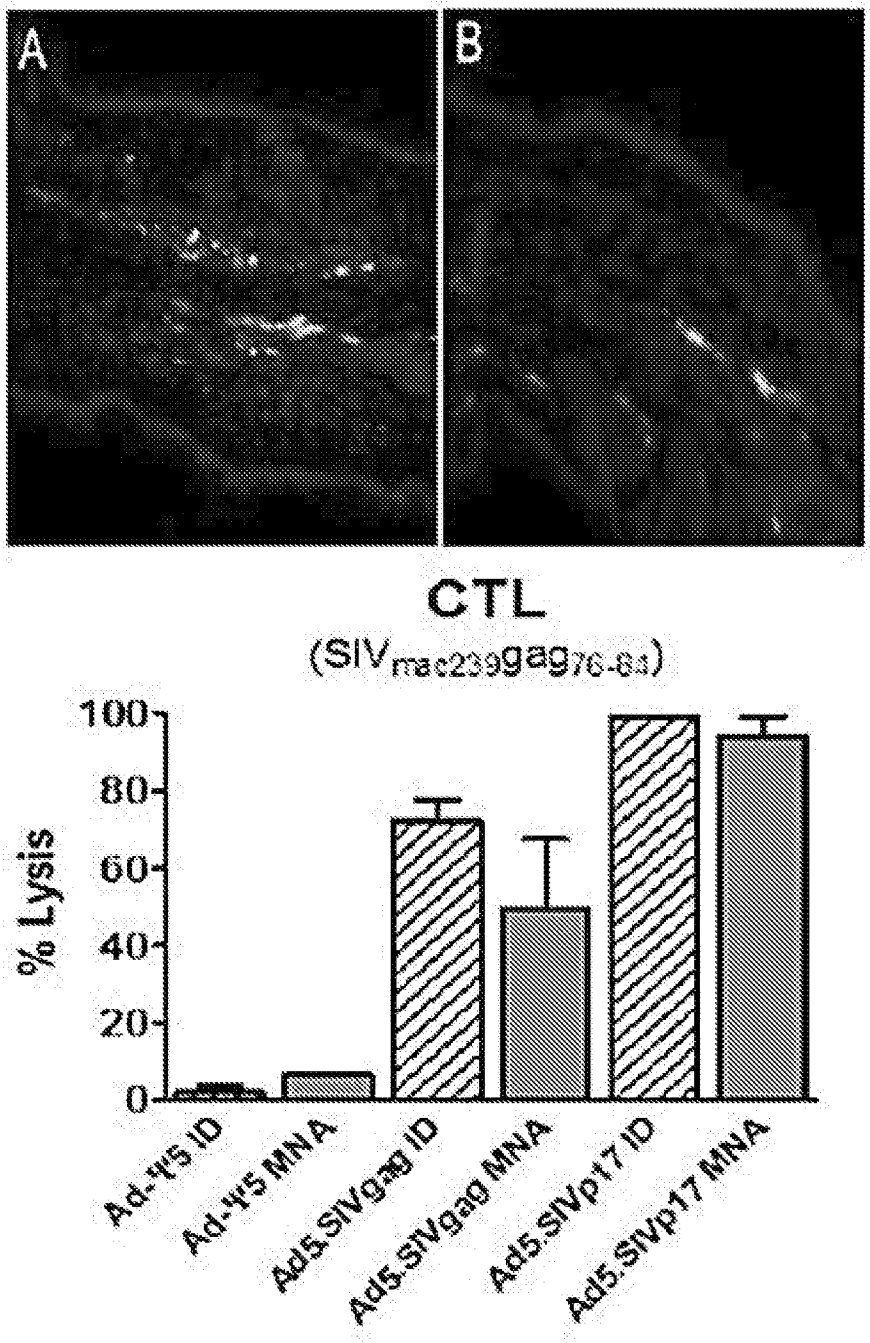
A
B
CTL
(SIVmac239gag76-84)
% Lysis
100
80
60
40
20
0
Ad-Y5 ID
Ad-Y5 MNA
Ad5.SIVgag ID
Ad5.SIVgag MNA
Ad5.SIVp17 ID
Ad5.SIVp17 MNA

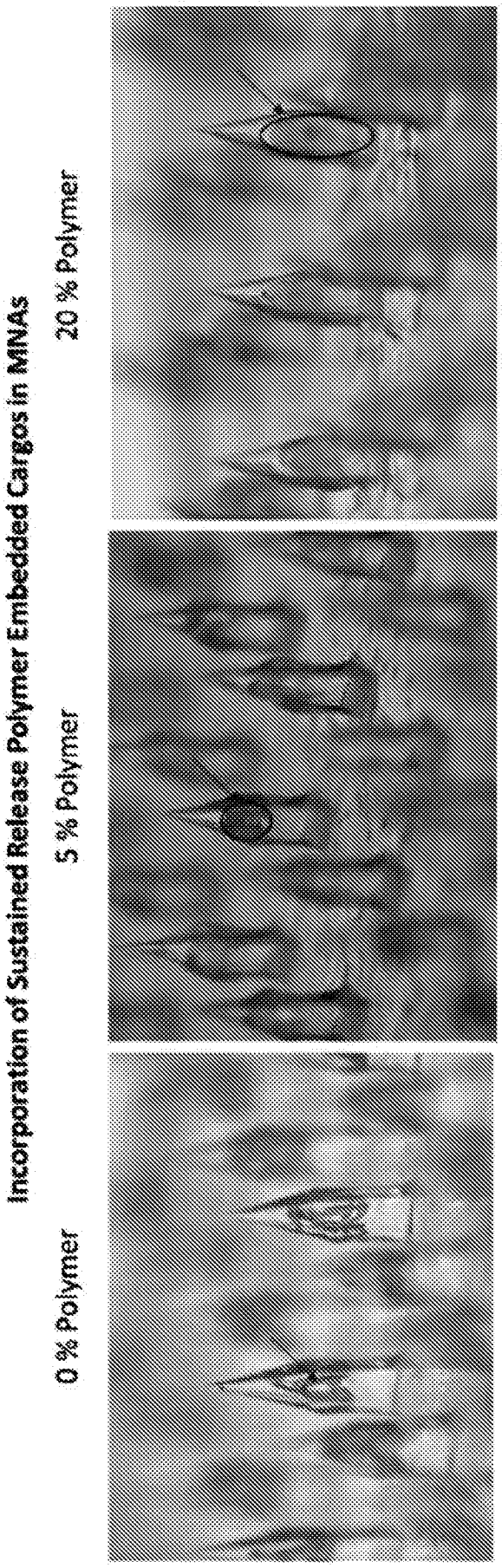

FIG. 38A

FIG. 38B

FIG. 38C

FIG. 39A FIG. 39B FIG. 39C

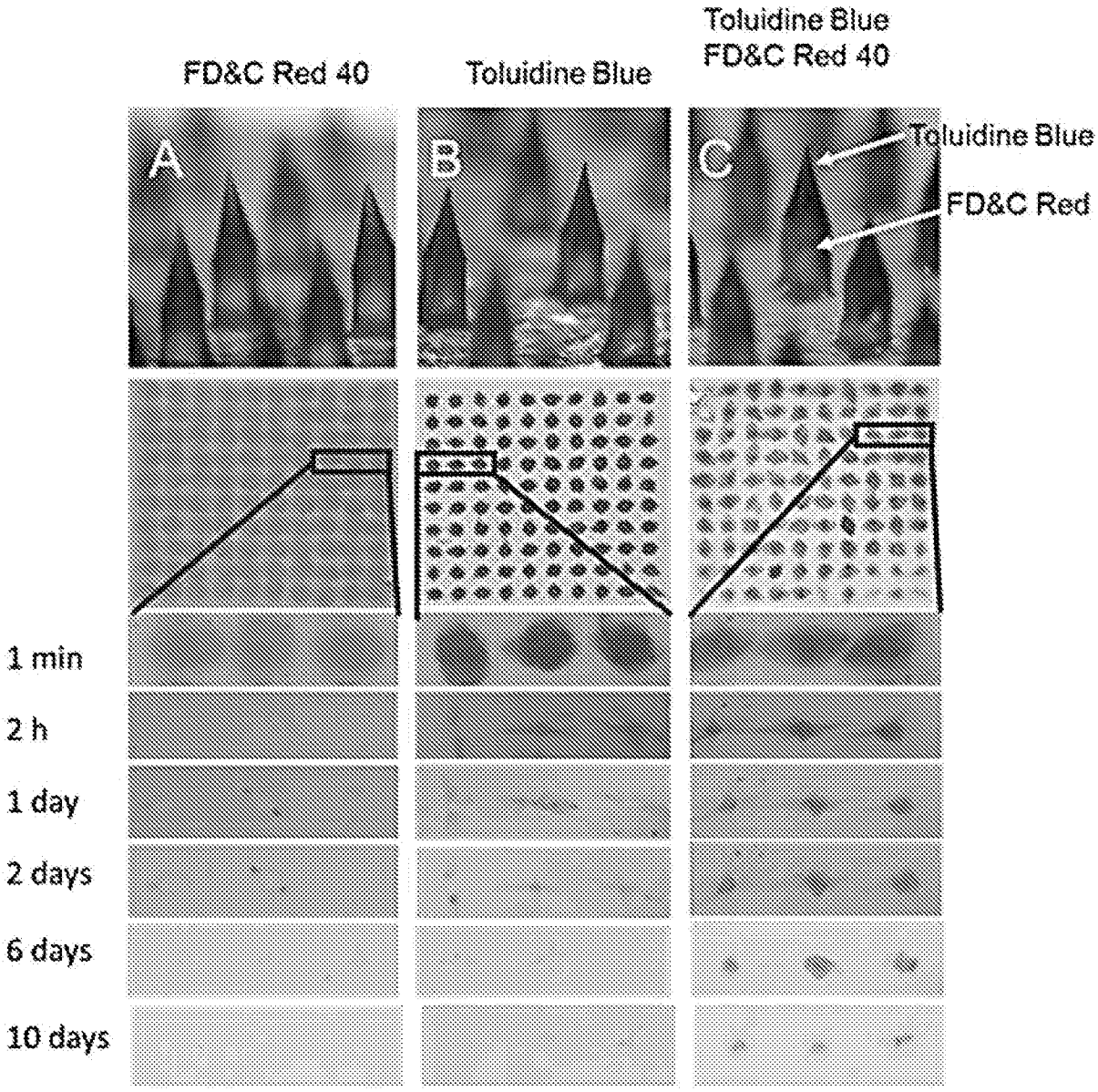

FIG. 40

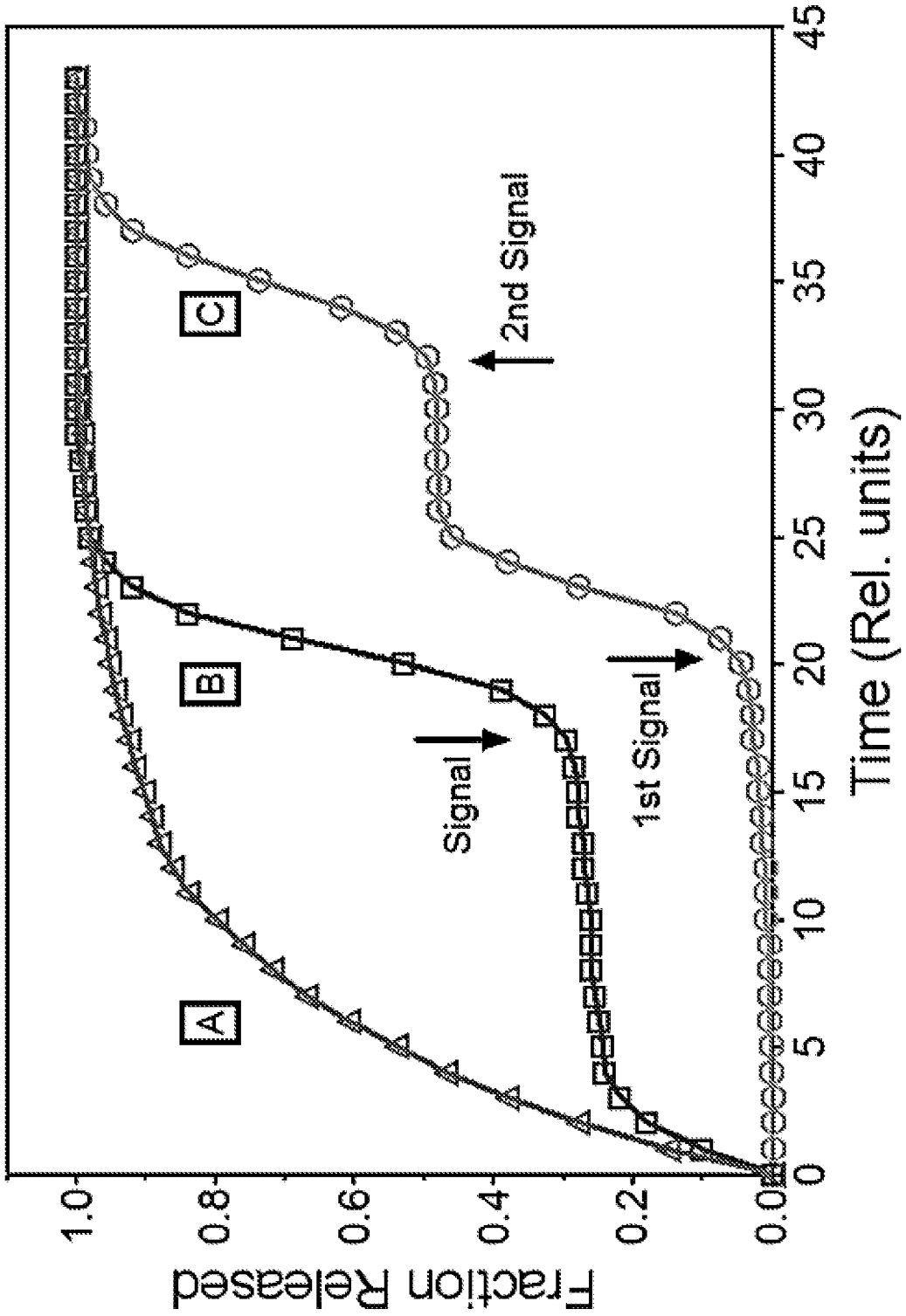
Fraction Released
1.0
0.8
0.6
0.4
0.2
0.0
0
5
10
15
20
25
30
35
40
45
Time (Rel. units)
A
B
C
Signal
1st Signal
2nd Signal

FIG. 41A

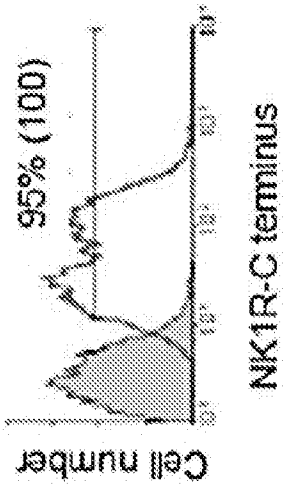

FIG. 41B

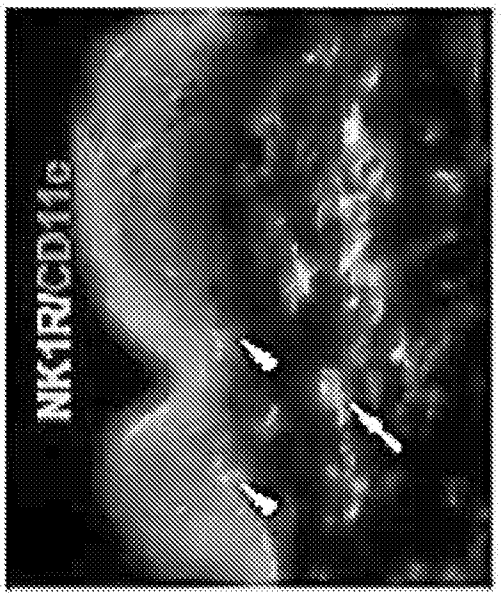

FIG. 41C

FIG. 41D

FIG. 42A

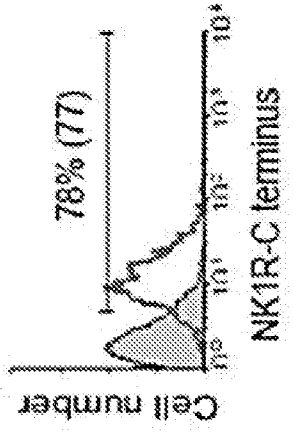

FIG. 42B

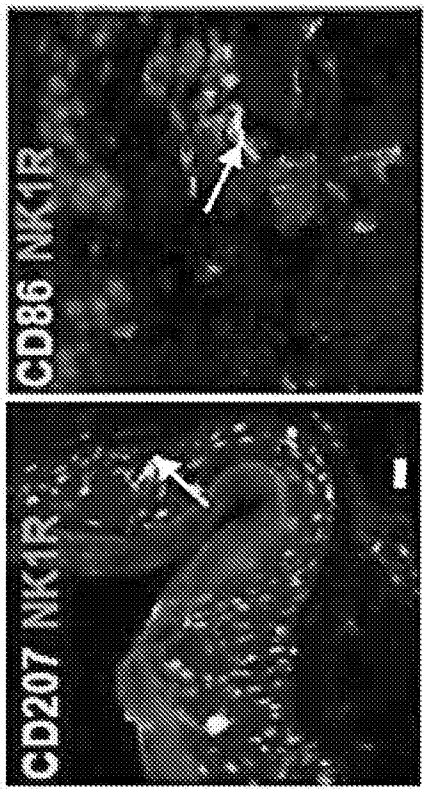

FIG. 42C

FIG. 42D

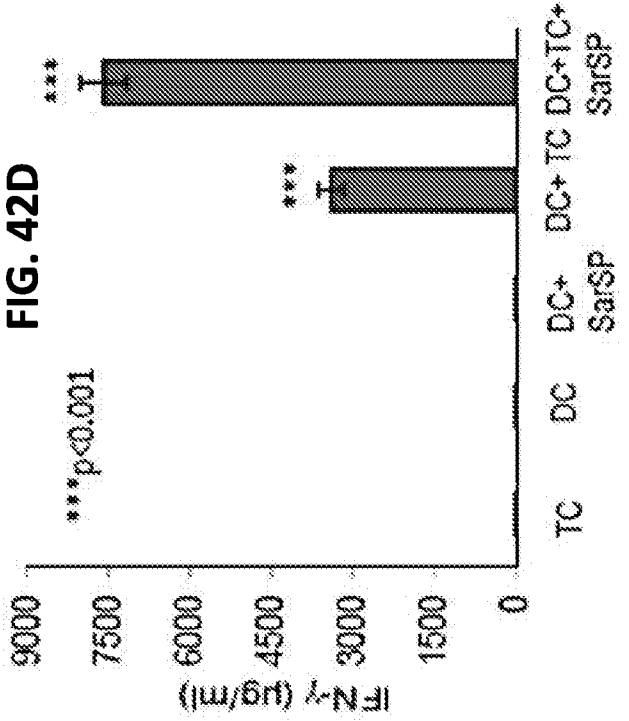

	MNA Pyramidal shape		MNA Obelisk shape	
Array Batches	c.p.m. / MNA	OVA transferred (µg / MNA)	c.p.m. / MNA	OVA transferred (µg / MNA)
AVG of 4 batches	3,068 ± 19%	2.12 ± 19%	11,919 ± 7%	8.24 ± 7%

MNA cargo delivery ratio:
$\frac{\text{MNA Obelisk}}{\text{MNA Pyramid}} = 3.89$

FIG. 43

FIG. 44A

FIG. 44B

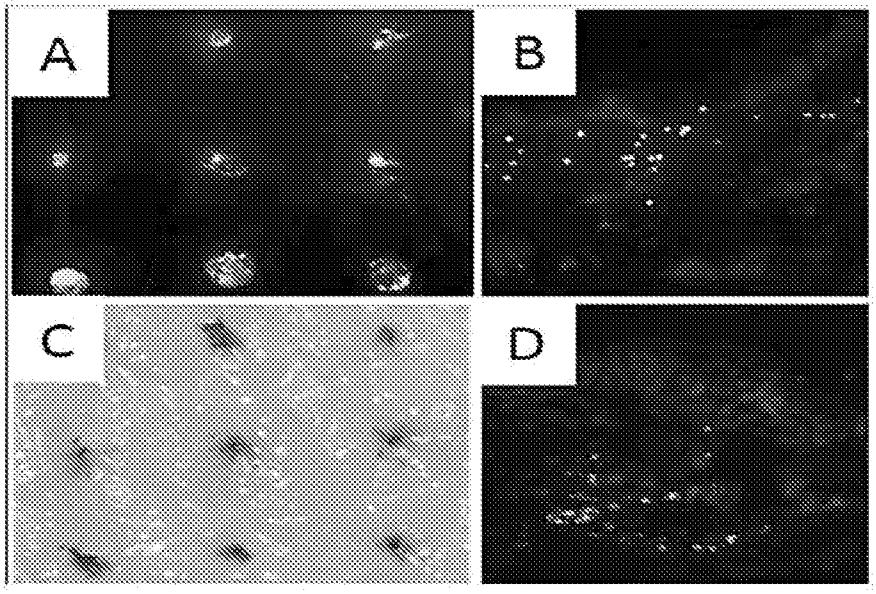

FIG. 44C

FIG. 44D

FIG. 45A

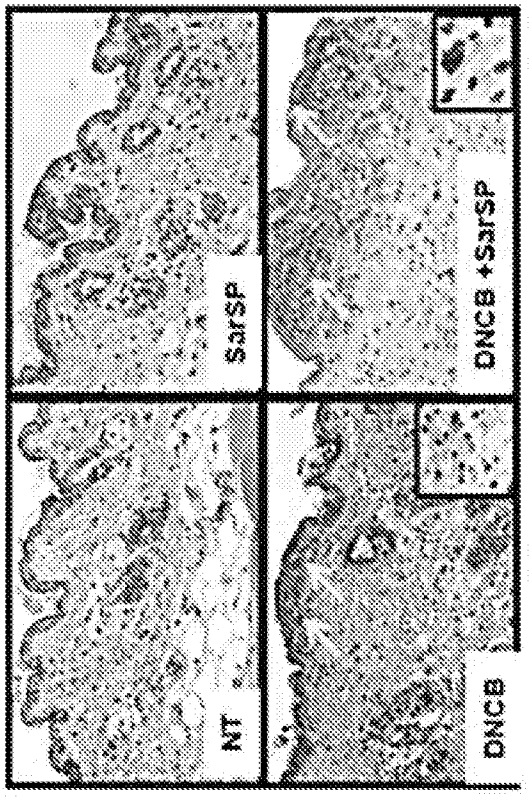

FIG. 45B

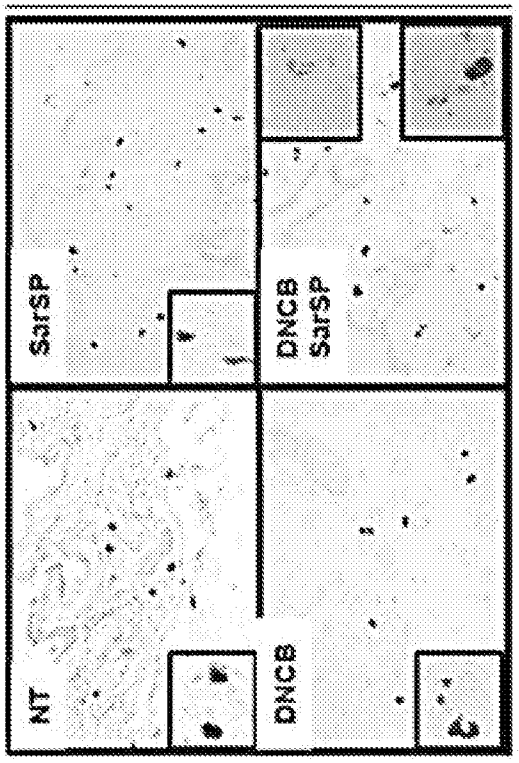

FIG. 45C

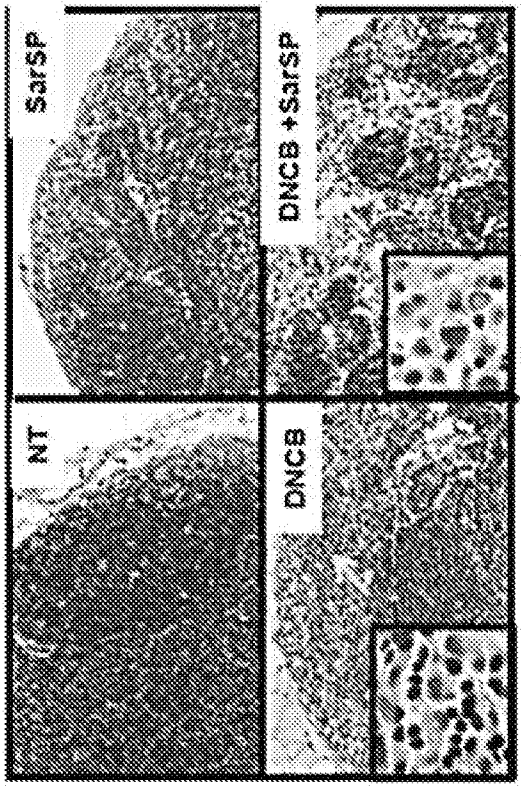

FIG. 45D

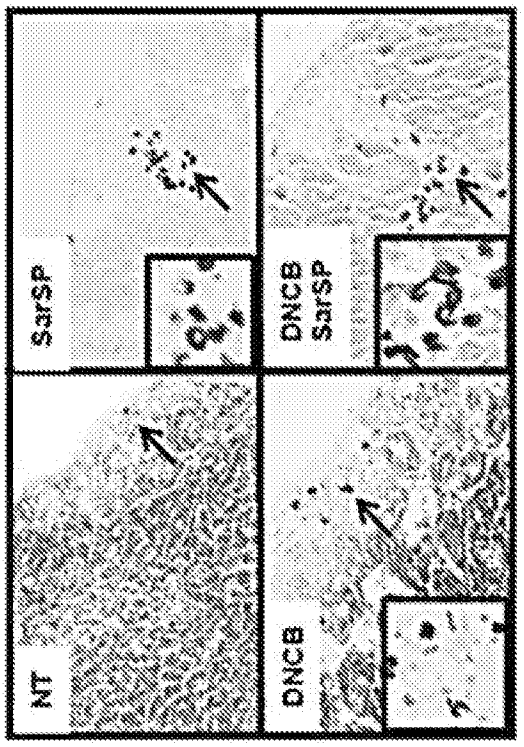

FIG. 46

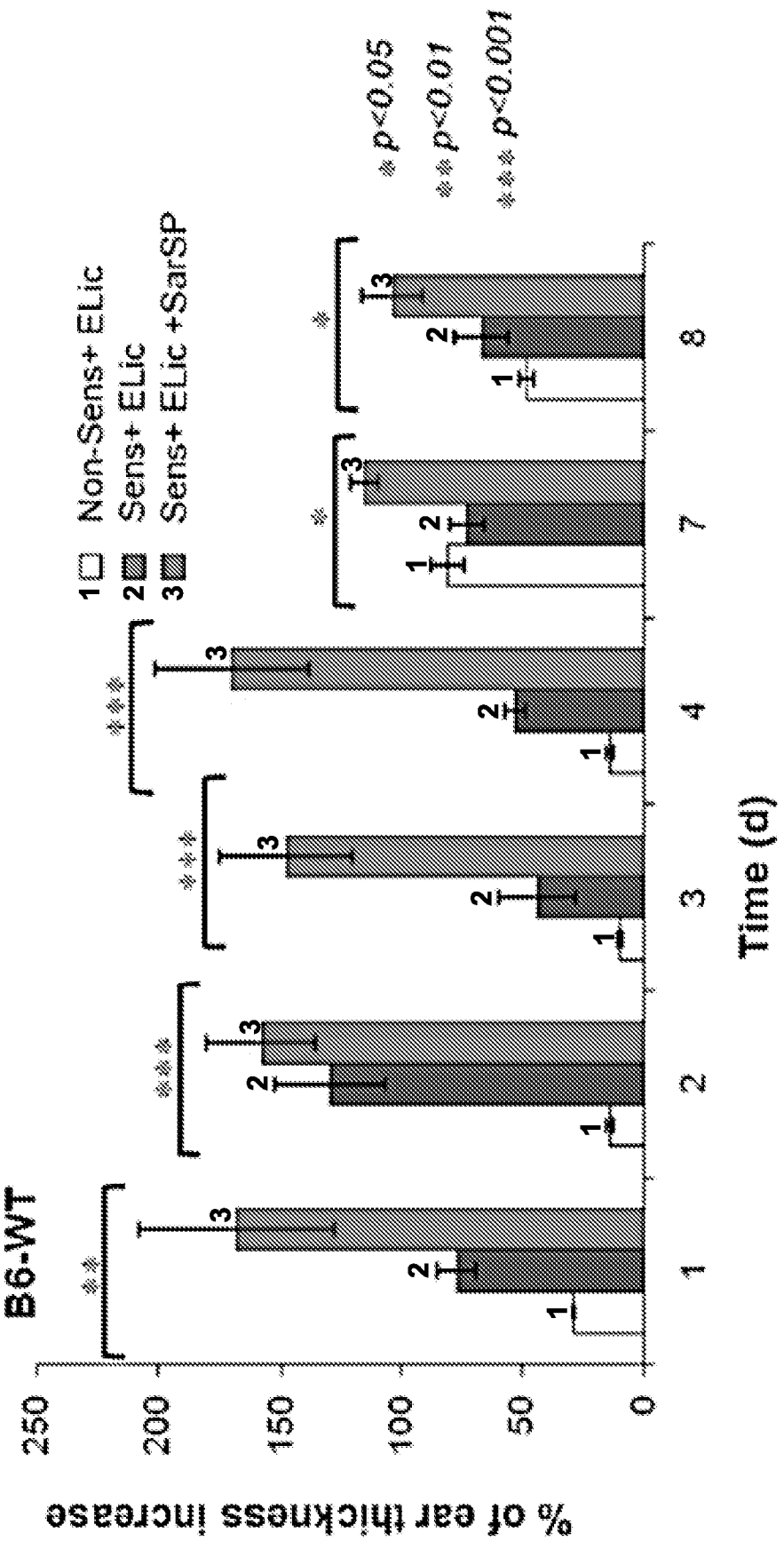
B6-WT
% of ear thickness increase
250
200
150
100
50
0
Time (d)
1
2
3
4
7
8
1 Non-Sens+ ELic
2 Sens+ ELic
3 Sens+ ELic +SarSP
* p<0.05
** p<0.01
*** p<0.001

FIG. 47A

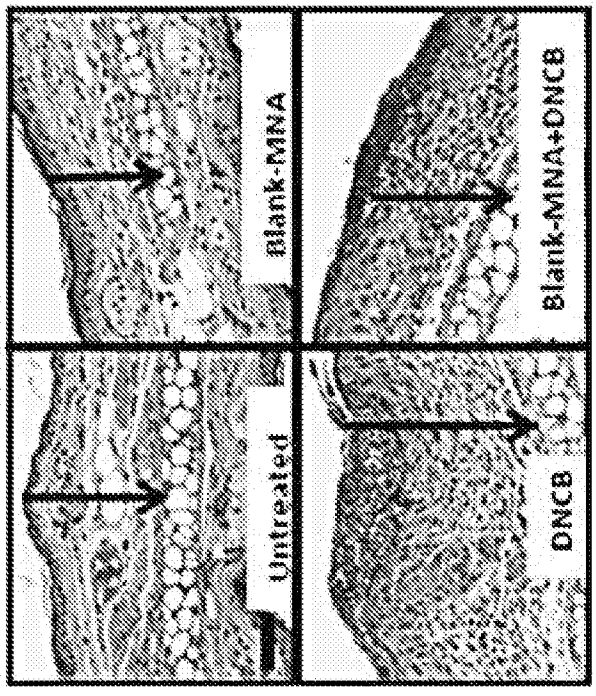

FIG. 47B

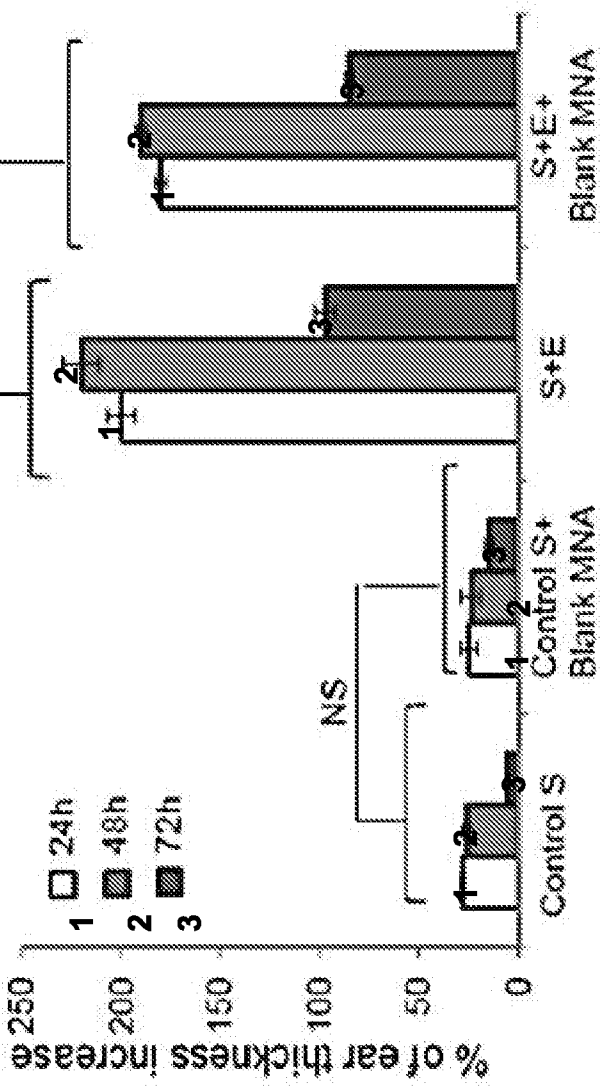

FIG. 48

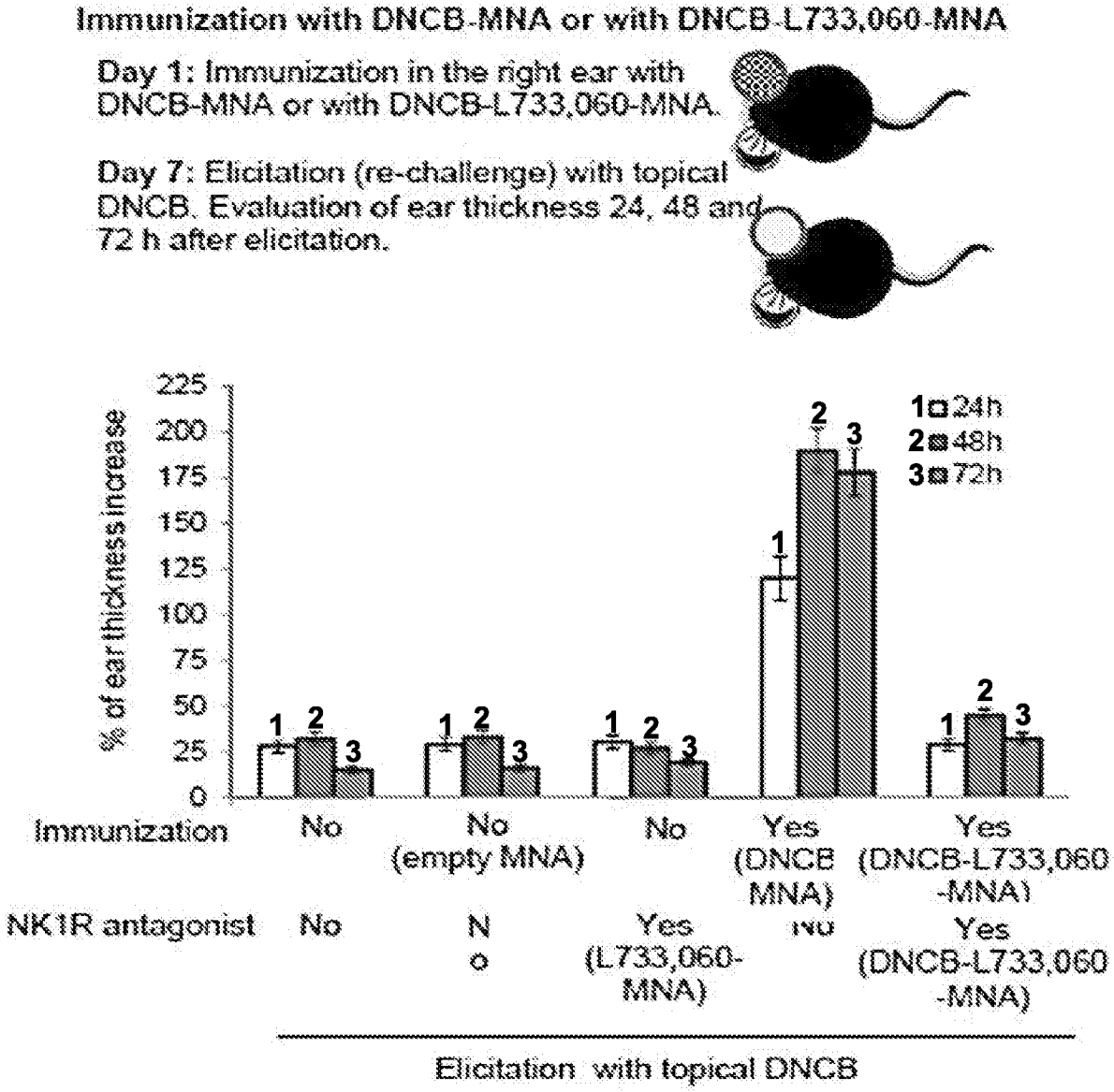
Immunization with DNCB-MNA or with DNCB-L733,060-MNA
Day 1: Immunization in the right ear with DNCB-MNA or with DNCB-L733,060-MNA.
Day 7: Elicitation (re-challenge) with topical DNCB. Evaluation of ear thickness 24, 48 and 72 h after elicitation.
% of ear thickness increase
225
200
175
150
125
100
75
50
25
0
1 24h
2 48h
3 72h
Immunization
No
No (empty MNA)
No
Yes (DNCB MNA)
Yes (DNCB-L733,060 -MNA)
NK1R antagonist
No
No
Yes (L733,060-MNA)
No
Yes (DNCB-L733,060 -MNA)
Elicitation with topical DNCB

FIG. 49A Desensitization of contact dermatitis by MNA negative immunization

Experimental Design

1) **Week 1: contact dermatitis induction**
Day 1: immunization with topical DNCB
Day 7: elicitation with topical DNCB.

2) **Weeks 2 and 3:** rest.

3) **Week 4: contact dermatitis desensitization**
Day 22: DNCB ± L733,060-MNA.

4) **Week 5: re-challenge + evaluation. Experiment endpoint.**
Day 29: topical DNCB.
Evaluation of ear thickness at 24, 48 and 72 h after elicitation (bar diagrams on B and C).

Re-challenge (right ear) to evaluate vaccine local effect. (B)

Re-challenge (left ear) to evaluate vaccine systemic effect (C).

FIG. 49B

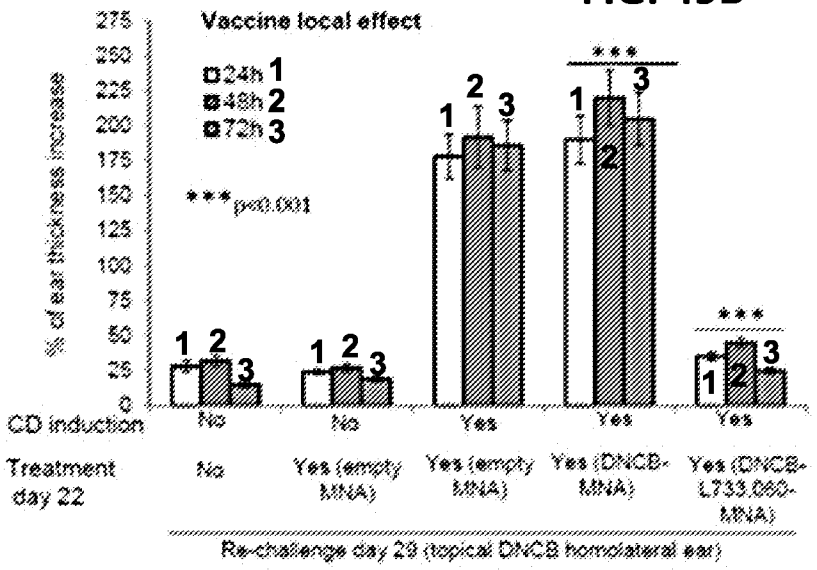

FIG. 49C

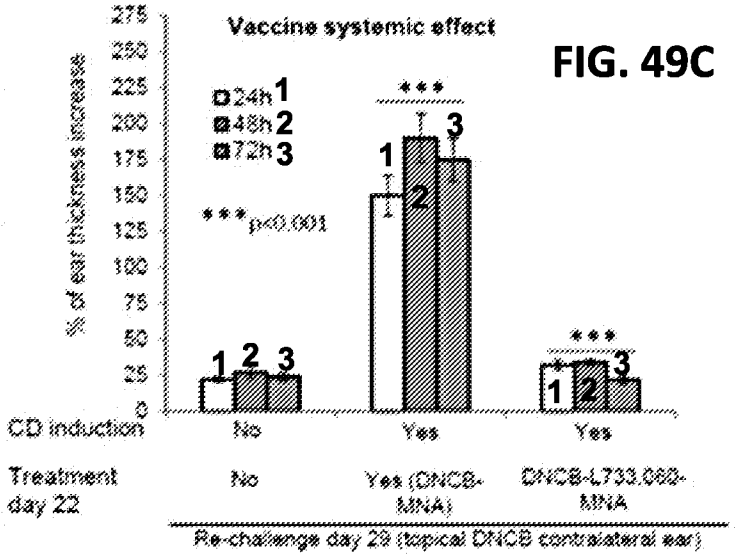

FIG. 50A

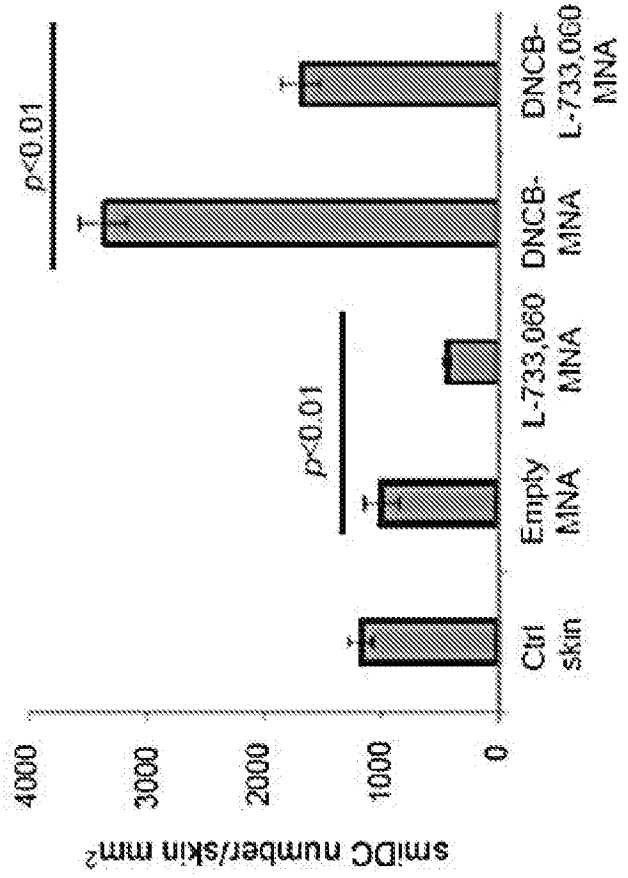

FIG. 50B

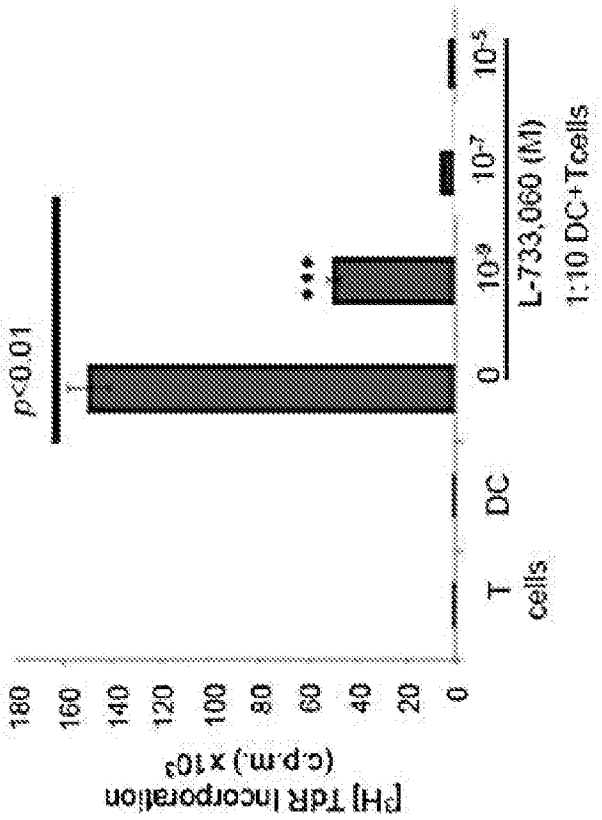

FIG. 51A

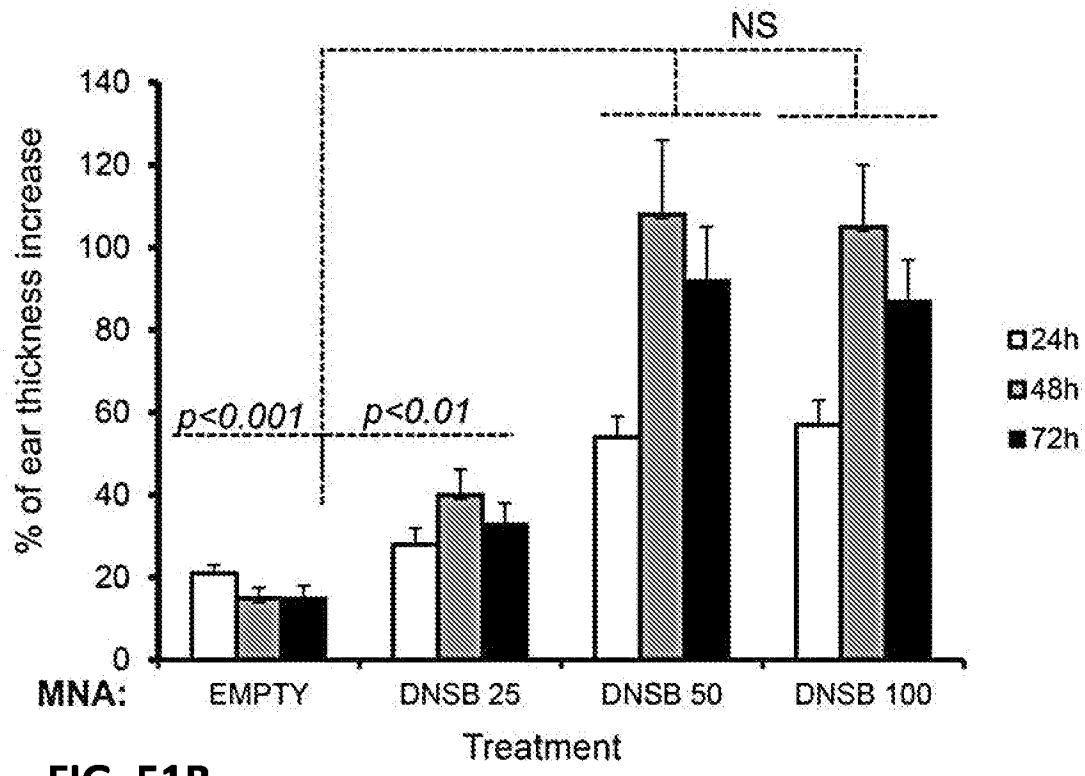

FIG. 51B

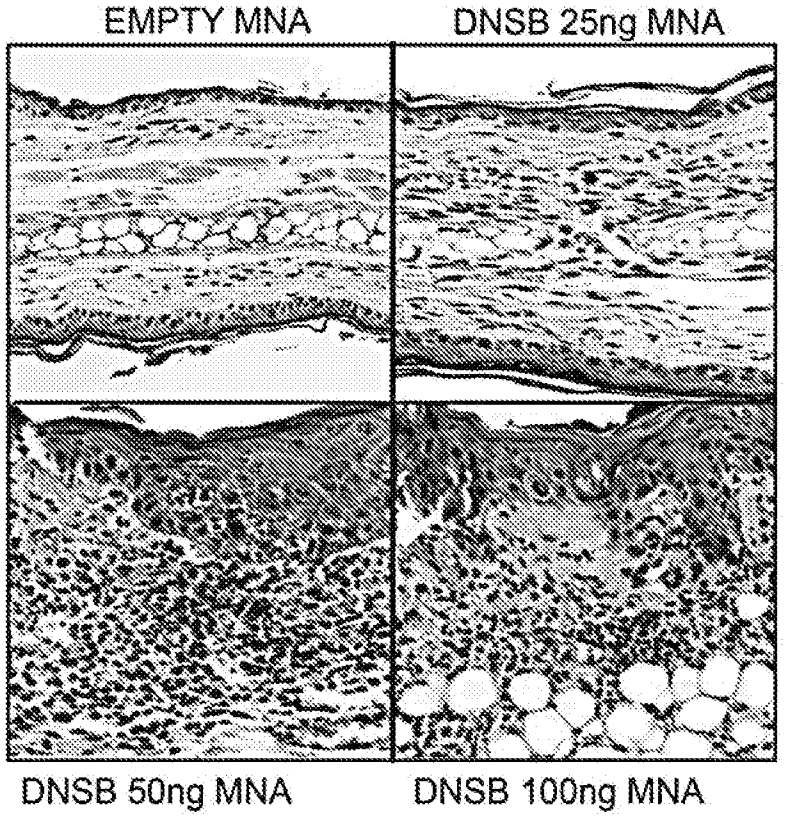

FIG. 52A

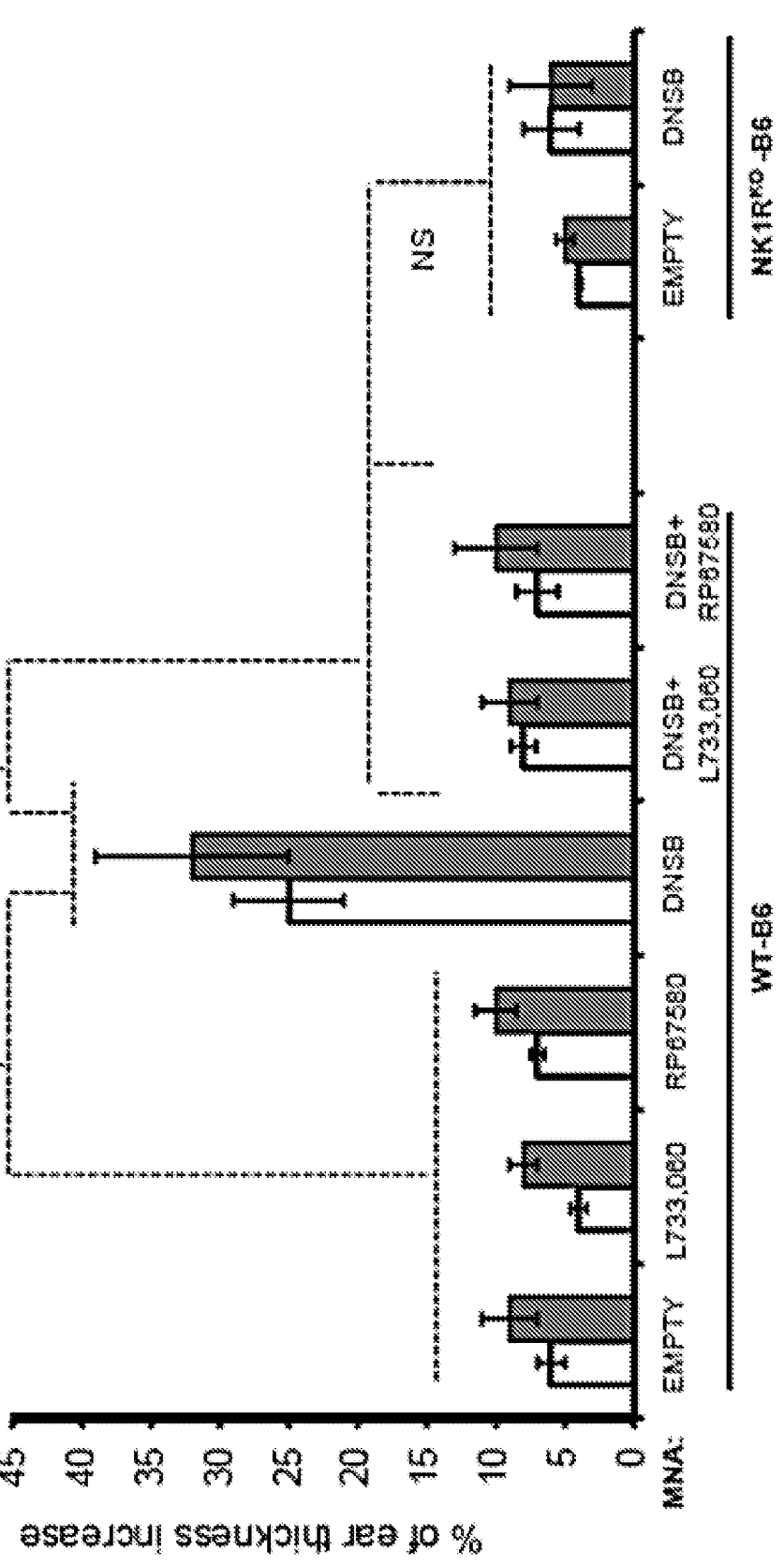
Mouse acute inflammatory response
% of ear thickness increase
45
40
35
30
25
20
15
10
5
0
***p<0.001
**p<0.001
NS
MNA:
EMPTY
L733,060
RP07580
DNSB
DNSB+ L733,060
DNSB+ RP07580
EMPTY
DNSB
WT-B6
NK1R^KO -B6

FIG. 52B

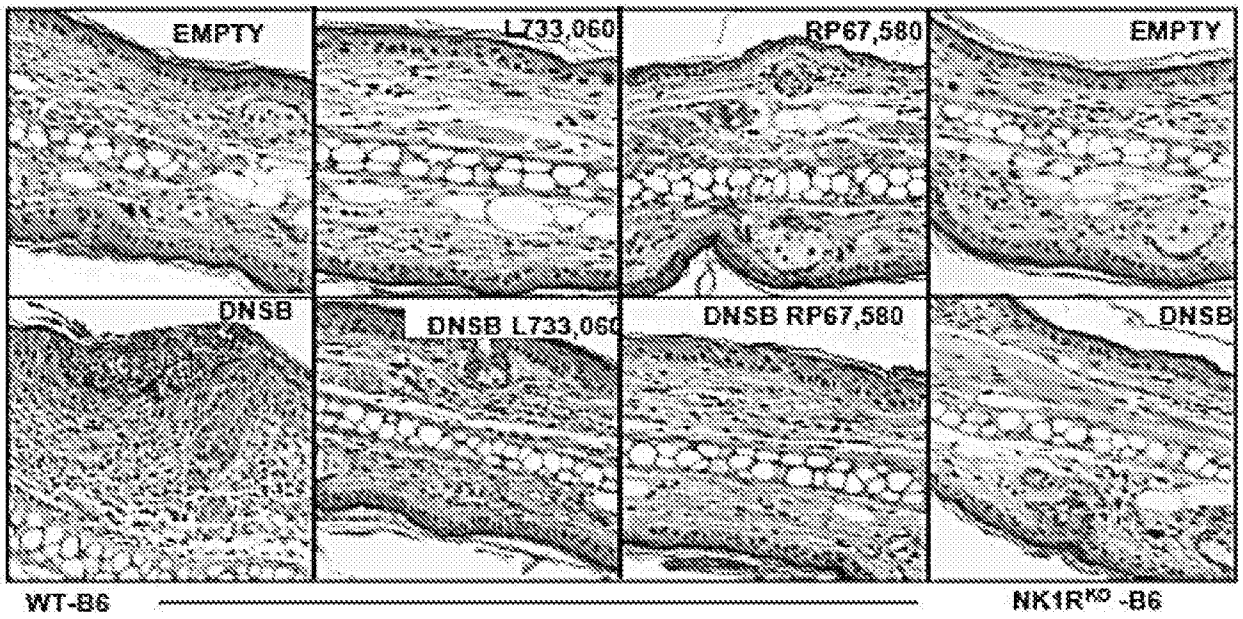

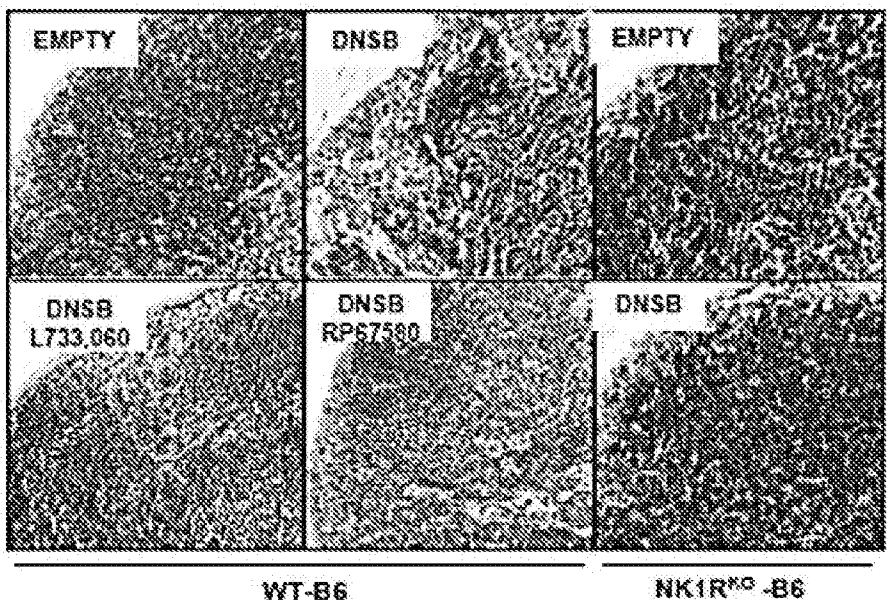

FIG. 52C

FIG. 53A

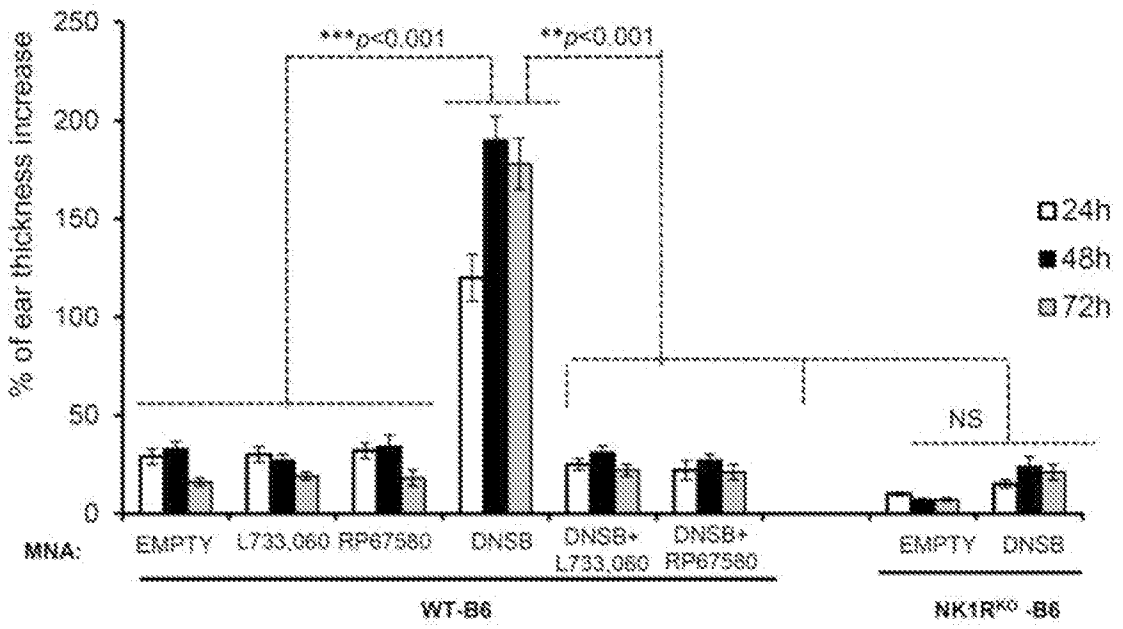

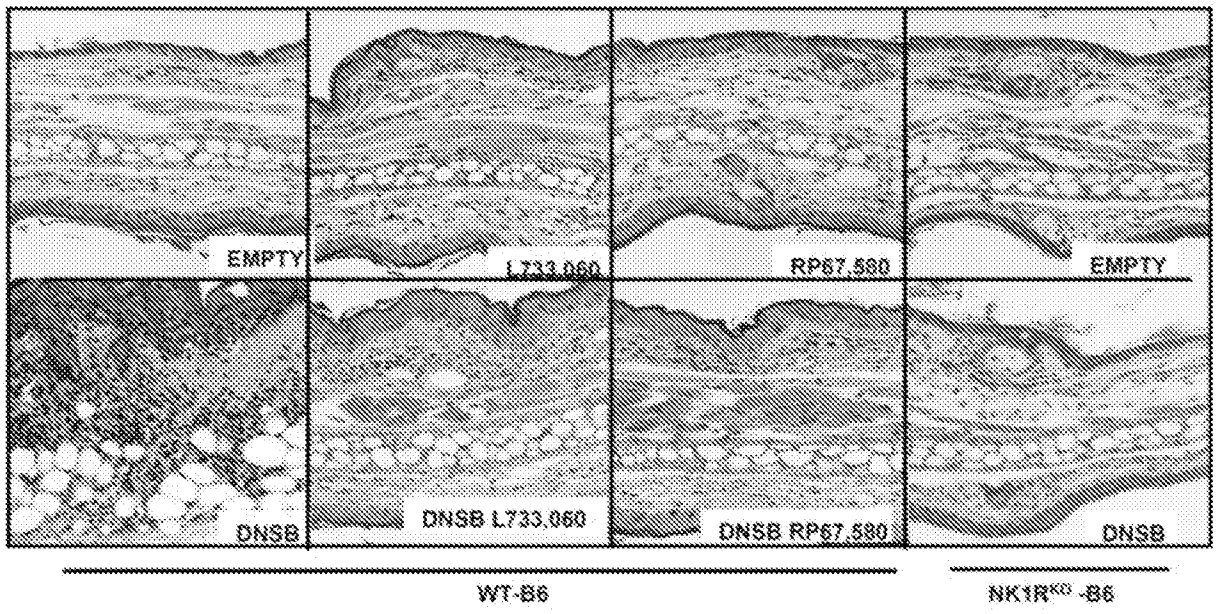

FIG. 53B

FIG. 54A

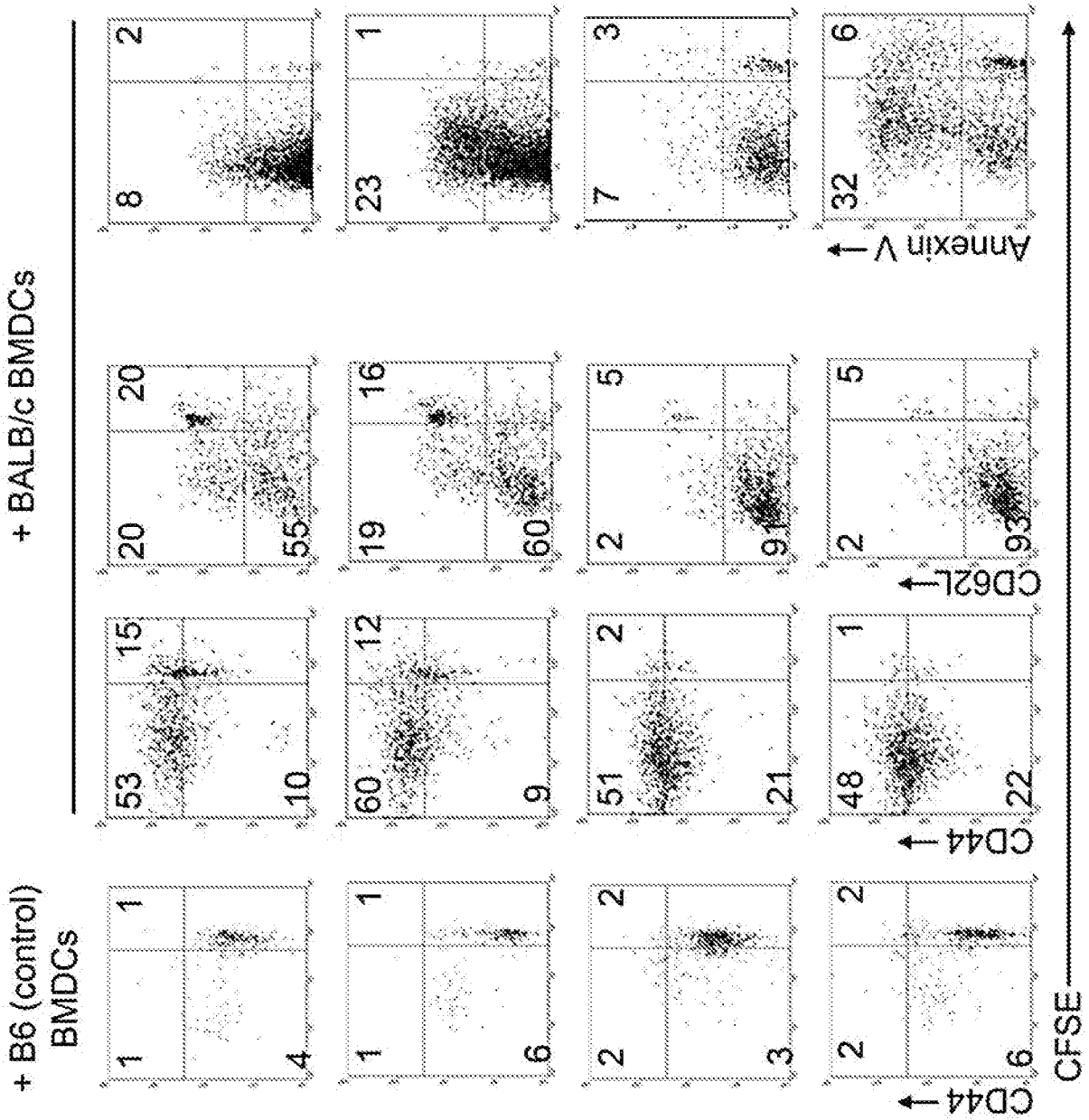
+ B6 (control) BMDCs
+ BALB/c BMDCs
Wt CD4 T
NK1R^KO CD4 T
Wt CD8 T
NK1R^KO CD8 T
CD44
CD62L
Annexin V
CFSE

FIG. 54C

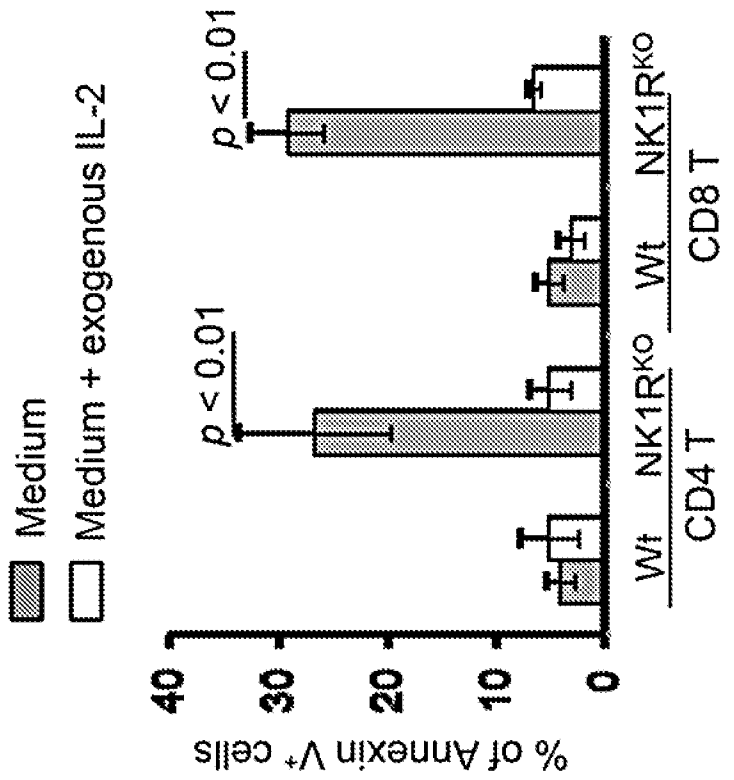

FIG. 54B

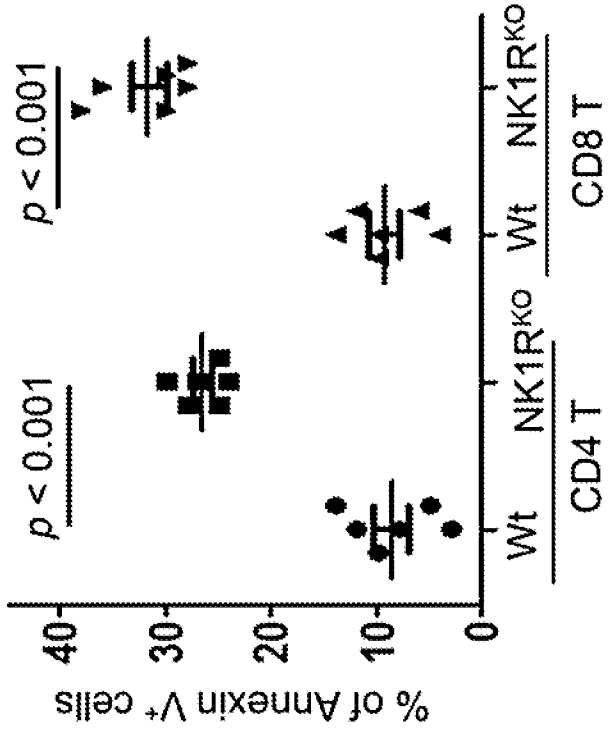

FIG. 55A

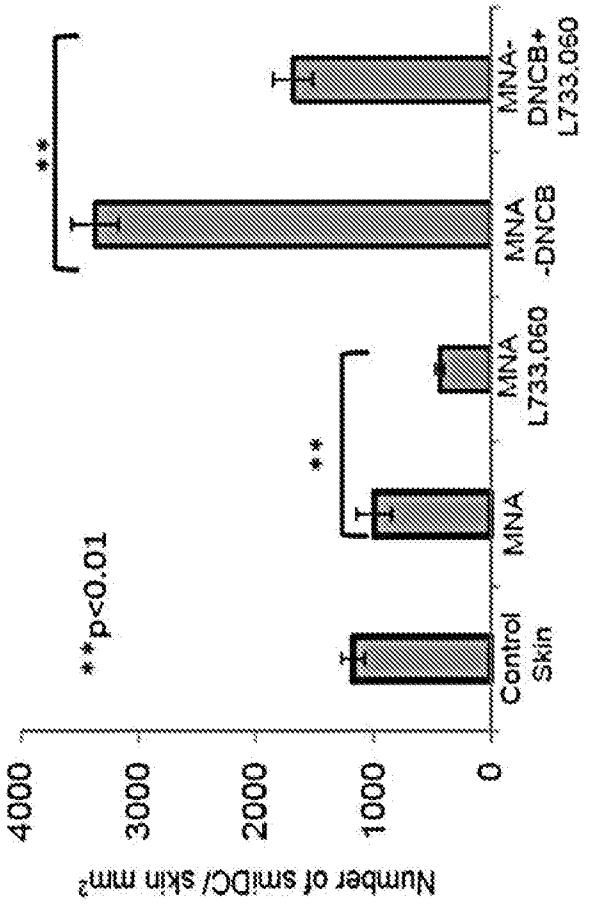

FIG. 55B

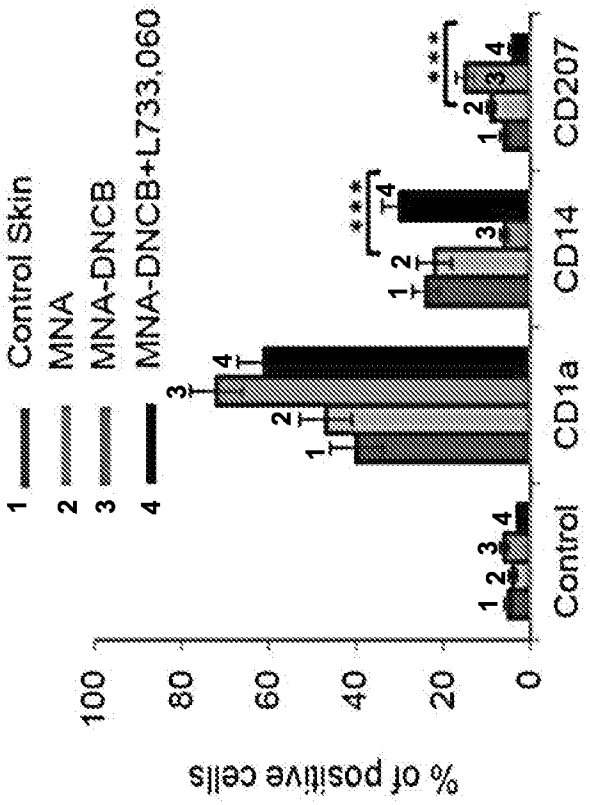

FIG. 55C

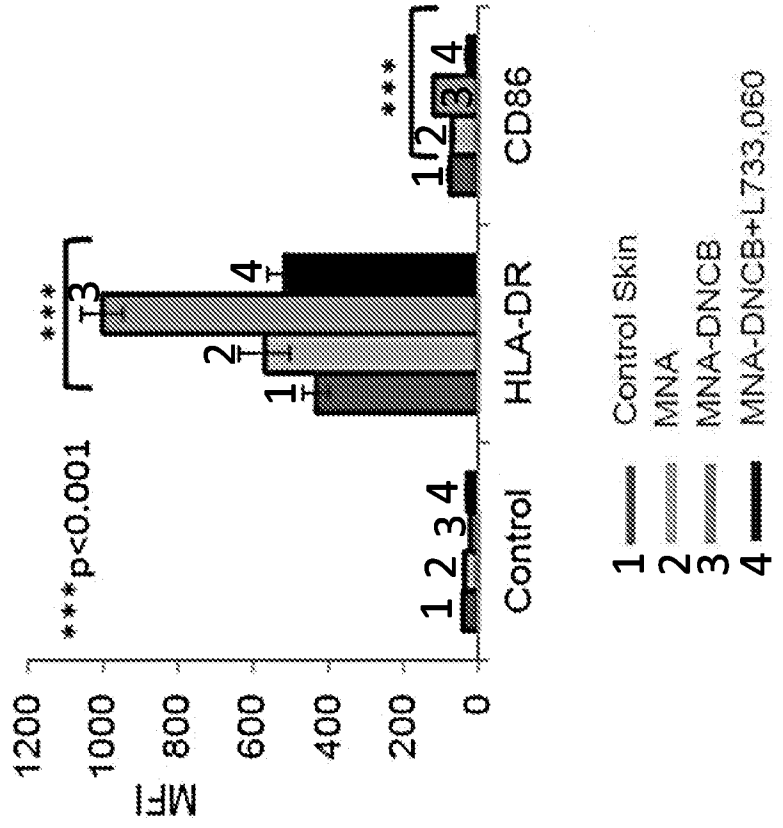

FIG. 55D

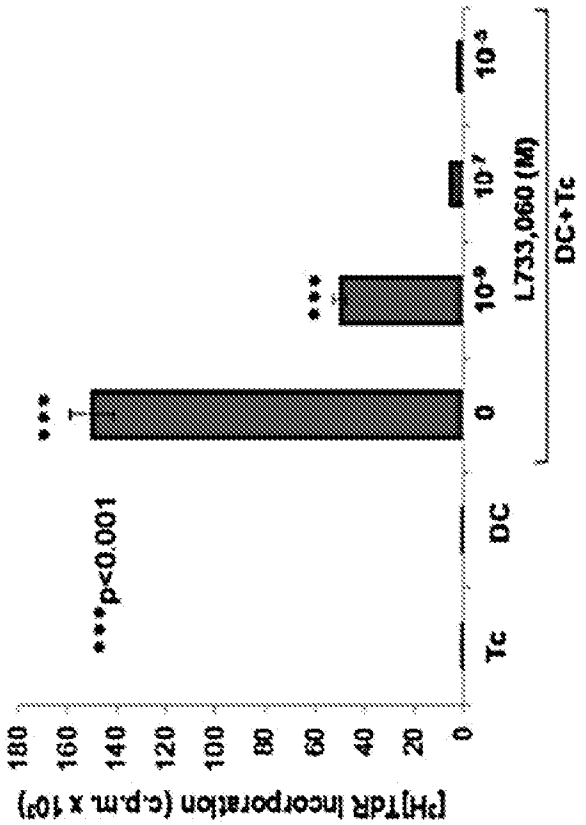

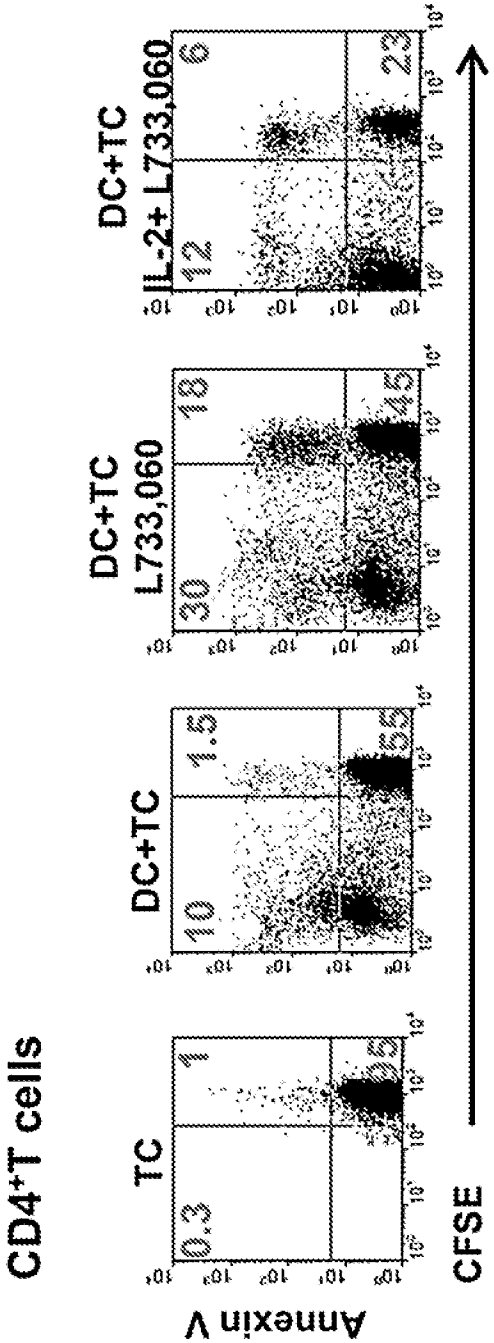

FIG. 56A

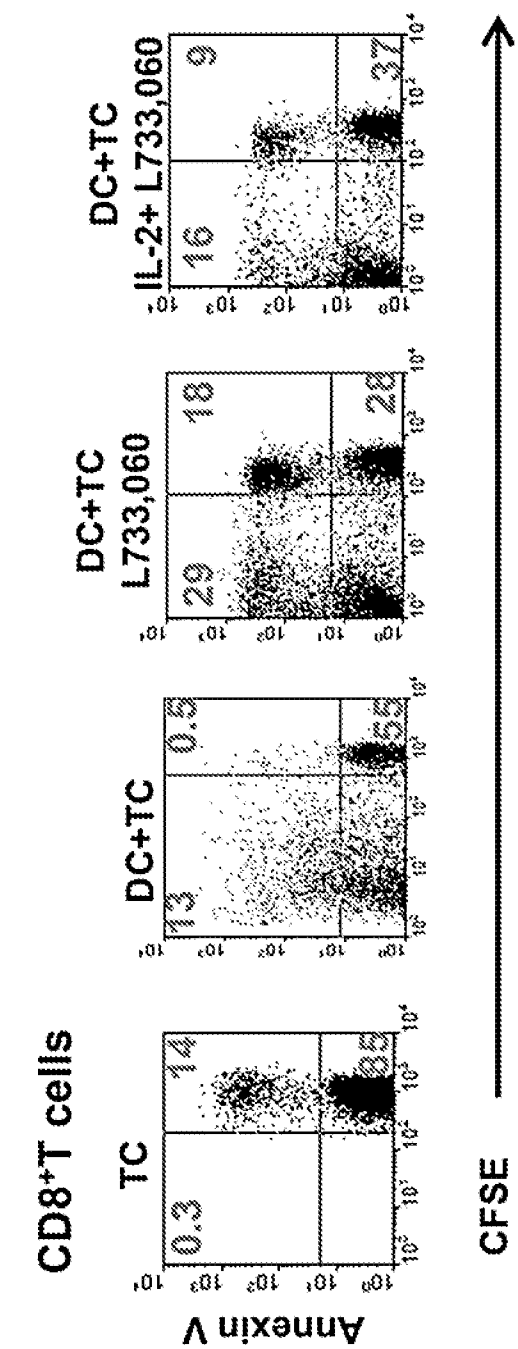

FIG. 56B

INTERNATIONAL SEARCH REPORT

International application No.
PCT/US2017/012315

Box No. II Observations where certain claims were found unsearchable (Continuation of item 2 of first sheet)

This international search report has not been established in respect of certain claims under Article 17(2)(a) for the following reasons:

1. ☒ Claims Nos.: 1-29
because they relate to subject matter not required to be searched by this Authority, namely:
Claims 1-29 pertain to methods for treatment of the human body by surgery or therapy, and thus relate to a subject matter which this International Searching Authority is not required to search (PCT Article 17(2)(a)(i) and PCT Rule **39.1(iv)).**

2. ☒ Claims Nos.: 43
because they relate to parts of the international application that do not comply with the prescribed requirements to such an extent that no meaningful international search can be carried out, specifically:
Claim 43 refers to an unsearchable claim which is not drafted in accordance with PCT Rule 6.4(a).

3. ☒ Claims Nos.: 6-9, 17, 28-29, 42
because they are dependent claims and are not drafted in accordance with the second and third sentences of Rule 6.4(a).

Box No. Ill Observations where unity of invention is lacking (Continuation of item 3 of first sheet)

This International Searching Authority found multiple inventions in this international application, as follows:

1. ☐ As all required addtional search fees were timely paid by the applicant, this international search report covers all searchable claims.

2. ☐ As all searchable claims could be searched without effort justifying an additional fees, this Authority did not invite payment of any additional fees.

3. ☐ As only some of the required additional search fees were timely paid by the applicant, this international search report covers only those claims for which fees were paid, specifically claims Nos.:

4. ☐ No required additional search fees were timely paid by the applicant. Consequently, this international search report is restricted to the invention first mentioned in the claims; it is covered by claims Nos.:

Remark on Protest

☐ The additional search fees were accompanied by the applicant's protest and, where applicable, the payment of a protest fee.

☐ The additional search fees were accompanied by the applicant's protest but the applicable protest fee was not paid within the time limit specified in the invitation.

☐ No protest accompanied the payment of additional search fees.

INTERNATIONAL SEARCH REPORT

International application No.
PCT/US2017/012315

A. CLASSIFICATION OF SUBJECT MATTER

A61K 39/35(2006.01)i, A61K 39/39(2006.01)i, A61K 38/19(2006.01)i, A61K 9/00(2006.01)i

According to International Patent Classification (IPC) or to both national classification and IPC

B. FIELDS SEARCHED

Minimum documentation searched (classification system followed by classification symbols)
A61K 39/35; A61N 1/18; A61B 17/20; A61M 5/158; A61M 5/00; A61M 37/00; B29C 37/00; A61K 39/39; A61K 38/19; A61K 9/00

Documentation searched other than minimum documentation to the extent that such documents are included in the fields searched
Korean utility models and applications for utility models
Japanese utility models and applications for utility models

Electronic data base consulted during the international search (name of data base and, where practicable, search terms used)
eKOMPASS(KIPO internal) & Keywords:microneedle array, promoting, reducing, desensitizing, immune response, allergen, antigen, adjuvant, skin, obelisk

C. DOCUMENTS CONSIDERED TO BE RELEVANT

Category*	Citation of document, with indication, where appropriate, of the relevant passages	Relevant to claim No.
X	W0 2013-166162 Al (UNIVERSITY OF PITTSBURGH - OF THE COMMONWEALTH SYSTEM OF HIGHER EDUCATION et al.) 07 November 2013 See claims 1-13; pages 4-7, **11,** 18-21, 30.	30-37,40-41
Y		38-39
Y	US 8321012 B2 (DELLA ROCCA, G. J. et al.) 27 November 2012 See claim *V*, columns 2-3, 14-15.	38-39
A	US 2011-0098651 Al (FALO, JR., L. D. et al.) 28 April 2011 See claims 12-19; paragraph [0022].	30-41
A	US 2005-0065463 Al (TOBINAGA, Y. et al.) 24 March 2005 See claim **1.**	30-41
A	KORKMAZ, E. et al, "Therapeutic intradermal delivery of tumor necrosis factor-alpha antibodies using tip-loaded dissolvable microneedle arrays" , Acta Biomater., 2015, Vol. 24, pages 96-105. See pages 96, 105.	30-41

☐ Further documents are listed in the continuation of Box C.

☒ See patent family annex.

* Special categories of cited documents:
"A" document defining the general state of the art which is not considered to be of particular relevance
"E" earlier application or patent but published on or after the international filing date
"L" document which may throw doubts on priority claim(s) or which is cited to establish the publication date of another citation or other special reason (as specified)
"O" document referring to an oral disclosure, use, exhibition or other means
"P" document published prior to the international filing date but later than the priority date claimed
"T" later document published after the international filing date or priority date and not in conflict with the application but cited to understand the principle or theory underlying the invention
"X" document of particular relevance; the claimed invention cannot be considered novel or cannot be considered to involve an inventive step when the document is taken alone
"Y" document of particular relevance; the claimed invention cannot be considered to involve an inventive step when the document is combined with one or more other such documents,such combination being obvious to a person skilled in the art
"&" document member of the same patent family

Date of the actual completion of the international search	Date of mailing of the international search report
27 April 2017 (27.04.2017)	**27 April 2017 (27.04.2017)**

Name and mailing address of the ISA/KR
International Application Division
Korean Intellectual Property Office
189 Cheongsa-ro, Seo-gu, Daejeon, 35208, Republic of Korea
Facsimile No. +82-42-481-8578

Authorized officer
PARK, Jung Min
Telephone No. +82-42-481-35 16

INTERNATIONAL SEARCH REPORT

Information on patent family members

International application No.

PCT/US2017/012315

Patent document cited in search report	Publication date	Patent family member(s)	Publication date
WO 2013-166162 Al	07/11/2013	AU 2013-256348 Al	18/12/2014
		CA 2871770 Al	07/11/2013
		CN 104703651 A	10/06/2015
		EP 2841147 Al	04/03/2015
		EP 2841147 A4	13/04/2016
		HK 1209658 Al	08/04/2016
		IN 10161DEN2014 A	21/08/2015
		JP 2015-515886 A	04/06/2015
		MX 2014013234 A	29/10/2015
		US 2015-0126923 Al	07/05/2015
US 8321012 B2	27/11/2012	US 2011-0150924 Al	23/06/2011
		US 2011-0152748 Al	23/06/2011
		US 2013-0079582 Al	28/03/2013
		US 2013-0131435 Al	23/05/2013
		US 8364258 B2	29/01/2013
		US 8725251 B2	13/05/2014
		US 8788037 B2	22/07/2014
US 2011-0098651 Al	28/04/2011	US 2014-0350472 Al	27/11/2014
		US 8834423 B2	16/09/2014
US 2005-0065463 Al	24/03/2005	DE 202004003389 Ul	06/05/2004
		US 8353861 B2	15/01/2013